Innovative Solution for Seafastening Offshore Wind Turbine Transition Pieces during transport

Wouter Hoeksema

February 2014

Seaway Heavy Lifting
offshore installation

TU Delft Delft University of Technology
Challenge the future

MSc thesis
Delft University of Technology
Faculty of Civil Engineering and Geosciences

Innovative Solution for Seafastening Offshore Wind Turbine Transition Pieces during transport

Wouter Hoeksema
February 2014

Thesis examination committee:

Prof. Ir. F.S.K. Bijlaard	TU Delft
Dr. Ir. P.C.J. Hoogenboom	TU Delft
Dr. Ir M.H. Kolstein	TU Delft
Ir. J.P. Breedeveld	Seaway Heavy Lifting
Ir. W.R. van Dalen	Seaway Heavy Lifting

Preface

This rapport contains the design of a new method of seafastening Offshore Wind Turbine Transition Pieces. This thesis study is part of my masters degree in Civil Engineering at the Delft University of Technology.

The success of the thesis would not have been possible without the contributions of my graduation committee. Many thanks goes out to Pierre Hoogenboom, Henk Kolstein and especially prof. Frans Bijlaard, who has helped me from the start in finding the right directions in the thesis.

Much gratitude goes out to all the employees of Seaway Heavy Lifting, where everybody was very kind and eager to help. I have special gratitude for Jan-Peter Breedeveld, who offered me this fascinating opportunity. Wouter van Dalen, who guided me through the art of thesis writing. Joep Niermeijer and Lars Bos, who helped me get started in this exciting industry with all their practical knowledge. Hans van Engelen, whose experience and methodological approach to problem solving taught me valuable lessons I will benefit from the rest of my career. Jason Yan and Kees Havik, who answered all my trivial, tedious and complex questions about ANSYS Software without losing patience. And above all, I would like to thank my parents, who made this all possible.

Wouter Hoeksema

Amsterdam, February 2014

Abstract

Seaway Heavy Lifting is an offshore contractor that transports, installs and decommissions offshore oil and gas platforms and offshore wind turbines. During transport, objects need to be secured on the deck, the so-called seafastening. In particular for parts of offshore wind turbines, called Transition Pieces, this proves to be difficult. The Transition Pieces are on average 25 m high tubular structures and weight 300 mT. The outside is covered with a special coating and various attachments, such as boat landings, ladders, and anodes for corrosion protection. The inside of the Transition Pieces contains various structures and equipment, such as groutskirts, shear keys, J-tubes and internal platforms.

Seaway Heavy Lifting currently uses clamps on the lower flange to secure the Transition Pieces in an upright position to the deck of the ship. This causes relative high stresses in the flange and weld and turned out to be a critical limiting factor during transportation for several projects. Due to this limitation, the workability of the vessels is suboptimal. Many other offshore contractors use the same or similar method of clamping the lower flange to the deck.

A new method for seafastening Transition Pieces is proposed to improve the securing strength, the safety, and workability of the vessels. This new method comprises of a tubular element, much like the monopile on which the Transition Piece will stand once on offshore location, welded onto the grillage. The Transition Piece can then be lifted over this tubular element. Mounted on the tubular element are hydraulic cylinders that extend outwards towards the inner wall of the Transition Piece. By exerting a force to the inner wall, the Transition Piece is effectively secured to the vessel. This method avoids using the rather weak lower flange.

Strength calculations have shown that this new method can withstand accelerations and accompanying forces caused by the ships motions that are nearly twice as high as the current method allows.

Because the new method is fully automated, it requires no manual labour and the seafastening can be activated and deactivated quickly, thus saving critical crane time. It also reduces the time frame where the Transition Pieces stands on the deck unsecured, as is the case with the current method which uses clamps and bolts, thus improving safety.

This thesis covers the invention of the new method, calculating the critical structural parts, and detailing those element that are crucial to the design.

Currently, a patent applications is pending.

Table of Contents

List of Abbreviations

AISC: American Institute of Steel Construction
API: American Petroleum Institute
CoF: Coefficient of Friction
CoG: Centre of Gravity
DNV: Det Norske Veritas
DP3: Dynamic Positioning Class 3
EMA: Extended Motion Analysis
EWEA: European Wind Energy Association
GW: Giga Watt
kWh: kilowatt hour
MW: Mega Watt
NREAP: National Renewable Energy Action Plan
OS: Oleg Strashnov
OWP: Offshore Wind Park
SHL: Seaway Heavy Lifting
SY: Stanislav Yudin
RAO: Response Amplitude Operator
RNA: Rotor Nacelle Assembly
TP: Transition Piece

List of Figures

List of Tables

1 Introduction

1.1 Offshore wind energy

The offshore wind energy industry is booming. Since the first pilot-projects in the 90's the industry has really taken off. In 2002 the first large wind farm was installed, Horns Rev. Since then, several new wind farms have been build each year, steadily growing in size. This growth was spurred mainly for two reason: rising fossil fuel prices and the political desire to be more independent of foreign energy supplies.

Traditionally wind energy was harvested on land. But social resistance grew due to visual and sound pollution. Furthermore, the available space on land is limited, the wind is less strong on land than on sea and it's more turbulent. If wind turbines are placed offshore, there are a lot of advantages, like more and steadier winds and lots of space. There are downsides. Conditions are harsher and electricity prices are higher

In figure 1.1 a graph is shown with the annually and cummulative installed offshore wind turbines in European waters. A clear increase, almost exponential rise can be observed.

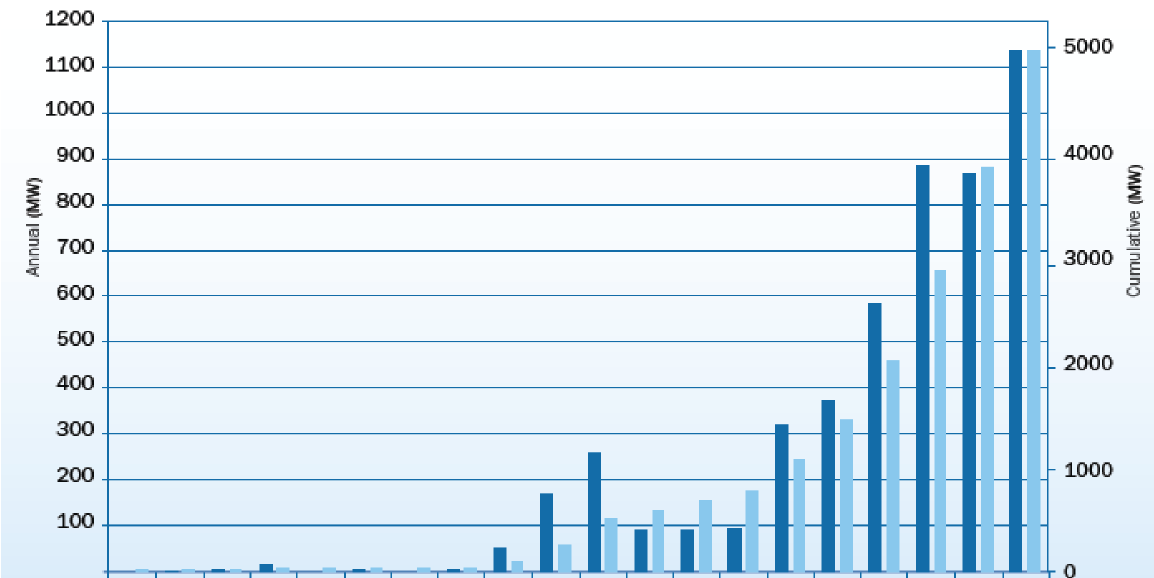

	1993	1994	1995	1996	1997	1998	1999	2000	2001	2002	2003	2004	2005	2006	2007	2008	2009	2010	2011	2012
Annual	0	2	5	17	0	3	0	4	51	170	276	90	90	93	318	373	577	883	874	1,166
Cumulative	5	7	12	29	29	32	32	36	86	256	532	622	712	804	1,123	1,496	2,073	2,956	3,829	4,995

Country	UK	DK	BE	DE	NL	SE	FI	IE	NO	PT	Total
No. of farms	20	12	2	6	4	6	2	1	1	1	55
No. of turbines	870	416	91	68	124	75	9	7	1	1	1,662
Capacity installed (MW)	2,947.9	921	379.5	280.3	246.8	163.7	26.3	25.2	2.3	2	4,995

Figure 1.1: Annually and cumulative installed offshore wind turbines in European waters [1]

It is expected that this rise will continue. European governments have set ambitious targets for future installments of wind turbines and for 2020 a 40 GW capacity is projected, see figure 1.2 .

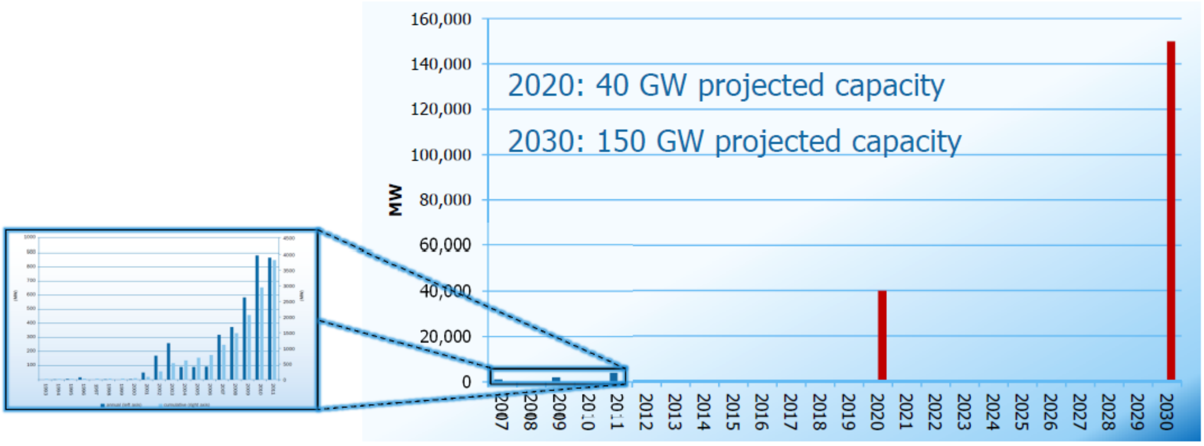

Figure 1.2: Projected capacity of offshore wind turbines in European waters [1]

How credible are these commitments? Looking back at a previous year, e.g. 2009, we can measure the difference between what was promised and what was built.

Looking at figure 1.3, it can be seen that the capacity that really has been built does lag somewhat behind the plans (NREAP's) and estimates (EWEA). NREAP's are the National Renewable Energy Action Plan's. In this figure the left column indicates the cumulative capacity that was planned by several European countries (e.g. UK, Denmark, Netherlands and Germany). The middle column indicates what European Wind Energy Association (EWEA) estimated beforehand. Real is what was actually built. Note that the numbers on the vertical axis do not start a zero [1]. So the actual building does lag behind the plans, but not more than 20%.

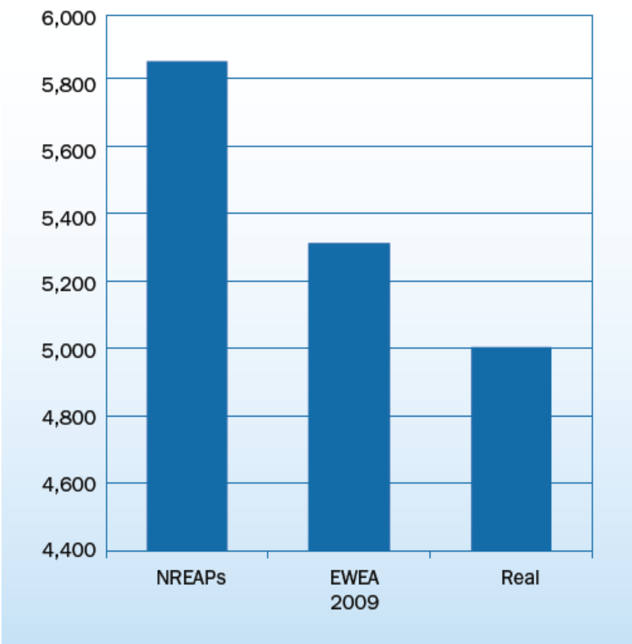

Figure 1.3: Planned vs. really build offshore wind turbines [1]

Looking further ahead (figure 1.4), Shell Global Solutions predicts a significant increase in new renewables (this includes all energy sources such as solar, tidal, wind etc.), and a significant decrease in conventional energy [2].

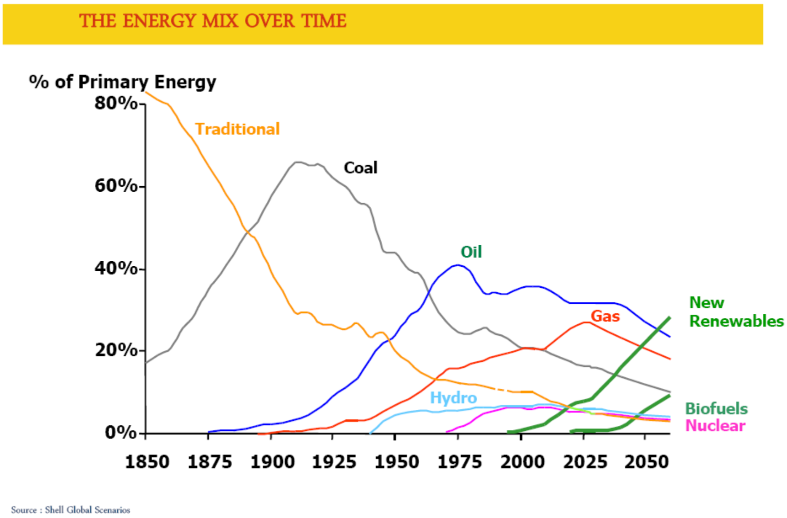

Figure 1.4: Overview of predicted mix of energy over time [2]

At the end of 2012 (figure 1.5) nearly 5 GW is online, almost 5 GW is under construction and over 18 GW is consented to.

The current biggest challenge for offshore wind is to reduce the cost per kWh. Currently the industry is heavily subsidized and cannot compete with conventional energy. But since it is a relatively young industry, a lot of steps to increase efficiency can be made.

The offshore wind industry still relies on Oil and Gas industry practice and experience. But there is an important difference: Oil & Gas are one-of projects, each project is unique, whereas wind projects are a lot of the same structures.

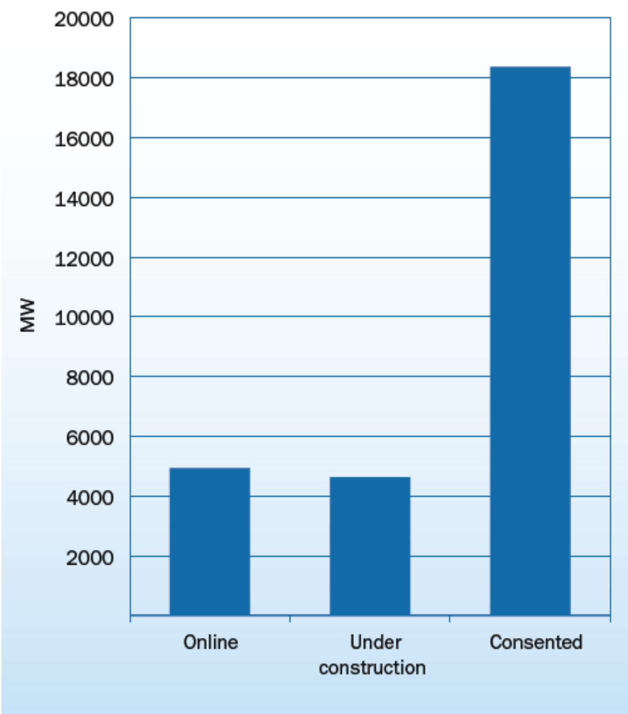

Figure 1.5: Currently consented to new offshore wind farms [1]

Concluding, offshore wind energy is here to stay and likely to increase very much in the near future. Since installing offshore wind farms is a repetitive action, it pays to optimize procedures.

1.2 Background

Seaway Heavy Lifting (SHL) is an offshore contractor that transports, installs and decommissions offshore structures like oil and gas platforms and wind farms. They are a key player in the global market with their two heavy lift crane vessels, the Stanislav Yudin and the Oleg Strashnov. Currently the offshore wind farm industry is developing very rapidly. A lot of questions remain however about optimizing industry practice. One of these questions is how to best transport Transition Pieces (TP). These 25 m high structures are full of delicate electronic equipment and the outside is painted with a special coating that should not be damaged during transport. The problem is that TP's are completely and solely designed for in-situ situation, not for transport.

1.3 Problem description

The current method the securing TP's on the transportation vessel is labour intensive and time-consuming. Current SHL practice is to place the TP on a grillage. This is a support structure, built up out of I-beams and welded to the deck of the ship. Its purpose is to spread the load towards strongpoints, i.e. frames and bulkheads, in the ship. Clamps are used on the bottom flange of the TP to hold it down against the grillage. These clamps are heavy (approx. 45 kg) and need to be carried by two men. The clamps are horizontally pressed and fixed against the TP using shim's and wedges, which can sometimes loosen during transport. Finally, the clamp is vertically fixed using two pretensioned M64 bolts. Each TP needs 16 of those clamps to be held down. Further problems arise when space is limited due to equipment and attachments on the outside of the TP right above the flange. Sometimes clamps don't fit or the bolts cannot be tightened. All this is done manually. Four TP's are transported each time. Since new wind farms are totaling over a hundred windmills (Walney 102 windmills, Greater Gabberd 140 windmills, London Array 175 windmills), installments of new wind farms requires a lot of repetitive actions.

1.4 Thesis objective

The objective of this thesis is to have a new method of seafastening TP's on the deck of the ship such that is faster and more effective than current methods.

1.5 Boundary conditions

A new method should abide by several boundary conditions.

Boundary conditions:

- no increase footprint
- no welding to TP
- cut out labour
- cut duration (faster)
- more effective (capable of withstanding higher forces)
- reusable
- no changes to TP can be made

Below is explained what these boundary conditions mean and why they exist.

No increase footprint. The footprint is the area consumed on the deck of the vessel by the object to be transported. Currently this means that the TP stands on a grillage, which is welded onto the deck. So for one TP transported, the area consumed is length x width of the grillage. The reason for this boundary condition is that on the deck of the vessel space is scarce (see figure 1.9). If a new method would require more space, then maybe less TP's can be transported, which would result in more trips back to harbour and this would increase the project costs and decrease profits.

No welding to TP. The outside of the TP is coated with a special paint. This may not be damaged in any way. Welding to the TP would damage the coating, which would need to be restored once the TP is in place. This is costly and difficult.

Cut out labor. The current method uses clamps that need to be installed and tightened manually. Because it is done manually, it takes time and there is a risk of injury. The old clamps weighed about 45 kg, but the new ones weigh over 200 kg and can only be slid into place.

Cut duration. This is one of the main goals to be achieved by the new method. Since operating a large vessel costs a lot of money, it pays to save as much time as possible. Particularly in the case of offshore wind farms, where frequent trips from the harbor to the offshore location and back are made, efficiency is important. The Oleg Strashnov has DP3 capabilities. This means that is can sail to a particular location offshore (e.g. next to a monopile where the next TP needs to be installed) and guarantee that it will maintain position without anchors. From this moment on the seafastening can be removed and TP installed. Because the current method requires the seafastening to be removed manually, again it takes time. Any time saved here, is time saved on the project and costs reduced and profits increased. Especially if wind farms consist of one-hundred-plus wind turbines, it adds up. For example, if 30 minutes could be saved on each TP, and a wind farm consists of 100 wind turbines, and a typical day rate of such a Heavy Lift Vessel (HLV) is 400.000,- euro per 24 hours, then over 800.000 euro's could be saved.

More effective. In this context that means stronger, i.e., capable of withstanding higher accelerations. The other main goal to be achieved by the new method. Although the accelerations the TP undergoes due to transport are often limited, it is expected that the industry will increase the limiting value and ultimately remove the limitation altogether. From then on the structure itself will be the limiting factor, as was already the case in the Gwynt y Môr project, where the weld between the flange and wall was not strong enough to withstand forces caused by accelerations higher than 3.57 m/s^2. This resulted in a lower workability. So, increasing the strength of the seafastening and using a method that ensures that the TP is not the limiting factor means that higher forces can be resisted, which means that higher accelerations can be experienced. Workability goes up, waiting for whether goes down, more TP's can be installed in a shorter amount of time, more projects can be executed in a season and profits go up.

Safer. Although already partially incorporated in a few boundary conditions mentioned above (i.e. stronger is safer and automation or no use of manual labor reduces the risk of injury), the new method should also be safer in that it should have more redundancy, or failsafe. If any component were to fail, the system should not.

Reusable. The current method uses 32 pretensioned bolts through 16 clamps to seafasten one TP. Since these bolts can only be used once, a lot of bolts are thrown away afterwards. If a method could be used that disposes of no materials, a slight increase in sustainability can be achieved, as well as cost savings.

No changes to TP can be made, i.e., it may not be assumed that within the near future SHL suggested changes will be incorporated in the design. This means that a method must be developed that can be applied directly to existing TP's. It would be very beneficial to make changes to the TP, e.g. like a stronger flange, which would make it much easier to seafasten. For now, SHL just gets TP's delivered as designers have designed them for in-situ loads, because at the moment of designing it is not yet known which company is going to install the TP's. Since different companies have different wishes regarding design changes, and all of these changes cost money, none of them are granted. Therefore, designers design TP's solely for in-situ loads and contractors are left to figure out on their own how to transport and install TP's.

1.6 Thesis approach

In the remainder of chapter 1 the terminology, current practice and available information on TP's will be reviewed.

Chapter 2 describes several alternatives for seafastening TP's. The best option is chosen as the solution to the problem and will be detailed further.

Chapter 3 determines the loads the seafastening structure has to resist. These loads result from the ships motions and accelerations. The TP has to follow these motions and thus needs to be accelerated in different directions. The seafastening structure has to provide the forces for these accelerations.

Chapter 4 determines the force distribution and describes the numerical model to check if a simplified model with two infinite stiff rings with springs in between is accurate enough. This numerical model is built in ANSYS in which accelerations can be applied as loads to a geometry.

In Chapter 5 a justification of the rotation point assumed in the dynamical model of chapter 3 will be described. This is done trough a static analysis of the TP standing on only one grillage beam. Besides the static analysis also a buckling analysis will be done, both using ANSYS finite element software. To verify the buckling analysis, a hand calculation will be used.

In chapter 6 the pretensioning force is applied to a part of the TP. This should result in stresses low enough so that the TP can be accelerated, causing an increase of the stresses, and not cross limiting values.

Chapter 7 will describe and calculate the model of the seafastening itself. It will be checked if the existing grillage of the Gwynt y Mor project suffices for the higher acceleration and different load application.

Chapter 8 describes the means with which enough friction is created to resist the overturning moment of the TP.

In Chapter 9 a few items will be detailed that are considered vital for this new method of seafastening Transition Pieces.

1.7 Terminology and current practice

In figure 1.6 a schematic overview is given on the major parts of an offshore windmill.

At the bottom of the wind turbine is the foundation pile or monopile (MP). This is a simple steel tube that is hammered into the seabed. Because it is hammered, it cannot be guaranteed that it is perfectly vertical. Also the top of the pile gets damaged in this process.

Indicated in yellow is the Transition Piece (TP). Typical characteristics are as follows: the lower 6m of this 25m high structure slides over the top of the monopile. Jacks are used to align the TP vertically to correct the MP skewness. Then the space between the TP and MP is grouted to fix the connection. Furthermore the top of the TP offers a nice flange for the tower to be bolted on.

After that the tower is installed on top of the TP. The Rotor Nacelle Assembly (RNA) is installed on top of the tower, sometimes in one go, and sometimes first the nacelle is installed and then each blade independently afterwards.

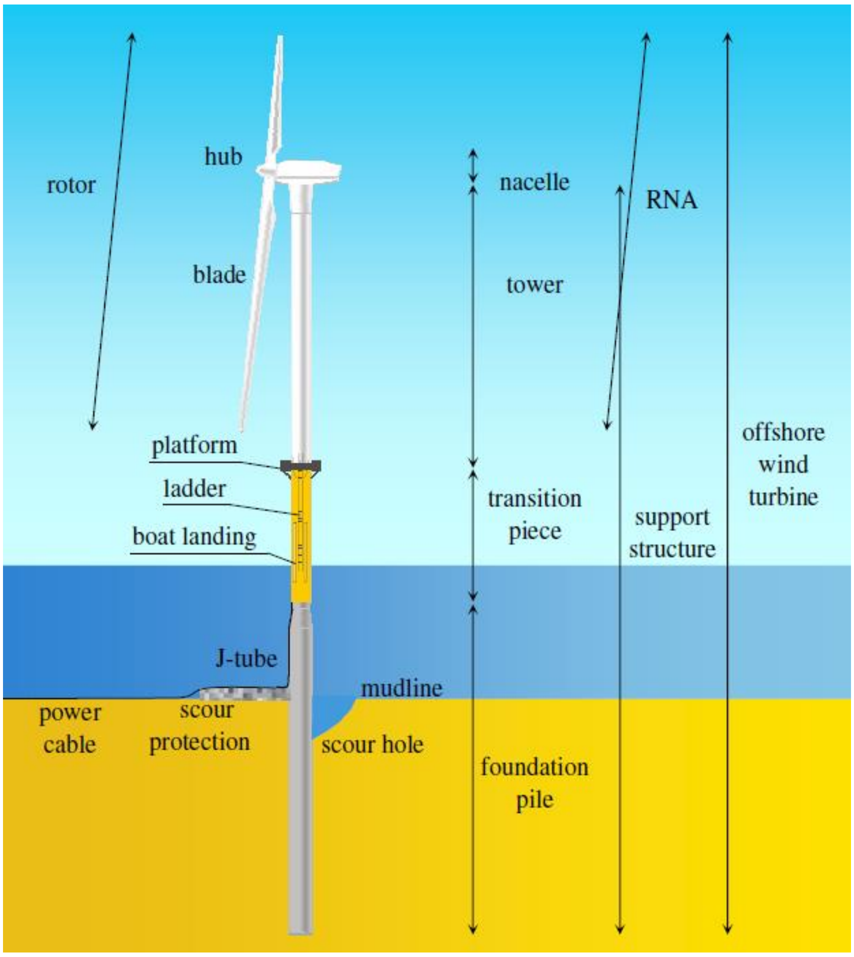

Figure 1.6: Overview of offshore wind turbine terminology

In figure 1.7 the clamps used to hold down the TP flange can be seen. For a more detailed view of the clamps, see Appendix A. The clamps are bolted onto the grillage, in this figure the grey I-beams. A torque wrench is used to apply the minimum required pretension in the bolts.

Figure 1.7: Clamps in place on grillage

In figure 1.8 two SHL employees can be seen placing a clamp. It's clear that in this case it's a difficult place to reach. The grey rectangles are anodes. These are a vital part of the corrosion protection and need to be at the bottom and outside of the TP.

Figure 1.8: SHL employees placing a clamp

Figure 1.9: Grillage on deck of heavy lift vessel

Figure 1.9 shows the grillage on deck. Four in a row as close as possible to the centreline of the ship to minimise forces due to ship motions. Grillages are build up out of I-beams. Their purpose is to spread the loads and direct them towards the strong points in the ship, namely the frames and bulkheads. Note there is not much space left on the deck. This should be taken into account when designing new method.

Figure 1.10 shows a side view of the TP standing on the grillage. Clearly the attachments can be seen on the outside of the TP.

Figure 1.10: Side view of TP on grillage

1.8 Alternative clamps

In this section a brief overview will be given of competitors methods of seafastening TP's.

As can be seen in the following figures, all seafastening is done on the lower edge of the TP. Mostly it involves a clamping device to press the lower flange onto the grillage.

Figure 1.11 shows small frames that are hinged on the grillage and placed over the flange. Then large bolts on either side are tightened to secure the TP. The frames are heavy and need to be handled with at least two men. Once it goes over its top dead centre, it is difficult to stop.

Figure 1.11: Alternative clamp 1

In figure 1.12 the primary guides are wedged into holders to restrain horizontal movement. Turnbuckles are used to restrain vertical and overturning movements. In this case 20 turnbuckles are used that require a lot of tightening, especially because tightening one may loosen another.

Figure 1.12: Alternative clamp 2

Figure 1.13 shows yet another form of grillage and a different clamp. This is slid over the flange. Two horizontal bolts force the clamp against the TP wall and two vertical bolts hold the flange down.

Figure 1.13: Alternative clamp 3

In figure 1.14 a method is shown that directly bolts the flange onto the supporting structure. This requires careful positioning and accurately fabricated bolt holes. In this particular case a sea state of up to 2.0 m significant wave height was limiting.

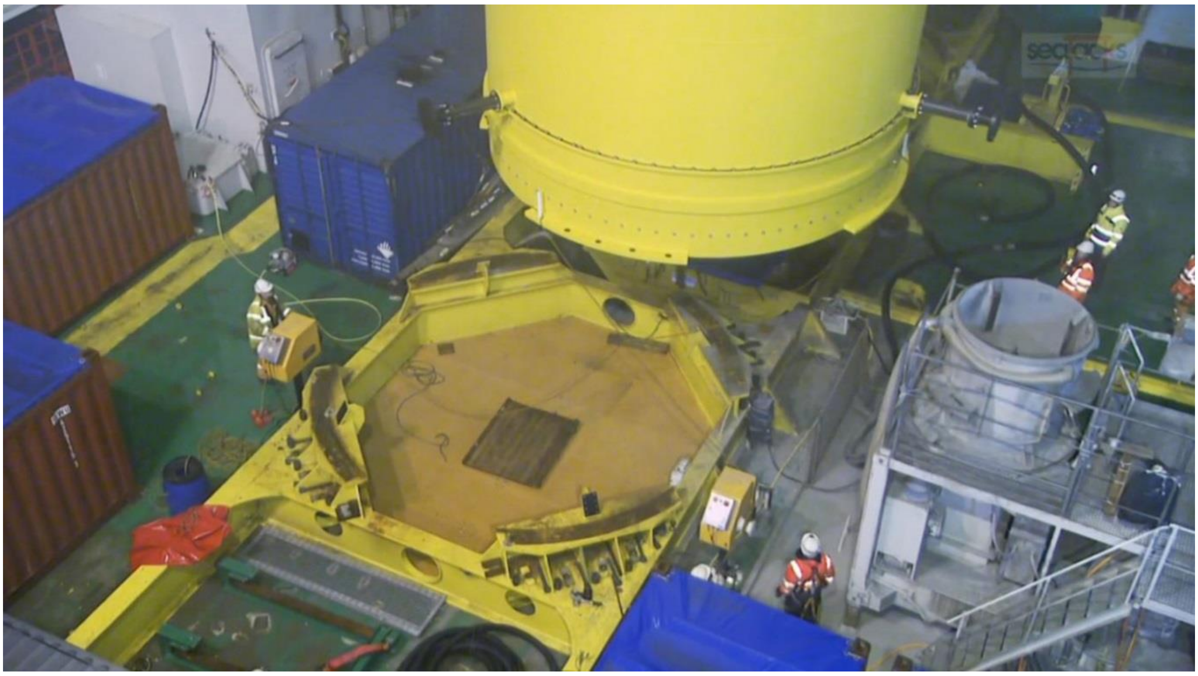

Figure 1.14: Alternative seafastening method

1.9. Transition Pieces

In this section four different TP's will be compared on important characteristics. SHL has been involved in these projects and so detailed information is readily available.

The four projects SHL has been involved in are Sheringham Shoal (2011), Meerwind (2013), Riffgat (2012) en Gwynt y Mor (2012 – 2013).

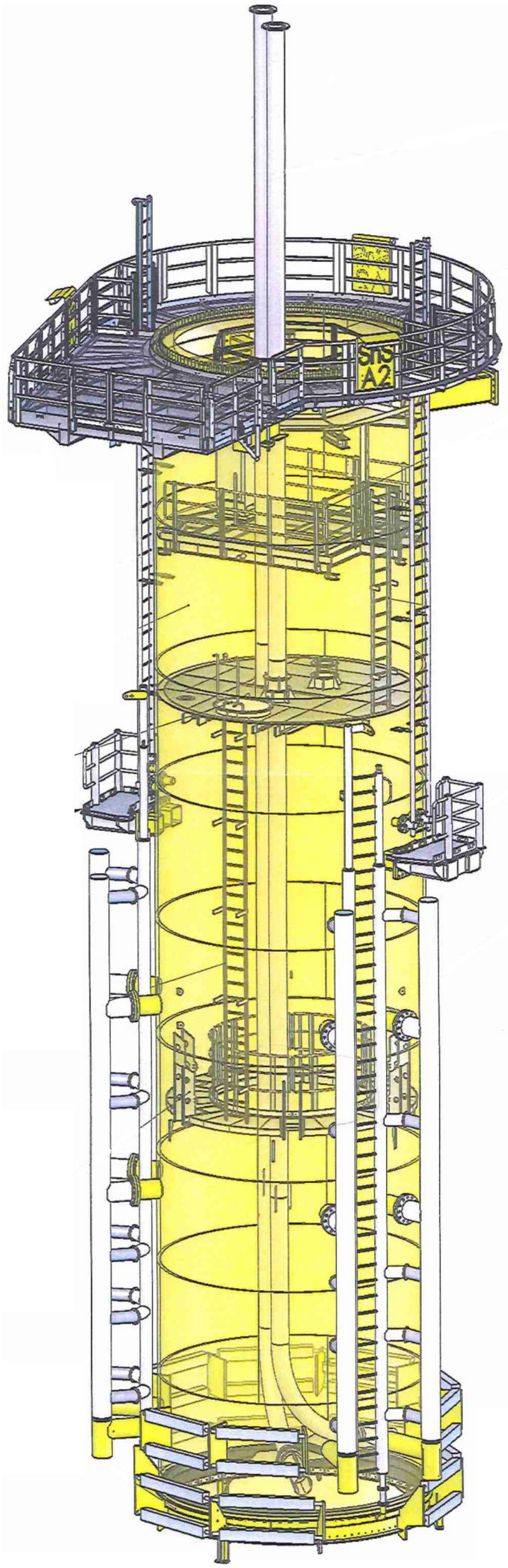

Sheringham Shoal TP particulars [4] :
Weight: 220 mT
Diameter: 5 m
Wall thickness: 30 ~70 mm
Height: 23 m
Height CoG: 11 m

Figure 1.15: Parametric view TP Sheringham Shoal [4]

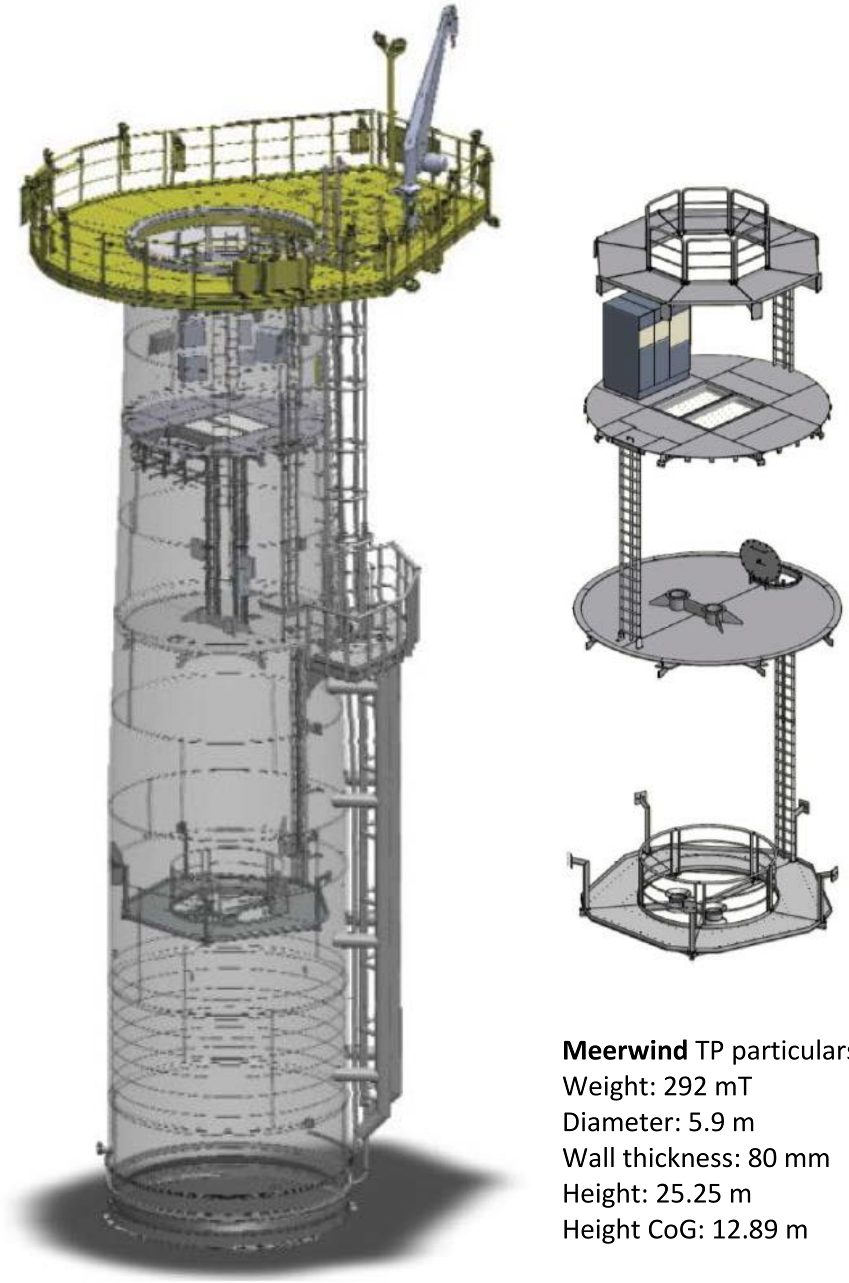

Meerwind TP particulars [5]:
Weight: 292 mT
Diameter: 5.9 m
Wall thickness: 80 mm
Height: 25.25 m
Height CoG: 12.89 m

Figure 1.16:Parametric view TP Meerwind [5]

Riffgat TP particulars [6]:
Weight: 290 mT
Diameter: 6 m
Wall thickness: 68 ~ 77 mm
Height: 26 m
Height CoG: 12 m

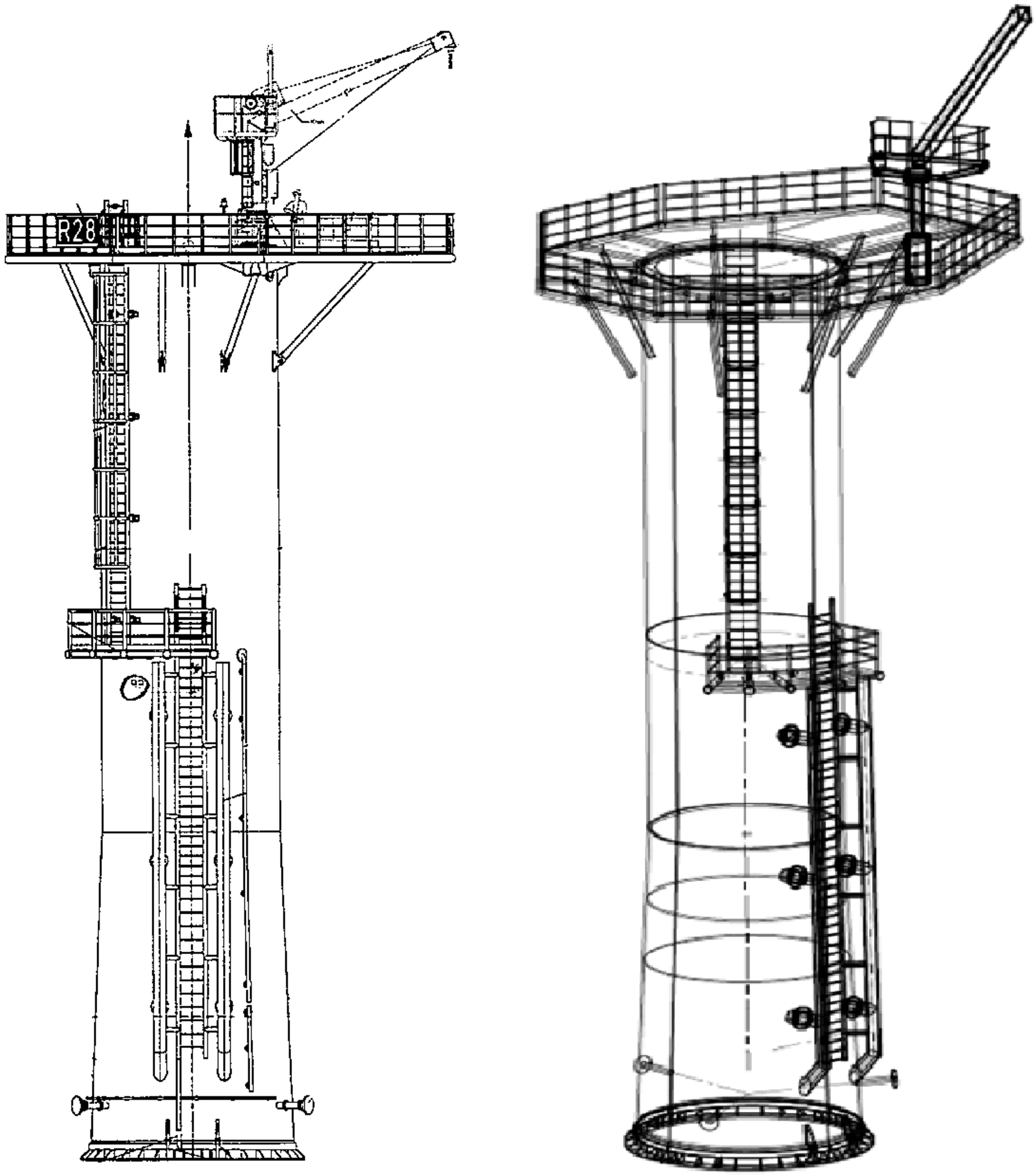

Figure 1.17 Side view and parametric view TP Riffgat [6]

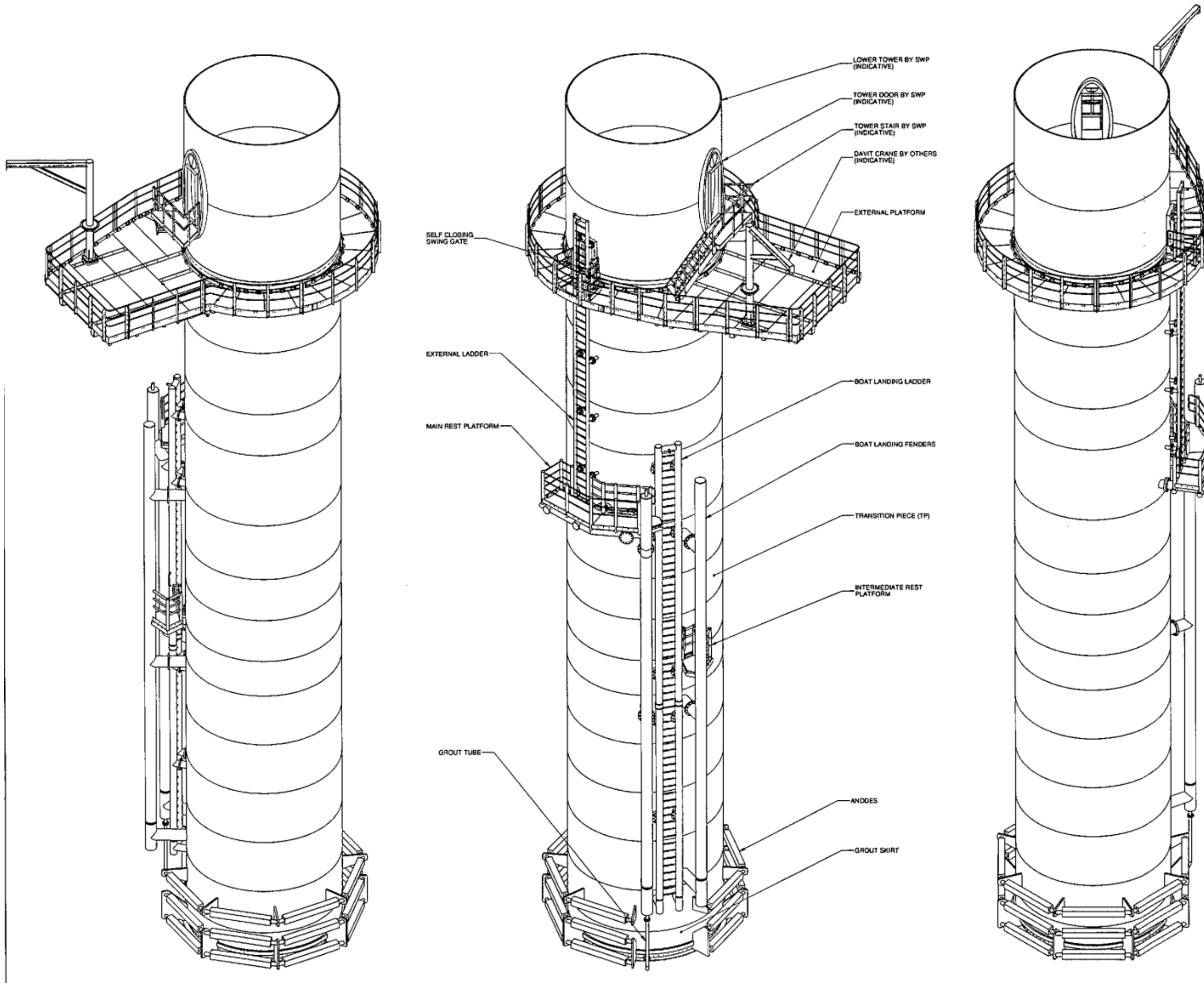

Figure 1.18: Parametric view TP Gwynt y Môr [7]

Gwynt y Môr TP particulars [7]:
Weight: 298 mT
Diameter: 5 m
Wall thickness: 55 ~ 85 mm
Height: 26.24 m
height CoG: 12.73 m

	Sheringham Shoal	MeerWind	Riffgat	Gwynt y Mor
Weight	220 mT	292 mT	290 mT	298 mT
Diameter	5 m	5.9 m	5.0 ~5.6 m	5 m
Wall thickness	30 ~ 70 mm	80 mm	68 ~77 mm	55 ~ 85 mm
Height	23 m	25.25 m	26 m	26.24 m
Height CoG	11.05 m	12.89 m	14 m	12.73 m
Height internal platform	7.51 m	8.50 m	6.70 m	8.82 m
J-tubes	Yes	No	No	No
Shear Keys	No	Yes	Yes	Yes
Inclination	No	No	Yes	No
Steel grade	S355	S355	S355	S355

Table 1: Transition Piece particulars[4][5][6][7]

Table 1 shows the characteristic TP features of the different projects SHL has been involved in. A seafastening method will be modeled on these characteristics. These projects are used because its detailed information is readily available. These projects are quite recent (2011; 2013; 2012; 2011), and, for now, are assumed to be representative for the industry. Future offshore wind projects might use bigger and or heavier TP's.

It can be concluded that the TP's are in general the same. An important difference is the use of J-tubes, as can be seen in figure 1.11. These tubes, meant to support the electric cables, run all the way through the TP (if internal) and come out at the bottom. These tubes will become obsolete in the future, and so this thesis will not take account of them.

Another important difference are the anodes on the lower outside part of the TP. All TP's have anodes, but the size differ. Sheringham Shoal (figure 1.15) and Gwynt y Môr (figure 1.18) use rather large, horizontal, rectangular anodes all around the TP. This is one of the reasons the current SHL method is somewhat troublesome, but would also make a new method difficult that operates in the same space. The anodes of MeerWind (figure 1.16) and Riffgat (figure 1.17) use only three much smaller anodes.

A third difference is the use of shear keys. These are small ribs welded onto the inner lower part of the TP to increase the sliding resistance between the grout and the steel and create compression diagonals so as to severely diminish settlement. Of the above projects only Sheringham Shoal didn't use these shear keys, but it is to be expected that in all future offshore wind farms they will be used.

1.10 Future Transition Pieces

Before finding a new method of seafastening, it is good to get an idea where the industry is going. In this case an indication can be gotten from the Tender Department. This department writes proposals for future projects, and thus has a view of what structures need to be installed and what they look like.

Looking back, from the start of offshore wind farms up until now, offshore wind turbine generators (WTG's) have steadily increased in size. What is true of the whole is in this case also true for each of its components, the foundation, the Transition Piece, the tower, the nacelle and the rotor diameter have all increased in size. From this trend it is expected that WTG's will keep increasing in size in the near future.

This expectation is further supported by observations by SHL's Tender Department. When SHL receives an Invitation To Tender (ITT), the client provides a document with specifications of the object which the client wants to be transported or installed.

These documents often describe the object as being between 12 m and 32 m high, weighing between 160 and 450 metric tonnes and having a diameter between 5 m and 7 m. It is difficult to engineer for this.

However, the experience of the people from the Tender Department indicates that the objects are often more towards the high end of this range than the low ends. A few years ago, the high end of the range was up to 26 meters height, 6 meters in diameter and 350 tonnes. Therefore it is expected that future TP will be bigger and heavier.

Unfortunately, no illustrations can be shown or projects named.

2 Concept solution

In this chapter several options to seafasten a TP are reviewed at a sketch level. After this the boundary conditions, as mentioned in section 1.5, are applied. Subsequently, a choice is made which option best suits the goals, given the boundary conditions.

2.1 Option 1: Wedge shaped clamps

Figure 2.1 shows a method similar to the current practice. In this case a wedge shaped clamp is hydraulically pushed towards the flange. When the clamps makes contact with the TP flange, the wedge is pushed upwards and the flange down. This is the force that keeps the flange and thus the TP fixed to the grillage. Because the clamp is pushed upwards it needs to be restrained vertically. This method has an important advantage in that it is faster. Because the TP is lifted into position and all the jacks can be simultaneously turned on, the TP is fixed immediately. Furthermore, the method abides by the boundary conditions, except for more effective/stronger. The current clamping method pushes the clamp all the way up to the TP wall to minimize the lever arm. This method maximizes the lever arm and thus maximizes the moment in the weld where the TP wall meets the TP flange. Experience with the Gwynt y Môr project has shown that this weld is a limiting factor and increasing the lever arm would further lower its limiting value.

This method could easily provide a better option than the current method, if the TP flange would be much stronger. Though this requires changing the TP, which is a good idea, but it proves difficult to get designers/manufactures to do so.

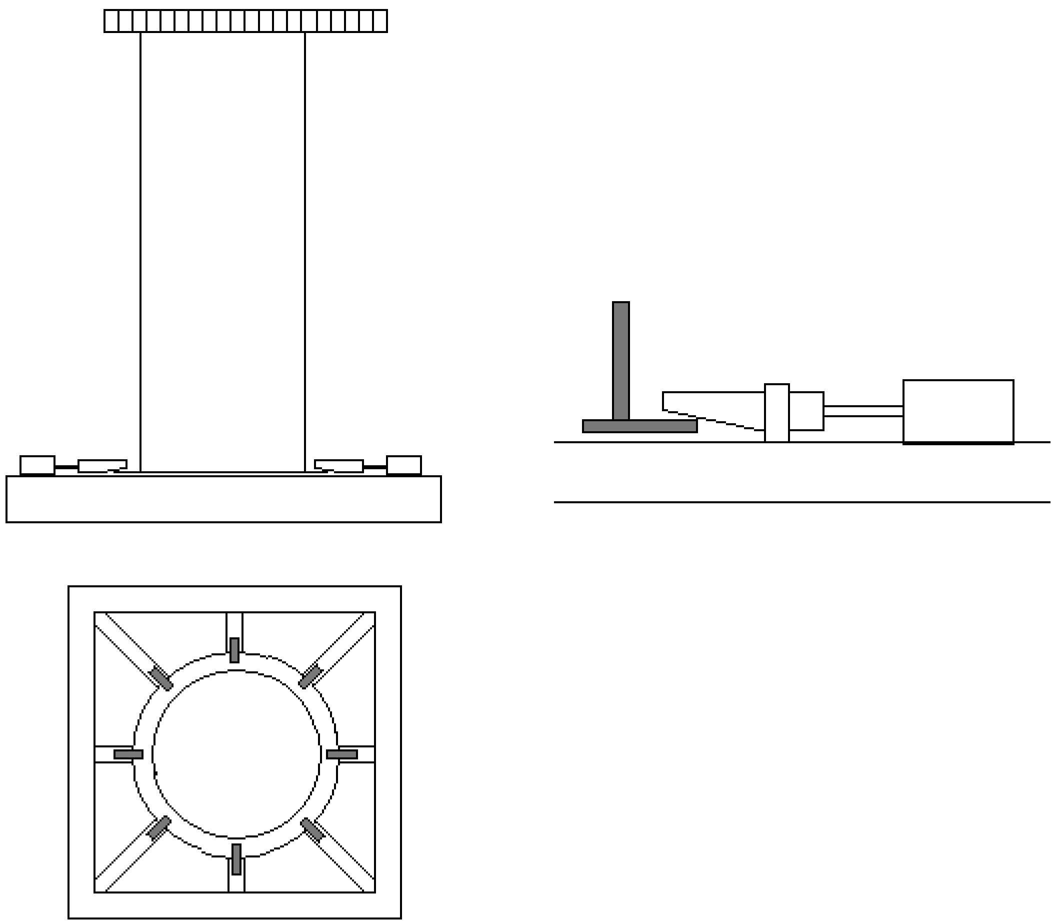

Figure 2.1: Horizontally jacked clamps

2.2 Option 2: Vertical jacks on the flange

Figure 2.2 shows a method to hold the flange down through the use of vertical jacks, either going through the flange or clamping its edge. If the jack goes through the flange, holes need to be drilled in the flange. This should not be a problem since the flange serves no purpose once the TP is in-situ and grouted to the monopile. Going through the flange has the advantage of lowering the lever arm but requires the extra work of drilling holes. Clamping at the edge maximizes the lever arm and is undesirable, because of before mentioned disadvantages. Furthermore, it is questionable if the flange is wide enough so it can still be clamped through a hole in its center and have enough width to accommodate the jack. Besides that, also the anodes could be in the way, either making it more difficult of even impossible to place the jacks.

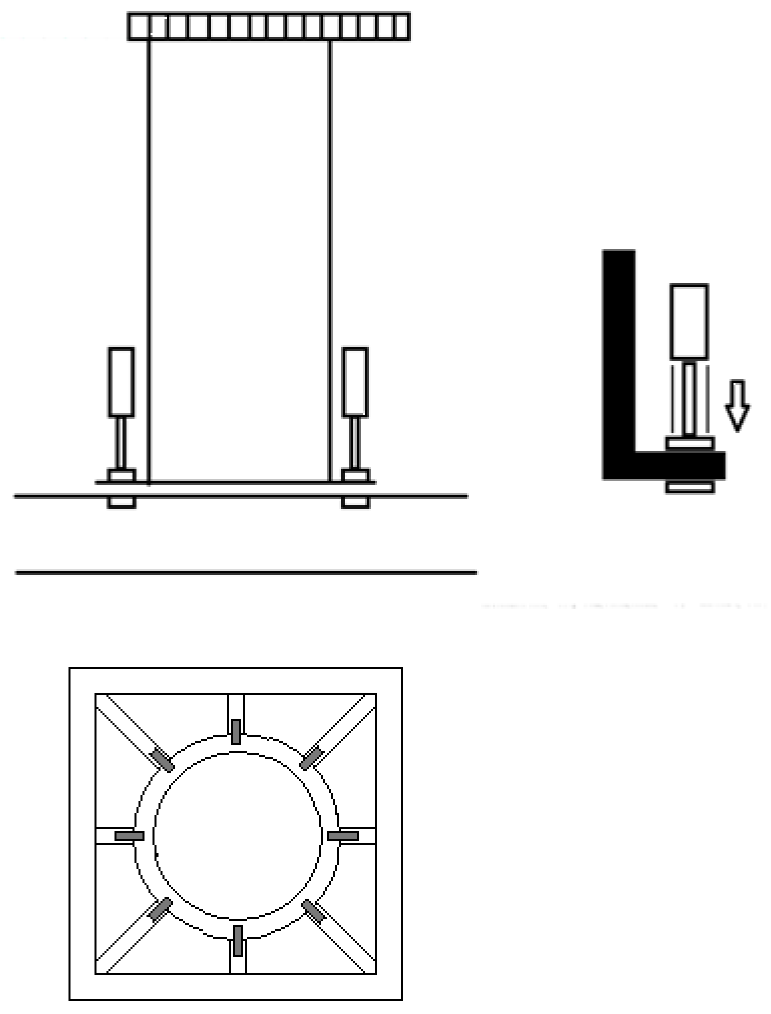

Figure 2.2: Vertically placed jacks clamping TP flange

2.3 Option 3: Rotating clamps on the flange

Figure 2.3 shows a method with rotating clamps, also holding down the TP lower flange. As the TP is lowered into place, the clamps rotate around the flange and then apply a downward force. This can be done as close as possible to the weld, so as to minimize the moment. All these clamps can be activated simultaneously and this is thus faster than the current method. Though only just as effective, because they clamp the force at the same location, near the weld. Furthermore, the anodes could also be in the way.

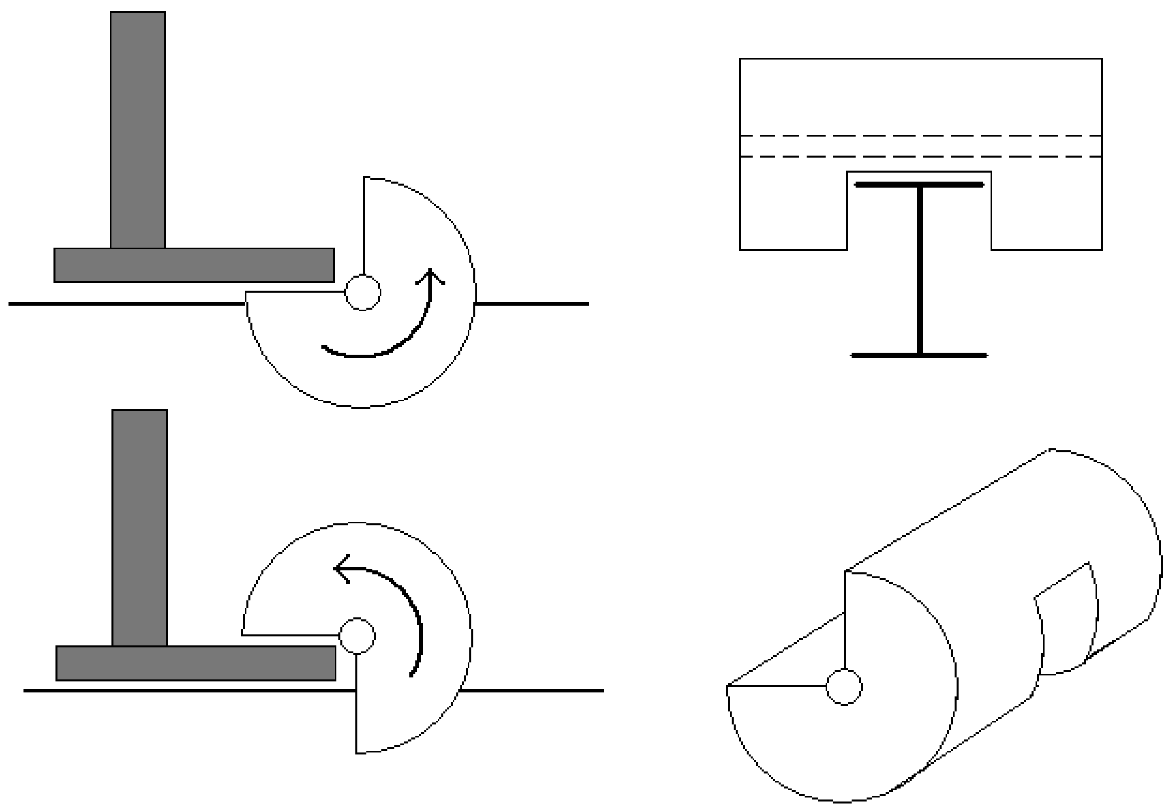

Figure 2.3: Rotating clamps

2.4 Option 4: Rotating wedges on the flange

Figure 2.4 shows rotating wedges. These have a round shape with a flat side. The underside is skewed, so when its turned, it will force the flange down. The flat side is there to enable the TP flange to be lowered passed the wedges onto the grillage. There need to be multiple of these wedges all around the TP. It has the advantage of being quick and easy. Because it takes up only little space there is no conflict with the anodes on the outside of the TP. The downside is that it forces the flange down on the outside. Just as option 1 it will maximize the lever arm and thus the moment in the weld. Prying forces due to repetitive loading could also loosen the wedges.

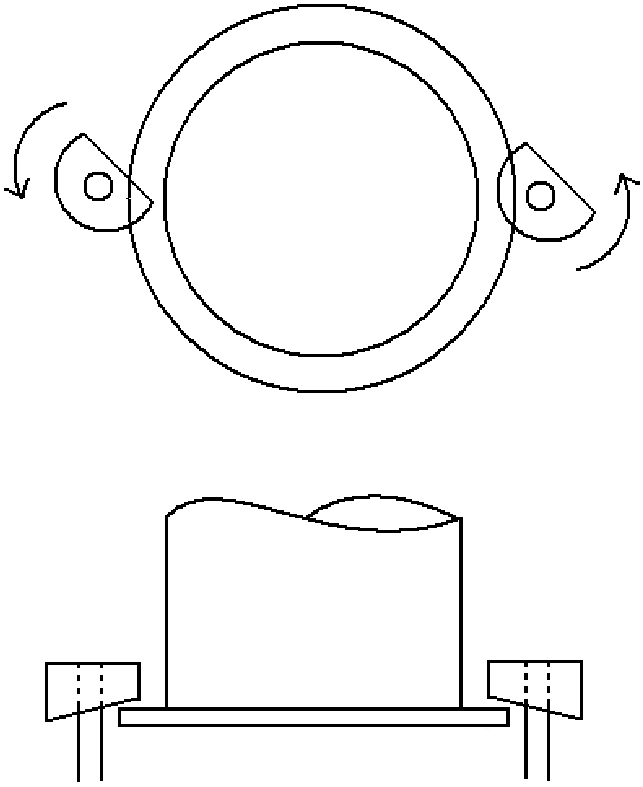

Figure 2.4: Rotating wedges

2.5 Option 5: External frames

Figure 2.5 shows a frame on the outside of the TP. Since forces in the lateral direction will be governing due to the roll motion of the ship, the frames are placed on the sides to take up these lateral forces. The frames can also take up forces in the longitudinal direction but these will be smaller and so the frame does not need to extend as much beyond the TP as in lateral direction. These frames can take up high forces, but also weigh more than manual labor could handle. So a crane is needed to put the frames in place. Also there is no easy way to attach the top of the frame to the TP other than welding. Furthermore, the footprint is increased significantly, that is, is takes up much more space on the deck, and this could conflict with other equipment and material placed on deck.

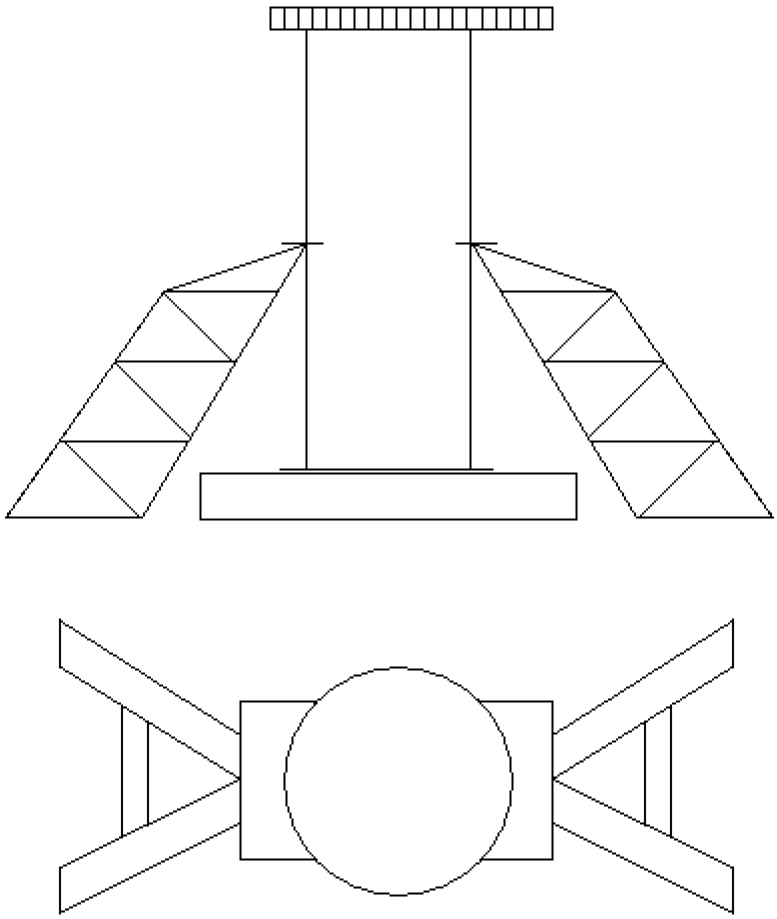

Figure 2.5: Frames on sides of TP

2.6 Option 6: Welded plates

Figure 2.6 shows a method that welds plates to the side of the TP and to the grillage. It is an easy method since it can always be made to fit. Though is it questionable if enough space is available on the grillage to weld plates on it that are strong enough to take up the lateral forces. If bigger plates are required, the footprint increases. Furthermore, there should be no welding to the TP.

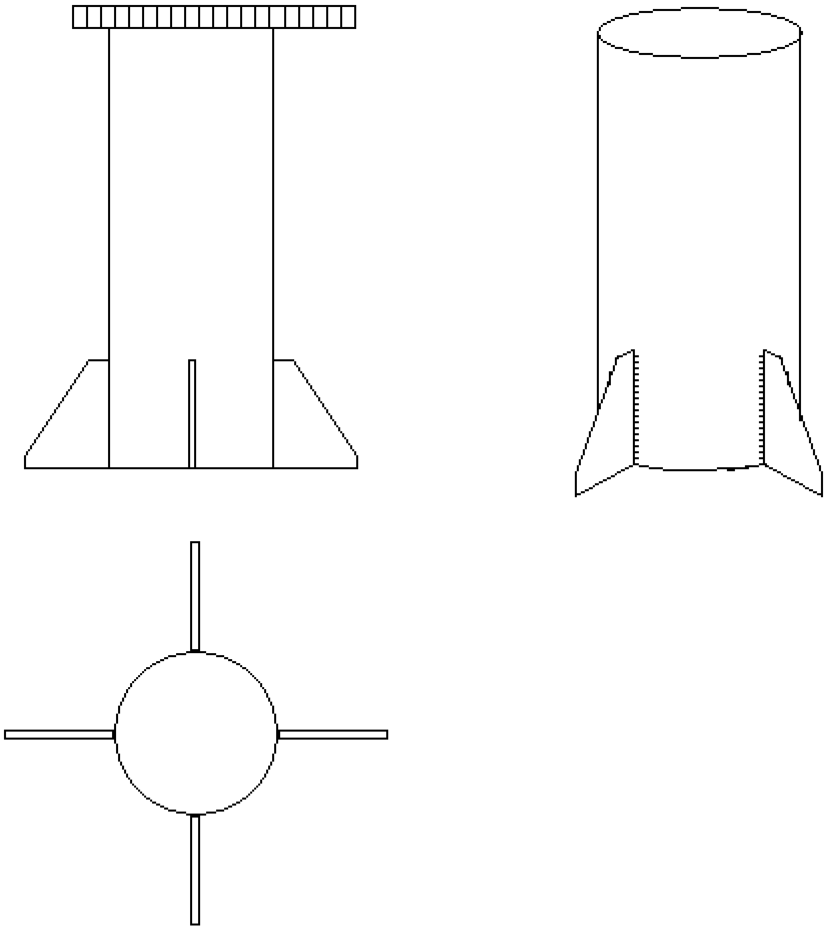

Figure 2.6: Plates welded to TP

2.7 Option 7: Integration in the ship structure

Figure 2.7 shows a method that integrates the seafastening in the ships structure trough “holes” in the deck. This is an interesting option for several reasons.

First, it lowers the objects center of gravity (CoG) relative to the ships center of gravity. Because of this smaller distance, the forces on the TP caused by accelerations due to ship motions are lower. Second, the TP is surrounded by a strong structure to which forces can be guided to. Third, when no TP’s are transported, the “holes” can be closed off with hatches, thus restoring the original deck space. Fourth, since the seafastening is integrated into the ships structure, there is no need to sail into harbor to pick up seafastening equipment such as grillages. This is especially beneficial since often last minute changes occur in the ships schedule.

There are also a few important downsides. First, these “holes” are going through the deck, frames and bulkheads. These are important for the ships structural integrity and stiffness and cannot easily be removed. Second, it’s the most costly method of all options considered here. Third, it’s no longer directly applicable to barges, which are also often used to transport TP’s.

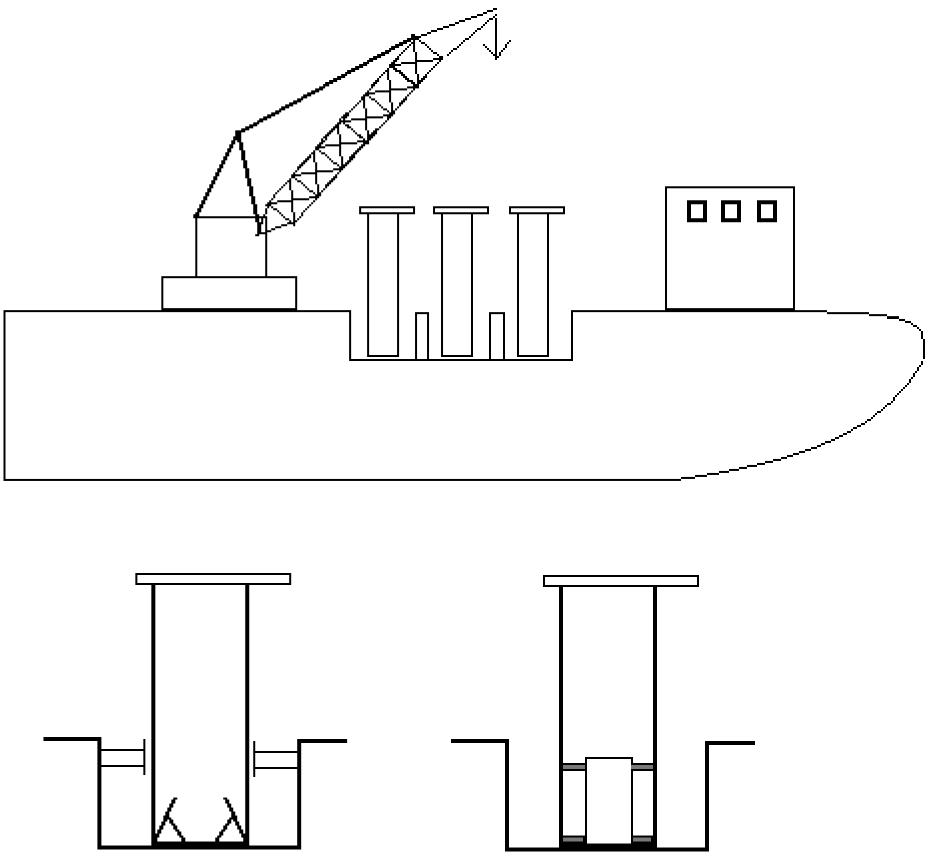

Figure 2.7: Integration seafastening in the ship

2.8 Option 8: Internal seafastening

Figure 2.8 shows a method that holds the TP fixed from the inside in a clamping manner. This is done by jacks placed around a tube that expand radially outwards. The tube itself is welded onto the grillage. This method has several advantages.

First, on the inside there is no coating that can be damaged. If small damages to the steel occur, like scratches or small dents, this poses no problem, since the lower part of the TP is grouted to the monopile and this remains unaffected by small discontinuities. Second, there are no attachments, like on the outside of the TP, except for the grout skirt at the bottom. It's the only part of "clean" steel on the TP. The outside of TP's differ for different projects, but since all of them are placed onto monopiles, the insides are all the same (except for diameter). Third, because it grips the object on its primary steel, a high force can be exerted. Primary steel is steel that is part of the load carrying structure of the object and thus often much stronger. Secondary steel, like the flange that serves no purpose of load carrying once in place, is much weaker.

A disadvantage is that it's difficult to vary in TP diameter. And since it uses jacks to exert a force, the steel is more stressed.

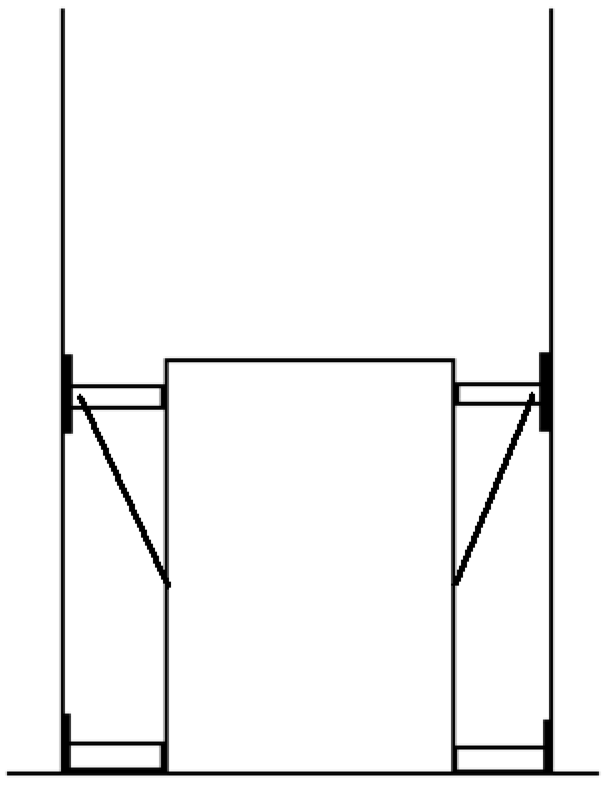

Figure 2.8:Tubular with jacks inside TP

2.9 Selection of the most promising conceptual solution

Below the several options shall be reviewed, the boundary conditions applied and judged which of these options is best suited to seafasten TP’s.

Boundary conditions are subject to economic considerations. Practically this means that if none of the suggested options abides by the boundary conditions, it must be weighed how important these conditions are and what the benefits of a new method would be. For example, if option 5 (frames on sides of TP) turned out to be extremely effective but does have the downside of increasing the footprint, it must be judged if the benefits outweigh the costs.

The first 4 options all are variations on one theme, namely fixating the TP via the lower flange. All are different than the current SHL method. All are faster but also suffer from the same defect that the flange is rather weak. They violate the boundary condition of being more effective.

Option 5 is more effective than the first 4, but increases the footprint significantly.

Option 6 uses welded plates to the TP.

Only option 7 and 8 violate no boundary condition. But there are differences. Integrating the seafastening in the ship is more costly and compromises the ships structural integrity. To maintain the ships strength and stiffness, a rather heavy structure must be built in. Option 8 is less devious while achieving the same result.

Overall option 8 is considered to be best. It abides by all the boundary condition and is also readily applicable on barges. In the next section this method will be further detailed and explained.

2.10 Further detailing chosen method

Now that the best conceptual option has been chosen, several other features need to be designed, e.g., the guides, method of force transfer, type of jacks, configuration of jacks, and how the groutskirt will be protected. Below the important aspects will be discussed, the difficulties explained and how the design will overcome these difficulties.

2.10.1 Groutskirt

An important issue to designing the seafastening is the groutskirt (figure 2.9). This seal is located at the bottom of the TP and narrows the diameter by 900 mm including the necessary clearance. This seal is also one of the reasons for the sliding guides. As can be seen in the two pictures below, in some cases the seal is pretty stiff (figure 2.9) and in other cases it's not stiff at all (figure 2.10). Although it is expected that in the near future the groutseal will likely disappear, they are still used today and thus the design will accommodate them.

Figure 2.9: Groutskirt or groutseal, a stiff rubber ring

Figure 2.10: Again the groutskirt, this time rather flexible

2.10.2 Guides

Guides are used to direct an object towards a specific desired location. Currently when the TP is lifted onto the grillage, guides on the grillage ensure that the TP is properly centered on its support structure. This is important for two reasons. First, it needs to be centered so the distance to the abutments on the grillage is the same all around (given a small margin), which in turn is important because the clamps used need to bridge that distance. Second, the forces on the seafastening are calculated for a specific location on the ship. Not centering the TP could result in higher forces and a different distribution of those forces, for which the seafastening may not be sufficient.

Also, guides mounted on the TP, extending below the lower flange, are used to orientate the TP on the grillage and when placing it on the monopile.

For the new method the guides would serve a third purpose, namely protecting the groutskirt. When the TP is lifted on the ship and placed over the seafastening tube, and on location it is lifted off again, the groutskirt, located at the bottom and inside of the TP, will “slide” past the tube, over the full length of the tube. This requires a very precise lifting operation. Wind and waves can make the TP sway. This risks the groutskirt colliding with the tube.

Needless to say the groutskirt may not be damaged. This means that enough clearance must be guaranteed between the tube and the TP and groutskirt.

Figure 2.11 and 2.12 show the guides used in two different projects. Welded onto the grillage, they center the TP when placed on deck.

Figure 2.11: Guides on grillage

Figure 2.12: Smaller guides on grillage

Alternatives for protecting the groutskirt are limited. One possibility would be to fixate the groutskirt as much as possible to the TP wall. This would increase the clearance and decrease the possibility of damaging the skirt. However, not all groutskirts are the same. Some are rather loose and can deform quite substantially, while others are firmer, inserted under much higher pretension and will not deform easily. SHL wants the method to be applicable to all TP’s (or as many as possible). Fixating the groutskirt against the TP wall does not constitute such a general solution.

From a jacks point of view, the distance between the seafastening tube and the TP is to be minimized, as to minimize the required stroke of the jack.

The above two requirements are opposite to each other. For the groutskirt it would be best to have a small seafastening tube and for the jacks it would be best to have a large seafastening tube. This results in a compromise such that the clearance on the groutskirt is minimized but guaranteed, and the space between the seafastening and the TP is as small as possible.

A way to achieve this is to use sliding guides, mounted on the top of the seafasteningtube, and will slide down with the TP to the bottom and “sink” into the interbeam space of the grillage. Once the TP is lifted up again, these guides will also slide up, always staying in contact with the TP. These guides guarantee that the groutskirts will not touch anything and remain undamaged, while at the same time also minimize the clearance necessary for the groutskirts. The guides need to be guiding the entire height of the seafastening, not just lower part, for sake of protecting the groutskirt, the TP and the seafastening itself. Guides currently used are not effective, since they can only direct the TP right above the grillage.

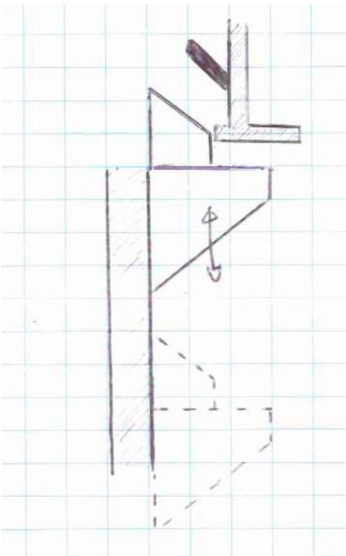

Figure 2.13: Sliding guide

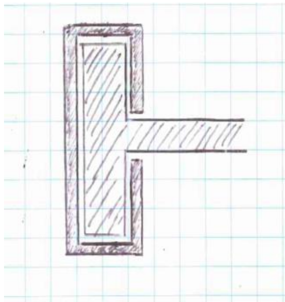

Figure 2.14: Casing sliding guide

Other alternatives: guides placed on TP would be effective in protecting the groutskirt, but difficult to remove quickly once on location. For example, TP standing on a ring, bolted to the flange. This ring has a smaller diameter than the groutskirt, thus ensuring that the groutskirt cannot be damaged by contacting the seafastening or jacks. This is a very effective and robust solution, but requires an extra operation offshore, namely to lift the TP off the seafastening and lowering it back again to deck height, so the ring can be removed. This is a very undesirable operation. It cannot be put down on the deck, because there is no grillage. It needs to be suspended or hovering above the deck, where it’s left swaying while the crew removes the ring. This can be dangerous.

A second alternative would be guides on the outside of TP/tube, placed on the grillage. These are possible but should be (approx. 6 m) and would pose difficulties because of attachments on the outside of the TP. This option is not considered to be sufficient.

The sliding guide is a steel structure, that slides trough a casing. The part that is in contact with the casing is covered with special sliding pads to lower resistance. Since guides starts at the top, then slides down with the TP, and when the TP is lifted up again, it needs to go up again, the system should be counterweighted so as to ensure that the guide itself is always forced up.

2.10.3 Jacks

Several options are available for making contact between the TP and seafasteningstructure: hydraulic jacks, pneumatic jacks and air bellows, to name a few. Air bellows would be very easy to use, cheap, low maintenance and have only one failure mechanism with a low probability. But they also have a low stiffness in the main direction and no stiffness in the transverse direction, so these would not suffice. Pneumatic jacks can deliver the required force but also have a low stiffness in axial direction. Only hydraulic jacks can deliver the required force and stiffness. The stiffness is important because only a high force in combination with a high stiffness (i.e., small displacements) ensures that the TP will remain at the required 90° angle compared to the ship's deck.

Two possibilities are considered for placing the jacks.

Option 1: Jacks placed at the top of the tube that extend radially outwards (horizontally), and make direct contact with the TP. This is the simplest way of fixating the TP. Although it may prove difficult to vary in diameter since the stroke of the jack is limited. Furthermore, since also forces have to be taken up that are not in the longitudinal direction of the jack but in transverse direction, a moment will occur on the piston of the jack. This is very undesirable, so a system needs to be in place to take up these forces. This could be done by a hinging arm, attached at the tube and at the end of the piston. This forms a triangle and thus prevents a moment occurring in the jack piston. A down side is that the jack-tube connection also needs to be hinging.

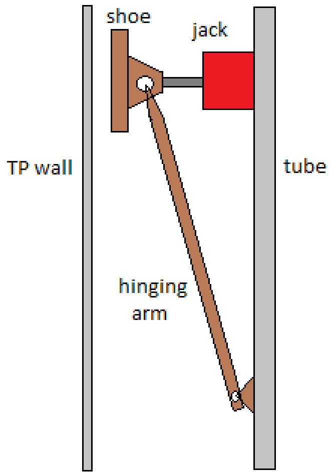

Figure 2.15: Hinging arm

Option 2: Jacks placed vertically and on the outside of the tube, extending towards the top of the tube. At the top of the tube are two wedges. The first is pushed upwards by the jack. The second is pushed outward by the first wedge until it makes contact with the TP wall. This option has several advantages compared to the first option. Foremost, no moment could occur on the piston. All forces that are in transverse direction of the jack are transferred trough the wedges toward the tube. The wedge will exert a reaction force downward, but that is in the longitudinal (strong) direction of the jack. Furthermore, if the wedge action is properly exploited, a smaller jack could be used to produce the required force. A smaller jack weighs less and would pose important advantages for the technical department concerned with maintenance.

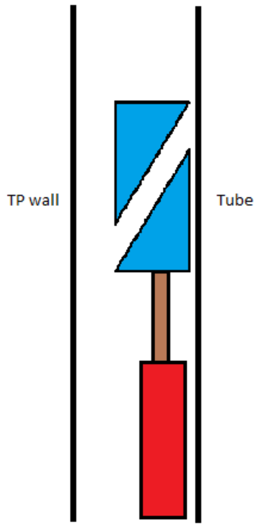

Figure 2.16: Vertical jacks

However, a significant disadvantage is that in this arrangement, if a jack would fail, it is very difficult to reach for repair, since it is in between two closely spaced tubes. Secondly, the distance that needs to be bridged by the wedge is approximately 500 mm. To do this with a wedge requires a very long wedge, especially if a wedge is used with a small angle.

Option 1 most efficiently bridges the distance to the TP. Also, the jacks are easily reached if repair during operations is needed. Therefore, option 1 is chosen as the most suitable fixating system.

2.10.4 J-tubes

J-tubes are large tubes inside the TP to accommodate the electrical cables. In the past not all TP's had internal J-tubes. Some are placed on the outside and some TP's don't have them at all or they are installed after the placing of the TP on the monopile. Of the four TP-installation projects SHL has been involved in, only one had J-tubes. The horizontal part of the J-tube had a length of about 3.5 meter. This means it will not fit inside the seafastening structure. Since the seafastening does no longer need to accommodate the J-tube inside, it also doesn't have to be an open tube. It can be closed to make it significantly stronger and more stable. In collaboration with the Tender Department at SHL, it became clear that in the future no more J-tubes are expected.

If internal J-tubes were to occur in future projects, a much simpler solution exist, namely to temporarily move the J-tubes upward inside the TP, so that they are above the seafastening structure. This is not only easier for transportation using this system, but also for installation on the monopile.

2.10.5 Variable diameter.

One of the wishes expressed by SHL is to make the seafastening applicable to as wide a range of TP diameters as possible. This could be done by using specific long stroke jacks, where standard models can have a stroke up to 1219mm. This would be sufficient for TP's varying in diameter from 5 m to 6 m.

Alternatively, smaller jacks could be used that would suit a specific diameter of TP. If a larger diameter TP would need to be seafastened, the jacks would have to be relocated manually to a more outward position. This is a preferable option since it is much lighter and less expensive.

2.10.6 Cylinder configuration

In the preliminary design a symmetrical configuration was used of eight jacks with equal spacing, see figure 2.17. Using this configuration, calculations have shown the TP will remain its structural integrity and its round shape.

Using a different configuration than the simple, symmetrical, eight jack system, e.g., more jacks in roll direction, cannot be done with the long stroke jacks proposed in 2.10.5. Figure 2.17 shows this configuration. Available spaced is mostly used up. Smaller jacks could form a different configuration, but this would be at the expense of the variable diameter.

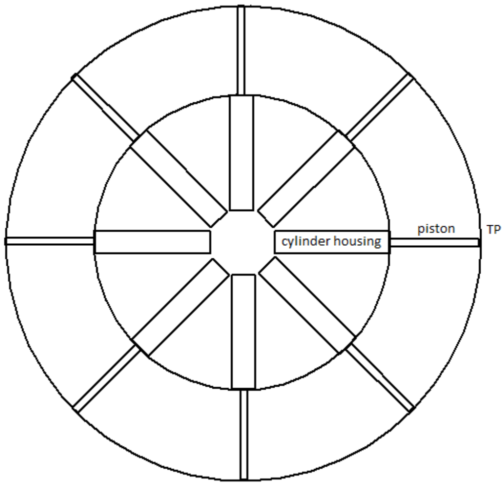

Figure 2.17: Symmetrical jack configuration

2.10.7 Shear keys

Shear keys are little ridges, often around 30 mm thick and 50 mm high, welded to the inside of the TP and outside of the top of the monopile. They are there to create compression diagonals in the grout, to prevent the two structures sliding past each other. Often the exact location of these shear keys is not known. Yet, they must be accommodated for. The distance between these shear keys can be up to 500 mm, but also as little as 250 mm. Therefore it is possible that the jack would make contact with the TP by pressing on the shear keys. This could produce high stresses in the shear key, because of the relative small contact area. If the contact area is enlarged, the stresses will reduce to an acceptable level. To this end special pads on the piston's end can be used, of alternatively, ensure to make contact with the TP wall in between of above the shear keys.

2.10.8 Pads

Pads are used to introduce the forces into the structure over a wider area to reduce the concentration of the load. Also, these pads are used to adjust to the different TP radii. The size and shape of the pads follow from necessary improvements of occurring stresses in the TP. A wide shaped pad would cause less bending of the TP wall and more hoop stresses, which are more efficient in transferring loads. Therefore it would make sense to use large, ring like, pads. However, there is a trade-off. Since the pads cannot retract into the cylinder housing, they will stick out. So more clearance needs to be reserved for this. This reduces the maximum stroke of the cylinders and thus reduces the range of different TP diameters that can be seafastened with one tool configuration, i.e., without changing the jacks. So, large pads are beneficial for the stress distribution but reduce the variable diameters. From this, it follows that the pads are to designed only as big as absolutely necessary.

For the lower jacks, much less clearance is required, because the groutskirt need not pass these jacks. Thus pads can be used without difficulties and with great benefits, namely reducing the distance between the application of the loads and increasing the area of load application if necessary.

2.10.9 Conclusion

The concept proposed to overcome the difficulties mentioned earlier comprises of a steel tube at the inside of the TP, see figure 2.18, much like the monopile on which it stands once in place. This steel tube is welded onto the grillage, which is welded onto the deck of the ship, to make it a solid structure to take up loads. The TP is lifted, placed over the tube and then lowered. It stands directly on the grillage, which take up the vertical downward loads.

At the top and bottom of the tube hydraulic jacks are placed. They expand radially outwards from the tube towards the TP to make contact with the TP and apply a force. Through this contact horizontal forces can be transferred from the TP to the tube and ultimately to the ship.

Since both at the top and bottom of the TP contact is made through the jacks, also any moment occurring can be resisted.

Vertical uplifting and overturning forces are transferred to the tube via special hinging arms which are attached to the jacks (figure 2.15). If the arm were left out, a moment could occur in the piston rod of the jack, resulting in stresses in the O-ring and ultimately causing leaking and failure of the jack.

Several jacks are placed around the tube, to take up forces from all directions and make sure the TP maintains its round shape. Needless to say this is a crucial part of the solution, or else the TP could not fulfill its function once in place.

The jack pushes the hinging arm towards the TP. At the end of this arm a hinging pad is placed. It's hinging so that it will rotate to align with the TP surface (some TP's have a vertical wall and some have a slightly inclined wall). Horizontal forces are transferred as normal forces. Vertical uplifting forces are transferred through friction between the TP surface and the surface of the jacking pad.

The lower jacks will use pads to spread the load. The upper jacks will also use pads, but their size needs to be determined from the required load spreading

Details could change as a result of the strength calculations.

Figure 2.19 shows the new seafastening method inside a TP

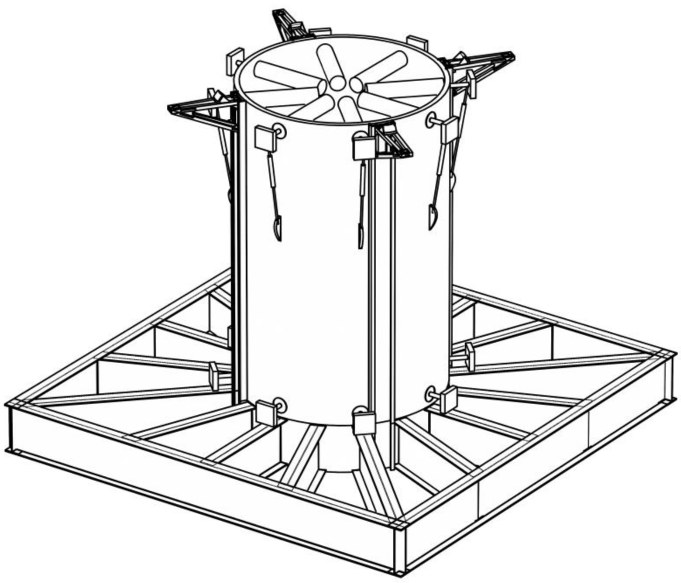

Figure 2.18: New seafastening method

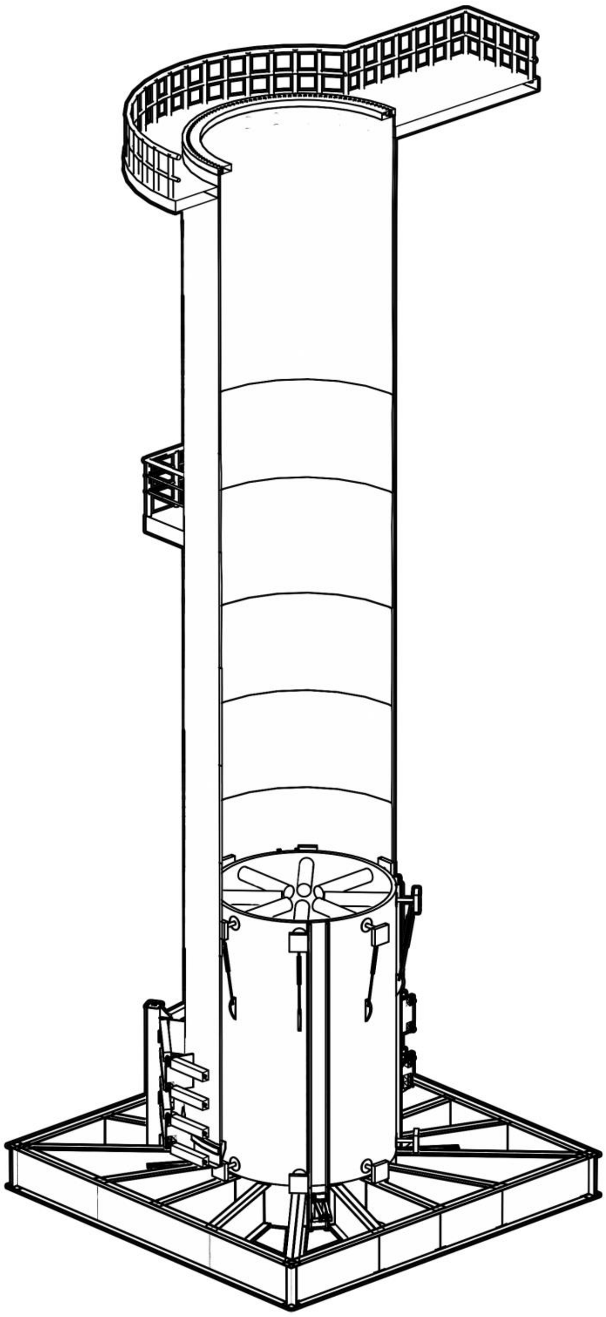

Figure 2.19: New seafastening method inside TP

3 Design loads transportation Transition Pieces

The forces on the seafastening result from accelerations of the ship. This section will first review the accelerations of previous installation projects that SHL has been involved in. Critical and limiting values will be determined and new design value presented. Sometimes the TP fabricator sets a maximum acceleration. This is because equipment and electronic measuring devices inside the TP could be damaged or may need recalibrating when subjected to higher accelerations. Other times the TP's structure is limiting. After this, a dynamical model calculates the forces resulting from those accelerations.

3.1.1 Accelerations

Four offshore TP installation projects have been executed by SHL:

Gwynt y Môr, located in the Irish Sea. For this particular project the lower flange, on which the clamps press down, turned out to be a limiting factor. The weld that connects the lower TP flange with the TP wall was set at a Unity Check of 1.0. From there SHL calculated backwards to find the maximum acceleration. It turned out that 3.57 m/s^2 was maximum in lateral direction (y-direction). The fabricator imposed no limits on acceleration.

Sheringham Shoal, located in the Greater Wash, off the east coast of England. The fabricator has set a limit of 0.5g acceleration in horizontal direction. SHL has calculated that a particular seastate of Hs=5 m will result in a maximum horizontal acceleration of 4.028 m/s^2. With the values of Table 2, this results in a Unity Check of the lower flange weld of 0.99. So in this case the weld is also limiting.

Meerwind, located in the German Bight, off the north-west coast of Germany. According to Vuyk Engineering, the TP is capable of withstanding 3.32 m/s^2 acceleration in y-direction. The accelerations from the extended motion analysis (table 2) are close to the limiting values imposed by the designer (table 3), but the weld was calculated only having U.C. = 0.65.

Riffgat, located a few miles above the Wadden Islands, on the border of Dutch and German territory. For this project the contract limits accelerations to 0.3g longitudinal, 1.0g lateral, 0.5g vertical (relative to g). This is a very sheltered area in shallow waters, so the extended motion analysis resulted in rather low acceleration, nowhere near the limiting values.

Table 2 shows an overview of the Extended Motion Analysis (EMA) accelerations for projects done by SHL. This means that a calculation was done to acquire the maximum acceleration the TP would be subjected to, if the HLV sailed at a particular draft, in a specific region, during a certain time of the year (summer season). The first two projects were limited by the flange weld. This means lower workability. The last two projects the EMA stayed within the fabricator imposed boundaries.

m/s^2	Gwynt y Môr	Sheringham Shoal	Meerwind	Riffgat
x-acceleration m/s^2	0.612	0.605	0.921	0.847
y-acceleration m/s^2	3.57	4.028	3.294	1.311
z-acceleration m/s^2	11.269	11.100	11.275	11.198
Limiting factor	*Flange weld*	*Flange weld*	*Fabricator*	*Fabricator*

Table 2: Extended Motion Analysis accelerations TP is subjected to[4][5][6][7]

Table 3 shows the limiting accelerations, if any, set by the fabricator/designer.

m/s^2	Gwynt y Môr	Sheringham Shoal	Meerwind	Riffgat
x-acceleration m/s^2	none	4.9	1.699	2.94
y-acceleration m/s^2	none	4.9	3.32	9.81
z-acceleration m/s^2	none	14.71	12.006	14.71

Table 3: Fabricator limited accelerations.[4][5][6][7]

The goal of this chapter is to decide upon a reasonable acceleration as basis for designing the new method of seafastening. The reason that it must be decided, is because one method should be applicable to all projects. Furthermore, it is expected that in the future Offshore Wind Parks (OWP) will be located further offshore, where sea conditions are harsher and the wind turbines may be bigger and thus heavier.

SHL has calculated a worst case scenario (figure 3.1), for both heavy lift vessels, the Stanislav Yudin (SY) and the Oleg Strashnov (OS) to transport a TP on the worst location of the ship, in the highest North Sea wave that is close to the natural frequency of the ship. This produces the highest accelerations the TP could possible experience in the North Sea. This is done via monthly wave scatter diagrams from 10 years of time series of wave parameters with 1 hour interval. This data set notes all the occurring wave (Hs) and wave frequency (Tp) combinations.

Table 4 and 5 show these accelerations. Comparing with table 2, all values are higher, so every project done by SHL would fall safely within these design values. The accelerations are calculated for the CoG of the TP.

	acc. worst case
x-acceleration	1.138 m/s^2
y-acceleration	4.623 m/s^2
z-acceleration	12.681 m/s^2

Table 4: Accelerations worst case scenario OS

	acc. worst case
x-acceleration	1.163 m/s^2
y-acceleration	6.476 m/s^2
z-acceleration	13.491 m/s^2

Table 5: Accelerations worst case scenario SY

The accelerations for the Stanislav Yudin are higher and will cause more severe loading on the seafastening. Forces will be calculated using the values from figure 3.2

Motions Oleg Strashnov at 13.45 m draft in Hs 7.5 m

Centre of Gravity vessel:

LCG = 72.498 m
TCG = 0.000 m
VCG = 12.130 m

Centre of Gravity Worst TP Location:

LCG = 102.000 m
TCG = -19.100 m
VCG = 32.430 m

Accelerations of Worst TP Location:

Without wavespreading

	X-acc	Y-acc	Z-acc	Roll-acc	Pitch-acc	Roll-angle	Pitch-angle
case 1	**2.077**	3.650	12.204	2.749	2.557	9.671	6.308
case 2	0.209	**5.974**	13.461	4.357	0.252	16.664	0.366
case 3	0.232	5.415	**13.723**	4.016	0.277	13.210	0.402
	m/s^2	m/s^2	m/s^2	deg/s^2	deg/s^2	deg	deg

With wavespreading (COS^4)

	X-acc	Y-acc	Z-acc	Roll-acc	Pitch-acc	Roll-angle	Pitch-angle
case 1	**1.777**	2.273	11.697	1.737	2.200	6.190	6.012
case 2	1.138	**4.623**	12.681	3.502	1.518	13.803	3.912
case 3	1.230	4.038	**12.812**	3.123	1.725	10.659	4.259
	m/s^2	m/s^2	m/s^2	deg/s^2	deg/s^2	deg	deg

NOTE that accelerations already include Roll and Pitch angles

X is longitudinal, Y is transverse, Z is vertical direction

Z-acc is including g. X-acc and Y-acc are including contribution of g due to roll and pitch angles

Bold indicates the maximum value for the degree of freedom, Normal font means associated values for the other degrees of freedom assuming the same heading and T_p

Coordinates of assumed CoG of Worst TP Location: X = 102.000 m fwd of aft perpendicular, Y = 19.100 m PS of CL, Z = 32.430 m above top of keelplate

Wave spectrum:

JONSWAP with gamma calculated for each wave height/period combination

Wave scatter diagram:

The calculations are based on the Deutsche Bucht, ALL YEAR wave scatter diagram

Other properties:

Hmax/Hs ratio = 1.86

Significant wave height = 7.50 m

Due to the maximum significant wave height at the natural Roll period the RAO's are based on a significant wave height of 7.50 m

Figure 3.1: Accelerations worst case scenario Oleg Strashnov

Motions Stanislav Yudin at 8.05 m draft in Hs 7.5 m

Centre of Gravity vessel:

LCG = 77.994 m
TCG = 0.000 m
VCG = 8.120 m

Centre of Gravity Worst TP Location:

LCG = 38.000 m
TCG = -13.000 m
VCG = 27.230 m

Accelerations of Worst TP Location:

Without wavespreading

	X-acc	Y-acc	Z-acc	Roll-acc	Pitch-acc	Roll-angle	Pitch-angle
case 1	**1.724**	3.653	12.087	4.774	2.407	13.111	5.601
case 2	0.176	**10.720**	15.199	12.123	0.248	28.321	0.332
case 3	0.176	10.720	**15.199**	12.123	0.248	28.321	0.332
	m/s²	m/s²	m/s²	deg/s²	deg/s²	deg	deg

With wavespreading (COS^4)

	X-acc	Y-acc	Z-acc	Roll-acc	Pitch-acc	Roll-angle	Pitch-angle
case 1	**1.403**	1.970	11.874	2.155	1.693	5.662	4.987
case 2	1.163	**6.476**	13.491	7.347	1.740	18.230	3.745
case 3	1.116	6.474	**13.554**	7.397	1.722	17.658	3.555
	m/s²	m/s²	m/s²	deg/s²	deg/s²	deg	deg

NOTE that accelerations already include Roll and Pitch angles

X is longitudinal, Y is transverse, Z is vertical direction

Z-acc is including g. X-acc and Y-acc are including contribution of g due to roll and pitch angles

Bold indicates the maximum value for the degree of freedom, Normal font means associated values for the other degrees of freedom assuming the same heading and T_p

Coordinates of assumed CoG of Worst TP Location: X = 38.000 m fwd of aft perpendicular, Y = 13.000 m PS of CL, Z = 27.230 m above top of keelplate

Wave spectrum:

JONSWAP with gamma calculated for each wave height/period combination

Wave scatter diagram:

The calculations are based on the Deutsche Bucht, ALL YEAR wave scatter diagram

Other properties:

Hmax/Hs ratio = 1.86

Significant wave height = 7.50 m

Due to the maximum significant wave height at the natural Roll period the RAO's are based on a significant wave height of 6.00 m

Figure 3.2 Accelerations worst case scenario Stanislav Yudin

Above accelerations result from complex calculations done by the Naval Department. In this, ship specific properties are used, as well as the heading of the ship relative to the waves and the fact that waves tend to come from all directions instead of just one.

As a model, the figures 3.3 and 3.4 can be used to get an idea of these motions. Displayed in the figures are the rotational acceleration and velocity of a ship. When the roll angle is maximum, the velocity is zero and the acceleration is also maximum.

When calculating the forces required to seafasten objects on the ship, it suffices to view only the case with the maximum roll angle.

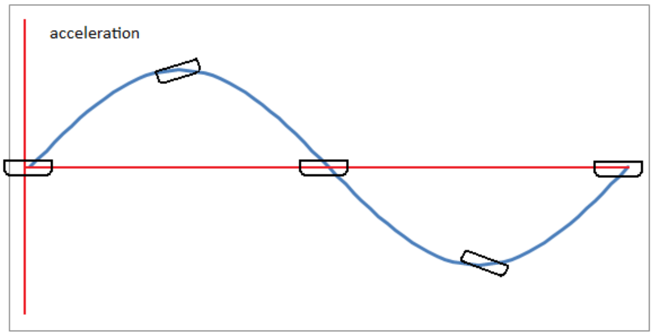

Figure 3.3: Acceleration and roll angle

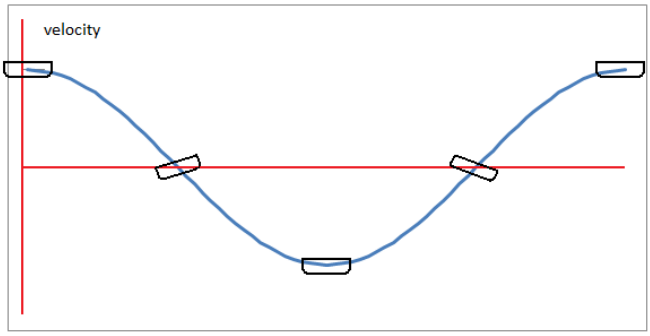

Figure 3.4: Angular velocity and roll angle

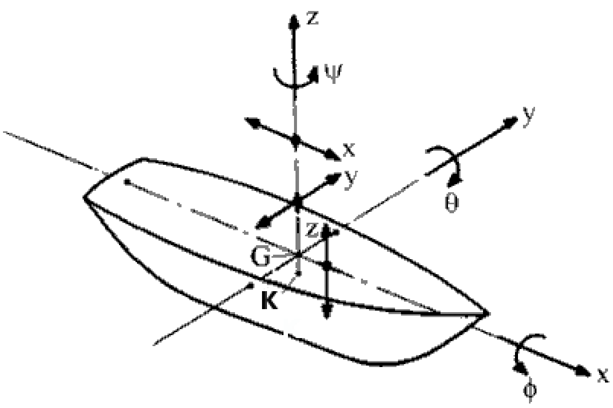

Figure 3.5: Axis and angles of rotation of the ship

Figure 3.5 shows the ships axis which are used in calculating the forces.

3.1.2 Wind loading

Wind loading is generally neglected by SHL for seafastening calculations. Experience has shown it to have a small contribution to the load compared to the forces induced by ship motions.

According to the DNV [20], the wind force acting on an object is:

$$F_w = \frac{1}{2} \cdot \rho_w \cdot v_w^2 \cdot A \cdot C_{ds}$$

In which

ρ_w is the density of air, 1.2 kg/m^3

v_w^2 is the airspeed. An airspeed of 25 m/s^2 corresponds with a significant wave height of 7.5 m.

A is the projected area of the object perpendicular to the wind direction. For TP's about 132 m^2.

C_{ds} is a shape coefficient. For cylinders with finite length, this is taken to be 1.0

From this, a total wind force of 49.5 kN acts on the center of the area of the TP. In the next section the forces acting on the TP from accelerations due to ship motions are calculated. These will prove to be much higher. The wind loading contributes only 2%, and therefore will also be neglected in this thesis.

3.2 Dynamical model

The forces for which the seafastening is calculated depends in part on the dynamical model that is used. The stick model below is the current method of SHL for calculating the clamp forces. All forces acting on the TP are translated to a moment acting around the base. Then the clamps and grillage provide a couple to resist this moment.

Below two models are described, differing in their rotational center (RC). The first is the conventional method used by SHL. The second is a more appropriate model for the new seafastening.

Model 1, rotational centre at base of TP; accelerations case 2 governing in roll-direction; case 1 governing in pitch-direction;

Accelerations case 2

x-acc = 1.163 m/s^2
y-acc = 6.476 m/s^2
z-acc = 13.491 m/s^2
xx-acc = 7.347 deg/s^2
yy-acc = 1.740 deg/s^2

Accelerations case 1

x-acc = 1.403 m/s^2
y-acc = 1.970 m/s^2
z-acc = 11.874 m/s^2
xx-acc = 2.155 deg/s^2
yy-acc = 1.693 deg/s^2

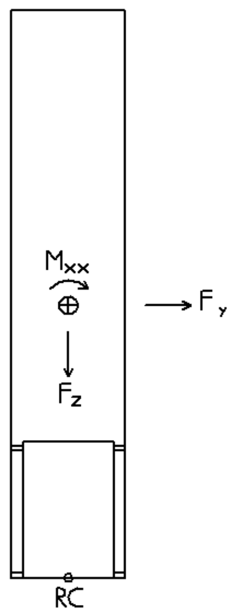

Figure 3.6: Rotational centre at base of TP

Gwynt y Môr TP:

m = mass = 307 mT
R = radius = 2.50 m
L = length = 26.24
Hcog = Height center of gravity = 12.73+0.5=13.23 m
Xcog= 0.19m.
Ycog=0.039m.
Hj = height hydraulic cylinders = 6 m

The height of the CoG is a calculated height from the fabricators models with an added contingency value of 0.5 m.
Ixx is the moment of inertia of a hollow cylinder.

Roll-direction

$$Ixx = Iyy = \frac{m}{12} \cdot (6 \cdot R^2 + L^2) + m \cdot (\frac{h}{2} - h_{CoG})^2$$

$$Ixx = Iyy = \frac{307}{12} \cdot (6 \cdot 2.5^2 + 26.24^2) + 307 \cdot (\frac{26.24}{2} - 12.73)^2 = 18689\ mTm^2$$

$$F_y = m \cdot a_y = 307 \cdot 7.143 = 1988\ kN$$

$$F_{z+heave} = m \cdot a_z = 307 \cdot 13.491 = 4142\ kN$$

$F_{z-heave} = m \cdot (2g - a_{z)} = 307 \cdot (2 \cdot 9.81 - 13.491) = 1882\ kN$

$M_{xx} = I_{xx} \cdot a_{xx} \cdot \frac{\pi}{180} = 18621.16 \cdot 7.347 \cdot \frac{\pi}{180} = 2399\ kNm$

$M_{xxtotaal} = M_{xx} + F_y \cdot h_{cog} + F_z \cdot y_{cog} = 28866\ kNm$

$F_{Ry} = \frac{M_{xxtotaal}}{Hj} = \frac{28866}{6} = 4811\ kN$

Pitch-direction

$Ixx = Iyy = \frac{m}{12} \cdot (6 \cdot R^2 + L^2) + m \cdot (\frac{h}{2} - h_{CoG})$

$Ixx = Iyy = \frac{307}{12} \cdot (6 \cdot 2.5^2 + 26.24^2) + 307 \cdot (\frac{26.24}{2} - 12.73)^2 = 18689\ mTm^2$

$F_x = m \cdot a_x = 307 \cdot 1.403 = 431\ kN$

$F_{z+heave} = m \cdot a_z = 307 \cdot 11.874 = 3645\ kN$

$F_{z-heave} = m \cdot (2g - a_{z)} = 307 \cdot (2 \cdot 9.81 - 11.874) = 2378\ kN$

$M_{yy} = I_{yy} \cdot a_{yy} \cdot \frac{\pi}{180} = 18621.16 \cdot 1.693 \cdot \frac{\pi}{180} = 550\ kNm$

$M_{yytotaal} = M_{yy} + F_x \cdot h_{cog} + F_z \cdot x_{cog} = 6945\ kNm$

$F_{Rx} = \frac{M_{yytotaal}}{Hj} = \frac{6945}{6} = 1157\ kN$

In roll direction, the accelerations from case 2 are governing. This model is conservative because it assumes a rotation point around base centre. This will produce the highest force in the axial direction of the jacks. This model assumes only a force in the axial direction and is a resultant force that is required to resist the overturning moment. The resultant can be spread over the horizontal component of the several jacks.

Model 2, rotational centre on the edge of TP; accelerations case 2 governing in roll-direction; case 1 governing in pitch-direction;

This model is more realistic and provides more information regarding where the forces are going. It does make assumptions that need to be justified afterwards, e.g., the rotation point should be able to withstand the high concentrated force.

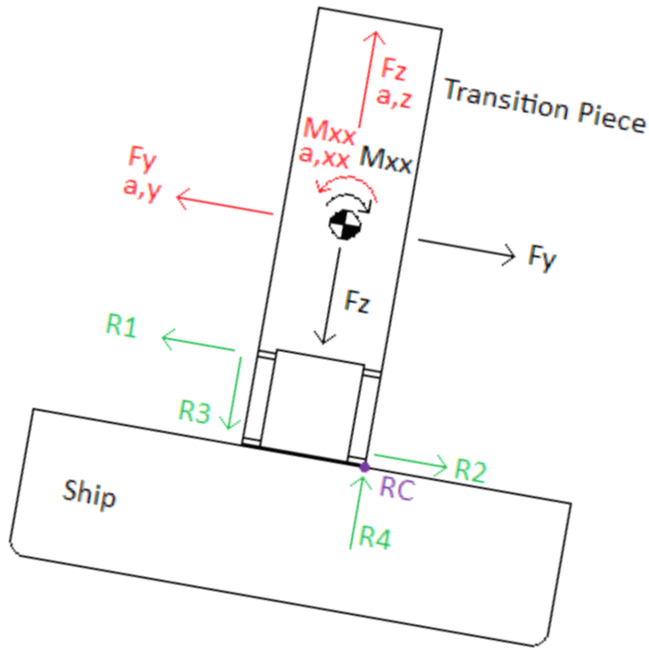

Figure 3.7: Rotational centre on edge of TP

The accelerations as given in figure 3.1 and 3.2 are calculated by the SHL Naval Department. These are accelerations that the TP needs to have at its centre of gravity to follow the motions of the ship such that it remains on its location on the deck. These are indicated in figure 3.7 by the red arrows. Accelerations multiplied by the mass will give the required forces. Those forces are to be supplied by the seafastening structure, indicated in figure 3.7 by the green arrows.

The maximum accelerations occur when the ship has reached its maximum roll angle and starts moving back towards the horizontal position. At this point the velocity of both the ship and TP are zero. The ship and the seafastening structure will need to apply a force to the TP to make it follow the ship motions.

To calculate the forces a rotational centre (RC) is assumed in the lower right corner of the TP, indicated in figure 3.7 in purple.

This is a dynamical situation, in which the green forces supply a resultant force that causes the accelerations (drawn in red). If, however, fictitious forces are drawn, equal in size and opposite in direction, the resultant force and thus acceleration is zero. The TP is in equilibrium and the equilibrium equations apply.

The values calculated from rotational centre 1 are used. It should be noted that, as mentioned in figure 3.1 and 3.2, that x- and y-accelerations already include contributions of g due to roll and pitch angles. This means that the forces act only parallel and perpendicular to the deck.

Accelerations case 2

x-acc = 1.163 m/s^2
y-acc = 6.476 m/s^2
z-acc = 13.491 m/s^2
xx-acc = 7.347 deg/s^2
yy-acc = 1.740 deg/s^2

Accelerations case 1

x-acc = 1.403 m/s^2
y-acc = 1.970 m/s^2
z-acc = 11.874 m/s^2
xx-acc = 2.155 deg/s^2
yy-acc = 1.693 deg/s^2

Gwynt y Môr TP:

m = mass = 307 mT
r = radius = 2.50 m
L = length = 26.24
Hcog = Height center of gravity = 12.73+0.5=13.23 m
Xcog= 0.19m.
Ycog=0.039m.
Hj = height hydraulic cylinders = 6 m

The height of the CoG is a calculated height from the fabricators models with an added contingency value of 0.5 m.
Ixx is the moment of inertia of a hollow cylinder.

Since R1 and R3 are coupled, i.e., they will always be at the same location, their force distribution follows from their stiffness relation. Because R1 represents the hydraulic cylinders loaded in axial direction, it will react less stiff than R3, which represents the steel rod diagonal, which is stiffer, and will therefore attract more force. Furthermore, since the width of the TP is 5 m and the height of the jacks is 6 m, the components of the displacement are unequal, i.e., for every 1.3 mm displacement perpendicular to the line connecting to RC, 1 mm is displaced in axial direction of the jacks and 5/6 mm is displaced in the vertical direction. Both these differences add up to a relation between R1 and R3 of 1 : 0.424. This means for every Newton that goes to the diagonal rod, 0.424 Newton goes to the jacks. This is detailed in Appendix H.

Roll-direction

$$Ixx = Iyy = 18689\ mTm^2$$

$$F_y = 1988\ kN$$

$F_{z+heave} = 4142\ kN$

$F_{z-heave} = 1882\ kN$

$M_{xx} = 2396\ kNm$

$\sum M_{RC} = F_y \cdot h_{cog} + M_{xx} - F_{z-heave} \cdot radius - R1 \cdot Hj - R3 \cdot 2r = 0$ → $R3 = 3181\ kN$
→ $R1 = 1349\ kN$

$\sum M_{RC} = F_y \cdot h_{cog} + M_{xx} - F_{z+heave} \cdot radius - R1 \cdot Hj - R3 \cdot 2r = 0$ → $R3 = 2432\ kN$
→ $R1 = 1031\ kN$

R2 can be calculated from horizontal equilibrium

$\sum F_H = F_H + R1_{-heave} + R2 = 0$ → $R2 = -640\ kN$

$\sum F_H = F_H + R1_{+heave} + R2 = 0$ → $R2 = -957\ kN$

R4 can be calculated from vertical equilibrium

$\sum F_V = F_{z-heave} + R3_{-heave} - R4$ → $R4 = 5063\ kN$

$\sum F_V = F_{z+heave} + R3_{+heave} - R4$ → $R4 = 6574\ kN$

Summing up the governing values of the acting forces in roll direction:

R1	1031	kN
R2	-957	kN
R3	2432	kN
R4	6574	kN

Table 6: Governing forces in roll direction for positive heave

R1	1349	kN
R2	-640	kN
R3	3181	kN
R4	5063	kN

Table 7: Governing forces in roll direction for negative heave

Note that the value calculated for R2 is negative, i.e., its direction is opposite to that drawn in figure 3.4. So R1 and R2 both work in the same direction. This is beneficial, because now the horizontal accelerations and thus forces can be introduced on two levels, keeping the stresses lower.

This effect is accomplished by the presence of R3. Without R3, the horizontal forces would have the direction as drawn in figure 3.4 and would be three times higher.

4 Force distribution

In this section the force distribution will be reviewed. Because of the ship motions, the TP will be accelerated back and forth. These accelerations require a resultant force. This resultant force will be supplied by a redistribution of the pretension forces. To this end a spring model is proposed.

4.1 Spring model

In the previous section different dynamical models were used to calculate the necessary seafastening forces. These are the resultant forces. They are to be produced by the summation of the jack forces. A resultant force in one direction requires the jacks in that direction to produce a higher force than the jacks in the opposite direction. Yet, in this opposite direction the contact force may never become zero, because this would mean that a distance between the jacks and the TP exist, and the TP could build up speed before re-establishing contact with the jack. Thus, an impact load could damage the TP or the jack and should be avoided at all time.

To avoid this losing of contact between the TP and the jack, an initial force needs to be present in the jack when pressed against the TP, the pretensioning force. This will elastically deform the TP and the jack. When moving back and forth, this elastic deformation first needs to be reduced to zero before contact between the TP and jack could be lost.

The spring model consists of two rings with springs in between, as shown in figure 4.1.

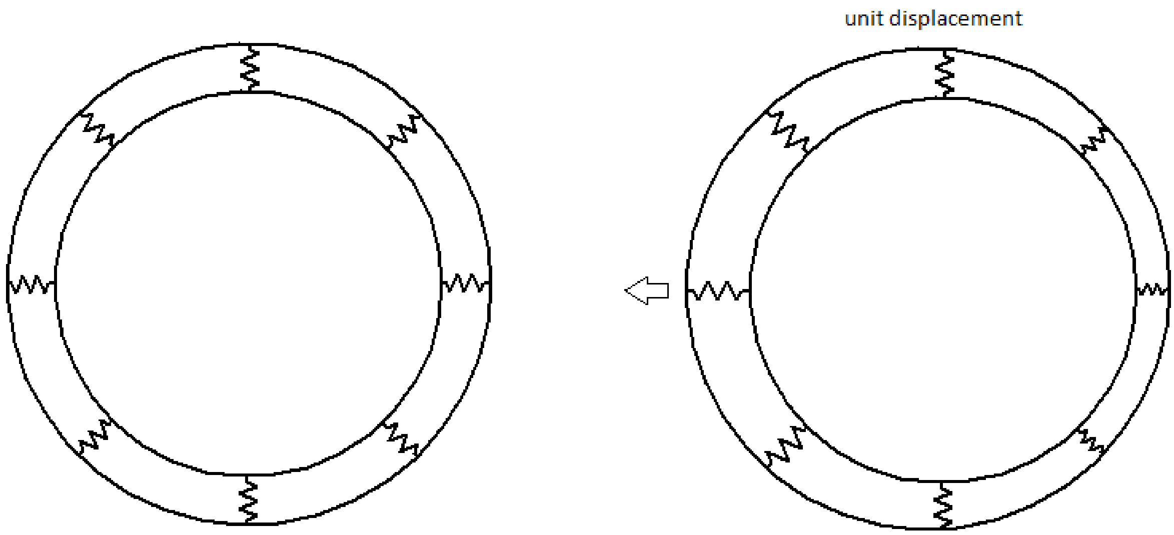

Figure 4.1: Spring model

The left part of figure 4.1 shows the model when no resulting force exist. The ship and TP are at rest, i.e., they experience no accelerations. All the springs have the same displacement and force. The right part of figure 4.1 shows the model when the ship has its maximum roll angle. Then the accelerations and resultant force are also at their maximum.

The required pretensioning force can be determined by giving the outer ring a unit displacement such that the springs on the left lose part of their initial force and springs on the right increase their force. This means a resulting force to the right. The minimum pretensioning force is found when the most left spring force equals zero and the sum of all spring forces equals the required resultant force.

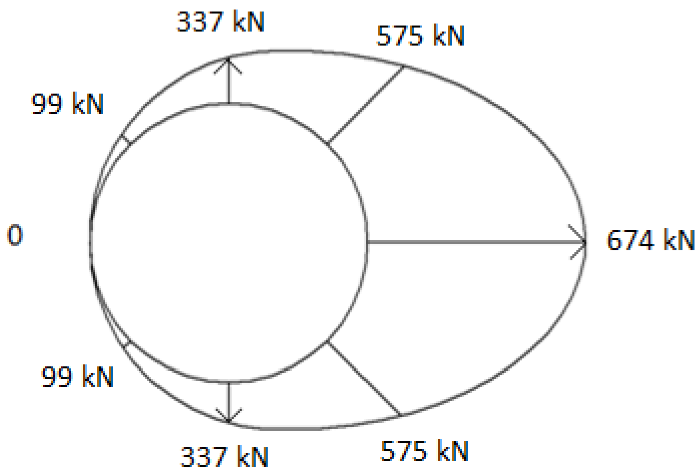

Figure 4.2: Radial force distribution

To achieve a resulting force of 1349 kN, all jacks need to be loaded at least up to 337 kN. Then, displacing the TP such that the left spring force equals zero, all the horizontal components of the jack forces as displayed in figure 4.3, result in 1349 kN to the right.

Figure 4.3 shows the horizontal and vertical components of the radial jack forces.

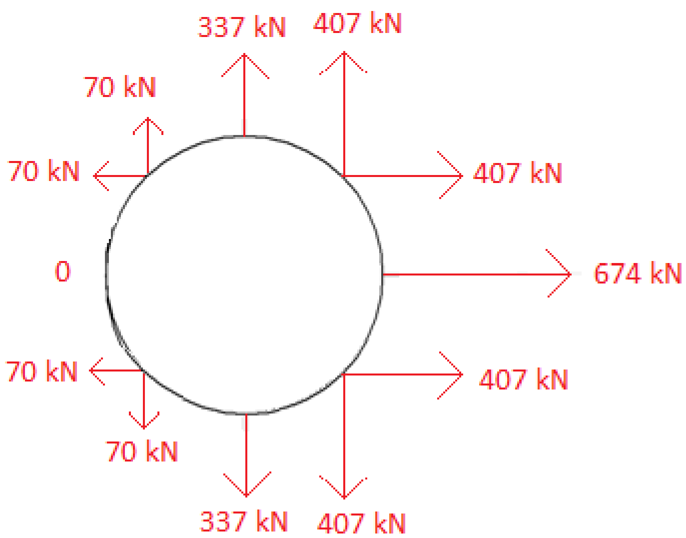

Figure 4.3: Horizontal and vertical components of radial jack forces.

Combinations of roll and pitch do not produce higher concentrated forces than 674 kN.

4.2 Vertical force distribution

The overturning moment is resisted by the downward reaction forces at the pads (R3 in figure 3.4). R3 represents all hydraulic cylinder and steel diagonal rod combinations that provide resistance against the overturning moment. The force distribution is linearly dependent on the distance from the hydraulic cylinder to the rotation point RC.

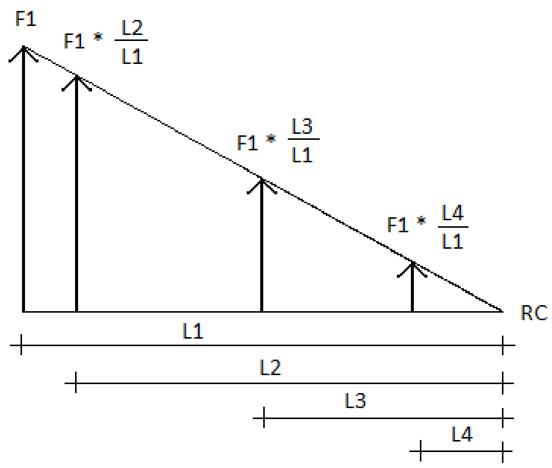

Figure 4.4: Linear vertical force distribution

The overturning moment they should resist equals $R3 \cdot L1 = 15905\ kNm$

The resisting moment they provide is given by the summation:

$$\sum F_i \cdot l_i = 15905\ kNm$$

This means F1 should at least be 1070 kN, and this is only for the roll direction. The pitch direction also requires a resisting moment, but this is very small compared to the roll direction, less than 2% and is therefore neglected.

4.3 Amount of pretension force

In section 4.1 the minimum amount of pretensioning was calculated using a spring model, to ensure that when the maximum acceleration occurs, no jack loses contact. Section 4.2 calculated the transverse force on the pads. This transverse force is almost 60% higher than the axial force. If this transverse force is to be transmitted through friction, this requires a coefficient of friction of 1.6. In practical cases this is not realistic. There are two arguments to increase the amount of pretension force.

First, the high transverse force requires a high amount of friction. This high amount of friction can be achieved by increasing the pretension force.

Second, when the maximum acceleration occurs, the least loaded jack should never lose contact, but also should never come near losing contact, i.e., a margin is needed.

Therefore, a pretension force of 1433 kN is chosen. The maximum force then becomes 1770 kN, which is 700 kN higher than the transverse force. Later it will be checked if this does not exceed allowable stresses and what the maximum pretension force may be.

4.4 Relative Stiffness

In the previous section a spring model was introduced to determine the distribution of forces when the TP is accelerated. Both rings were considered infinite stiff and all displacement was possible because of the elastic deformation of the jacks. However, the TP itself might also deform. This could result in a different distribution of forces.

First, the relative stiffness's of the jacks and the TP need to be determined. Then it can be concluded if the above model suffices.

The stiffness of the jacks follows from Hooke's law. The elastic medium is mainly the hydraulic oil. This has an average modulus of elasticity of 250.000 psi [11], or 1750 N/mm^2 . For elaboration see Appendix G.

$$k_{jack} = \frac{\Delta F}{\Delta L} = \frac{\Delta P \cdot A}{\frac{\Delta V}{A}} = \frac{\Delta P \cdot A^2}{\frac{\Delta P \cdot V}{E}} = \frac{A^2 \cdot E}{A \cdot S} = \frac{E \cdot A}{S}$$

In which S is the height of the oil column, and A the area of the piston.
If a TP of 5 meter in diameter is to be seafastened, then this piston needs to be extended 500 mm. So, S is taken as 500 mm, E is 1750 N/mm^2, and A is 45730 mm^2. This makes k_{jack} to be 160055 N/mm.

This stiffness of the TP or ring can be determined by applying two forces opposite to each other and establishing the deformation in horizontal and vertical direction. Rotating the system 90 ° such that the forces act in the horizontal plane, this create a system with 4 forces. The ring will ovalize, if two forces are applied. If two forces are applied at a 90° shift, the ovalization will be in the other direction, i.e., opposite to the first applied forces. The displacements can be added to arrive at the displacements of the whole. From this displacement an indication of the stiffness can be determined.

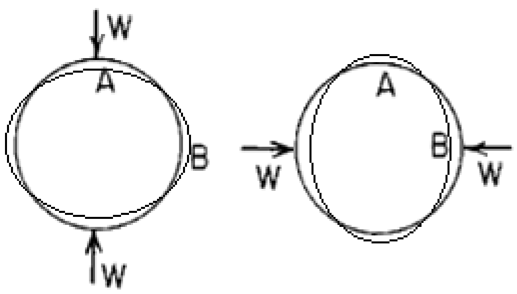

$$\Delta D_H = 0.1366 \frac{WR^3}{EI}$$

$$\Delta D_V = -0.1488 \frac{WR^3}{EI}$$

Figure 4.5: ROARK's ring

Because the coefficients 0.1366 and 0.1488 are close together, it is expected that the points of zero displacement are at approximately 45° angle from the horizontal. This means that also applying the diagonal jack forces will cause only small displacements in A and B and are therefore neglected.

To calculate the section modulus of the ring, an effective width is used of 894 mm. This is detailed in the Appendix E.

Calculating the horizontal and vertical displacement for a test load of 1 N.

F=W=1 N

R=2500 mm

E= 2e5 N/mm^2

I=4,58e7 mm^4

ΔD_H=-2,22e-4

ΔD_v=2,42e4

$\Delta D_A = \Delta D_h + \Delta D_v$=1,98e-5

K=F/Δ=100800 N/mm

(if only two forces were applied, the displacement would be much higher, resulting in a stiffness k of 8300 N/mm)

So, adding extra forces makes the ring react much more stiff. Also, the stiffness of the ring and the stiffness of the jacks are somewhat comparable, i.e., they are of the same order. This suggest that the previously proposed spring model needs to be refined, because the deformation of the ring could influence the forces exerted by the jacks, which could in turn influence the deformation of the ring.

A numerical model in ANSYS has been built to calculate more accurately the influence of deformation of the TP on the force distribution exerted by the jacks.

4.5 Numerical spring model – ANSYS

ANSYS is a general finite element package that can be used to carry out numerical calculations on a wide range of complex problems. In this thesis is has been used to calculate if the TP will deform enough to influence the force distribution of the jacks.

4.5.1 Build-up of the model

The model is build up out of two cylinders, one with a diameter of 5 m and one with a diameter of 4 m. These are respectively the TP and the seafastening tubular. Both cylinders are built up out of Shell181 elements. In between the cylinders are link elements, called Combin14 elements, to represent the hydraulic cylinders. These are the springs. In figure 4.6 half of the cylinder model is displayed.

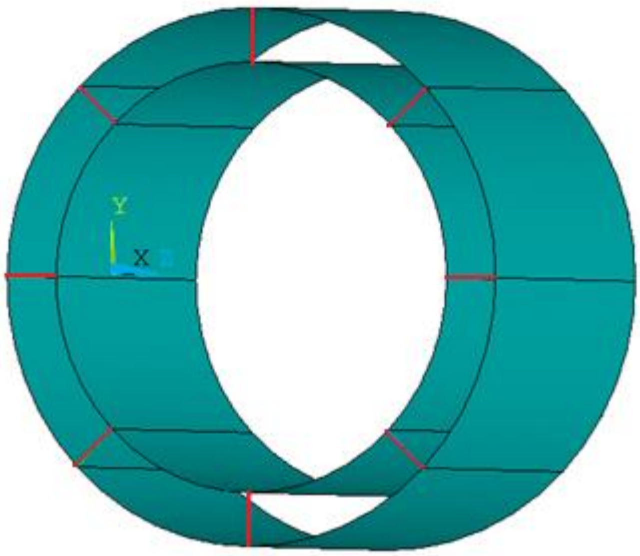

Figure 4.6: Build-up of the model

Only a 6 m part in axial direction of the TP is modeled. It is always a goal in numerical analysis to keep the model as small as possible, so as to keep computation time to a minimum.

The outer cylinder, representing the TP, has a local wall thickness of 85 mm. In this model it is the only part that has a density, so that when an acceleration load is applied, only this part will be forced to translate. The inner cylinder has no density.

The inner cylinder is restrained in all directions. The outer cylinder is restrained in axial direction over the entire circumference of both outer edges of the cylinder. The same edges are restrained on two discrete locations in y-direction, so the model cannot rotate around the x-axis. No restrained is applied in z-direction other than the springs. This means that the outer cylinder can translate in only in z-direction.

The springs have a spring stiffness and an initial force. In ANSYS this is modeled by giving the Combin14 elements an initial length that differs from the length given in the geometry. ANSYS then calculates itself what the force in the spring is. It should be noted that the model shows local deformation because of the spring force, even before the acceleration load is applied. This local deformation cause the spring to relax a little. A small iteration was done to make sure the springs have the right spring force after the cylinder deformed locally. For a detailed overview of the results, see Appendix I.

4.5.2 Model validation

The model is validated against the hand calculated model proposed in section 4.1. This is done by giving both cylinders an infinite stiffness, i.e., E=2e14. The springs have their normal stiffness and initial length to provide the required pretension force.

The first check is done with zero acceleration applied. No change in spring force should occur, and this is the case.

The second check is done with the occurring acceleration. This should produce the force distribution as given in figure 4.2 and 4.3. This is also the case.

From this it is concluded that the model behaves as expected. Now the stiffness parameters can be changed to realistic values and its effect observed.

4.5.3 Realistic values of stiffness

If for the outer cylinder a realistic value of the stiffness is used, i.e. E=2e5, the force in the springs will change, due to local deformation, the spring is relaxed a little. In reality the hydraulic cylinders will also elastically deform the TP locally, but they continue to exert a force until the required pretension force is achieved. To also realize this in the numerical model, the initial length of the springs needs to be increased, so that after local deformation the correct spring force remains.

The value of the local deformation, DMX = deformation = 1.41 mm. This corresponds with the loss in pretensioning force. After compensating for this loss, the initial force is 1433 kN and the local deformation is 1.66 mm.

When also the acceleration is applied, the total deformation plus displacement is 3.77 mm. Furthermore, the heaviest loaded spring now has increased its force with 337 kN

To see if the TP would deform under the influence of the spring force, also a model with only two springs opposite to each other was made. A clear ovalization was observed. As was stated in section 4.3, there was reason to believe that the stiffness of the TP was of the same order as the stiffness of the jacks. Adding more jacks stiffens the TP and makes the systems response much more like the kettle formula.

Figure 4.7 shows the displaced TP.

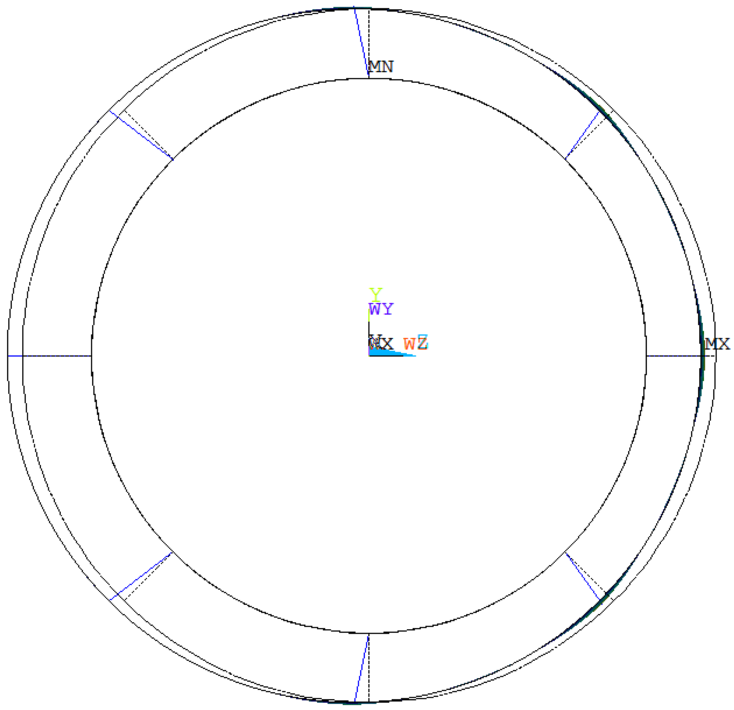

Figure 4.7: Displaced TP ring. The displacement is exaggerated trough a scaling factor so it is better visible.

4.5.3.1 Linear analysis

If a linear analysis is performed, the results show no difference with the model proposed in section 4.1. This means the TP reacts much stiffer than expected, namely close to infinitely stiff. It will not deform enough change the force distribution.

4.5.3.2 Nonlinear analysis

If a nonlinear analysis is performed, the result show only a difference of less than 1% with the model of section 4.1. This analysis make a series of linear analysis, where the outcome of a previous step is input for the next step. Since each step greater than 1 takes the deformed geometry into account, a slightly different result is expected, due to the extra component present in springs with a slight angle.

The difference is small enough to conclude that a nonlinear calculation is not necessary.

4.6 Conclusion

The goal of the analysis in this chapter was to find out the force distribution on the TP. A simple model consisting of two infinite stiff rings with springs in between is suitable for determining the force distribution. An numerical calculation done in ANSYS showed no significant difference. So, the TP will not deform enough to change the force distribution.

The local stresses in the TP follow only from the local spring forces and follows a linear relation, i.e., if a spring force is doubled, then so will the stresses.

5 Buckling of wall Transition Piece

The model used in chapter 3.2 calculated different forces that are necessary to accelerate the TP such that it will follow the ship motions. This model assumed a rotation point in the lower right corner of the TP. In the worst case the TP will stand only on this one spot. Here the vertical reaction force is introduced into the TP in a relatively small area, namely the width of the grillage beam, in this case 400 mm. To ensure that this point can be used as a rotation point, the capacity of the TP wall needs to be checked. This chapter will view the static capacity, the buckling strength of the TP wall, as well as the parameters that are of most influence.

A buckling analysis will be carried out in ANSYS, to find the ultimate load the TP can withstand. Furthermore, Teng & Rotter [12] describe failure due to buckling of thin metal silos on discrete supports. They propose design rules to prevent the buckling of these silos. The working closely relates to the TP standing on grillage beams.

5.1 Build-up of the model

The ANSYS model is build up out of Shell181 elements. The thickness of the flange is 40 mm. Its length is 350 mm. The flange is connected to the TP wall. The lower part of this wall has a different thickness than the part above is. The thickness is 55 mm for the first 1000 mm. After that the thickness increases to 85 mm in a tapered way. In the figure on the right the lower part of the TP wall can be seen, as well as the groutskirt, a packer, and the wall of the monopile.

It is expected that this lower part is the most likely to buckle because of its reduced thickness and high concentration of stresses. The stresses dissipate quickly in the structure.

The lower 7 m of the TP will be modeled, all around. The top of the TP will be constraint in all directions and the load applied below the flange in upward direction.

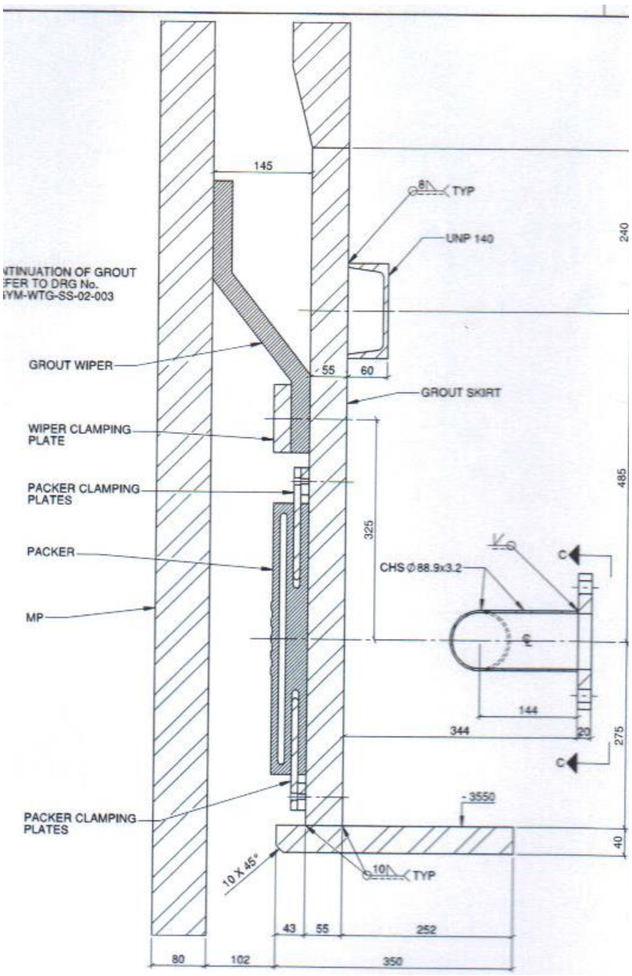

Figure 5.1: Drawing of TP wall when placed on top of the monopile (MP)

The length of load application is 400 mm. This is the width of one HE 1000 grillage beam. The beam has plate stiffeners at the location where the TP wall makes contact with the beam, therefore the full width of the beam can be utilized for force introduction.

Where the load is introduced, the mesh in the model needs to be finer. The rest of the model can suffice with a coarser mesh.

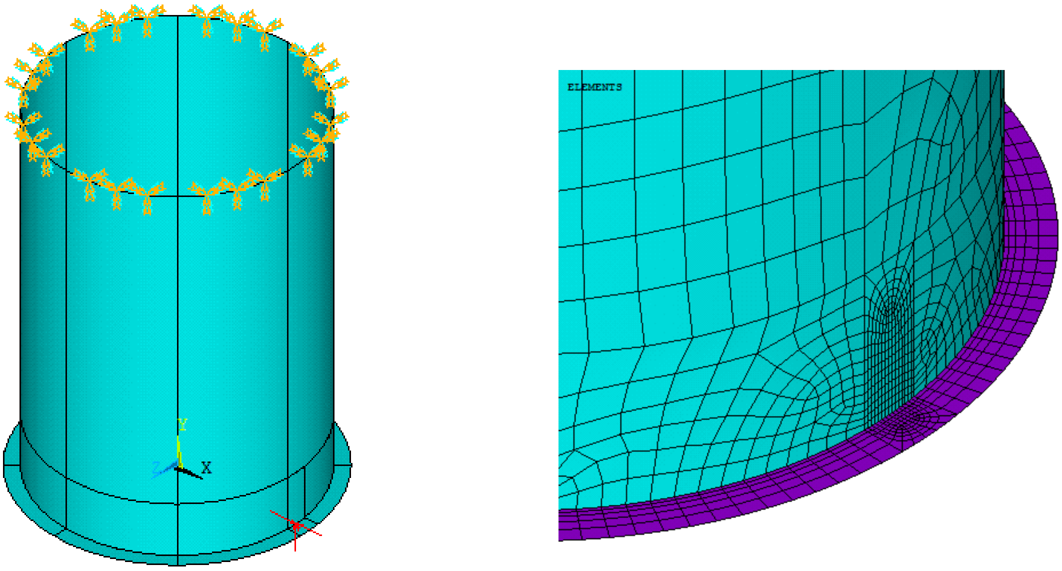

Figure 5.2: Build-up of the model in ANSYS

In figure 5.2 the build-up of the model is shown. The TP is constrained in axial (y) direction along the entire circumference. The load is applied on a 400 mm wide line at the bottom, also visible in figure 5.2 (left). The right half of the figure shows the mesh and the refinement at the area of load application.

5.2 Static analysis

First a static analysis is carried out. This is an important step because here is can be checked if the model behaves as expected. In this case local force introduction should lead to relatively high stresses that spread and dissipate quickly into the structure. The stresses should correspond with the force applied at the line or area.

The force specified in chapter 3 is 6574 kN. This force is introduced over a length of 400 mm. The thickness of the plate is 55 mm. So, $\frac{6574 \cdot 10^3}{400 \cdot 55} = 298\ N/mm^2$. This is the stress that is expected to occur locally. From figure 5.3 and 5.4 it can be seen that the stress concentration is very local above the force introduction and quickly decreases further away. ANSYS gives a maximum stress of 279.5 N/mm^2.

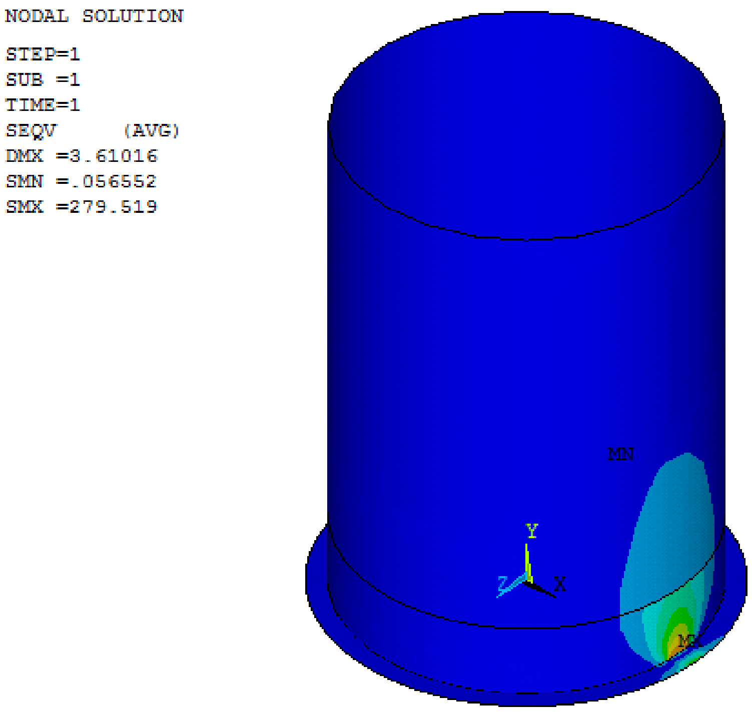

Figure 5.3: Static analysis TP wall

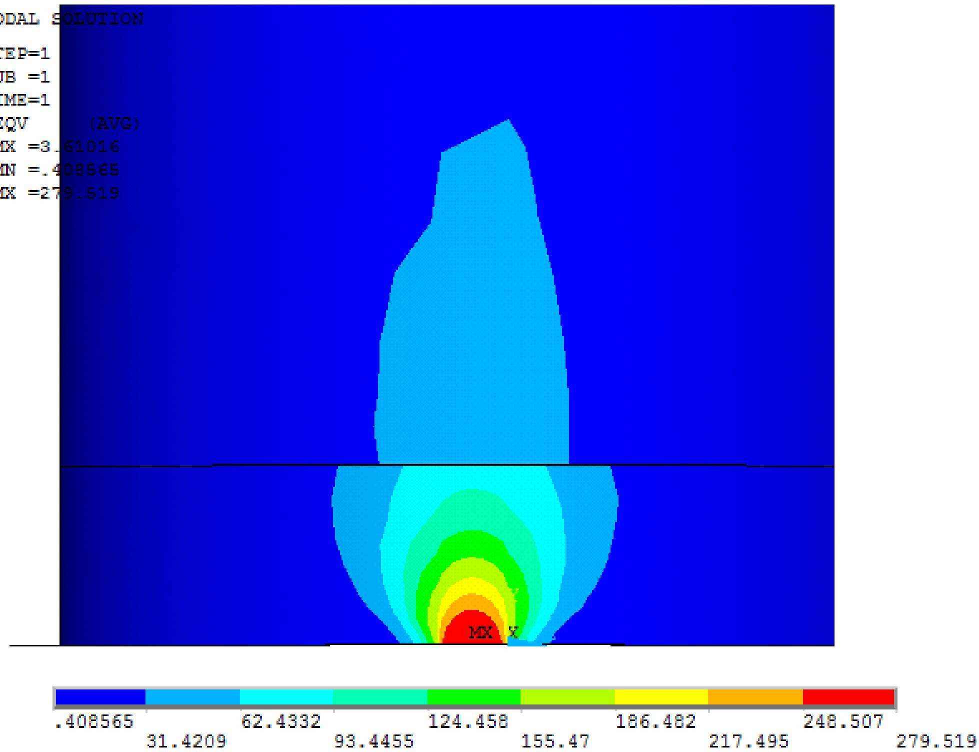

Figure 5.4: Local stress concentration

5.3 Eigenvalue buckling analysis

Eigenvalue buckling analysis predicts the theoretical buckling strength of an ideal elastic structure. This is also known as the Euler buckling strength. The analysis does not take into account initial imperfections and nonlinear behaviour. Therefore, the real buckling strength is much lower. This overestimation can be compensated for by for example, the use of a knock-down factor.

The model is the same as for the static analysis, only now ANSYS will do a eigenvalue buckling analysis. Figure 5.5 shows the buckled shape of the TP wall. The buckling is very local, as is expected, since only high stresses occur here.

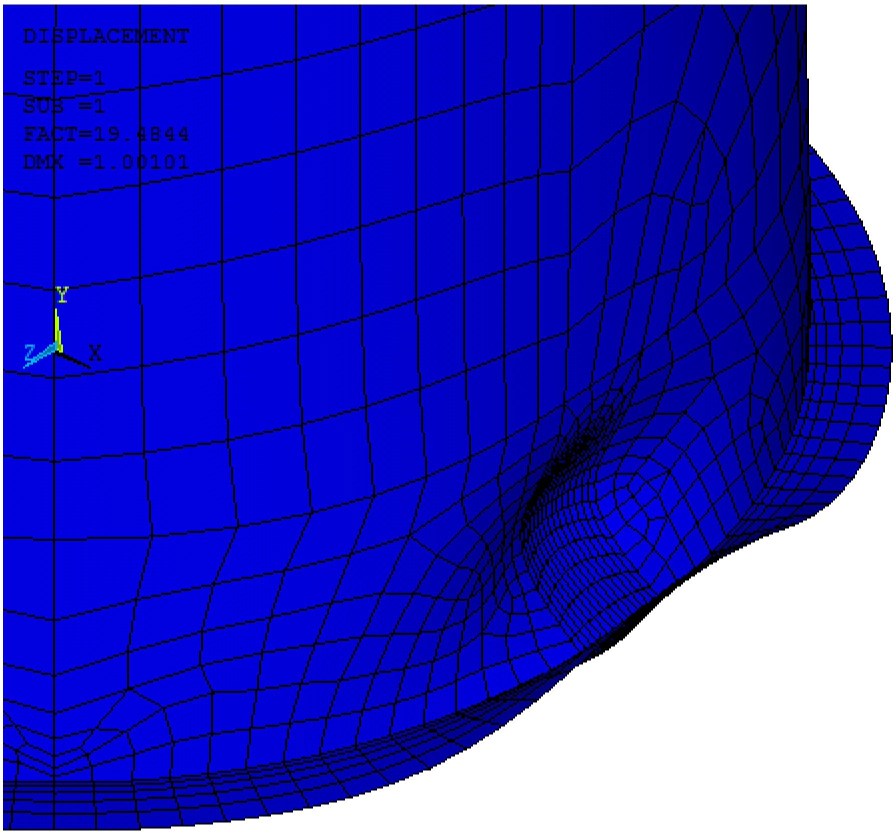

Figure 5.5: Buckled shape of TP wall. The deformation is scaled with a factor of 350.

The value of the eigenvalue buckling analysis is given in table 8. TIME/FREQ is specified as 19.484, this means that the load that applied in the model needs to be multiplied by 19.4 to equal the load required for the structure to buckle. This is only the theoretical buckling load and needs to be reduced to compensate for geometrical imperfections. Since no measurements are available, a conservative knock-down factor is used of 1/6. This provides a new buckling value of 3.247 times the applied load, i.e., 21345 kN, which would produce a very high local stress. This is much higher that the yield stress, namely over 892 N/mm^2. Therefore local yielding is the limiting criteria and buckling is not likely to occur.

The conservative knock-down factor is derived from experiments done by Andrew Robertson, who axially loaded a variety of cylinders and found the real buckling load to be much lower than the theoretical buckling load. The real buckling loads were never lower than 1/6 of the theoretical value.

***** INDEX OF DATA SETS ON RESULTS FILE *****

SET	TIME/FREQ	LOAD STEP	SUBSTEP	CUMULATIVE
1	19.484	1	1	1

Table 8: Eigenvalue buckling

5.4 Non-linear buckling analysis

A non-linear buckling analysis would provide a more accurate result than the eigenvalue buckling analysis. This analysis employs non-linear, large deflection, static analysis to predict the buckling load by gradually increasing the load until the structure becomes unstable.

Although is it more accurate, it also is more difficult. And since the eigenvalue analysis produced a value already satisfactory after using a conservative knock-down factor, there is no need for a more accurate calculation.

5.5 Hand calculation

Rotter & Teng [12][17] proposed design rules for cylindrical shells above local supports. They used it mainly as a guide for the design of thin metal silos on discrete supports. But it also correlates strongly with a TP standing on grillage beams.

Using those design rules, it is concluded that given this geometry, no buckling will occur prior to local yielding.

$$\sigma_{cr} = \frac{F_{cr}}{d * t} = k_{2;local} * f_y$$

$$\lambda = \sqrt{f_y/\sigma_{cl}}$$

$$\sigma_{cl} = \frac{E}{\sqrt{3 * (1 - \nu^2)}} * \frac{t}{R}$$

$$\varepsilon = \sqrt{235/f_y}$$

$$Cc = -0.43 + 5\epsilon - 3.57\epsilon^2$$

$$Ce = -0.87 + 6.38\epsilon - 4.51\epsilon^2$$

$$\eta = d/R$$

$$k_{2;local} = \frac{\sigma_{cr}}{f_y} = 0.19 + \frac{0.0283 * Cc}{\eta * \lambda^{0.77*Ce}} - 1.04 log\lambda$$

In which:

d = support width = 400 mm.
R = radius = 2500 mm.
t = thickness = 55 mm.
fy = steel used = 355 N/mm^2

What this calculation does, is calculate the critical force immediately above the support so that no buckling occurs. The factor k2 is limited to 1.0 or 1.15, above which local yielding would occur.

The calculation produces a k2 value of 1.28. Since this is higher than 1.0, local yielding will occur before buckling. It should be noted that this calculation is for an unstiffened cylinder. The TP has a significant stiffener at its lower edge and so the outcome of the hand calculation can be considered a lower bound for the TP.

5.6 Unstiffened cylinder

The design rules of Rotter & Teng [12][17] are based on the unstiffened cylinder. In ANSYS also this calculation is done. This produces a theoretical buckling load of 7.3411 times the applied load, see table 9.

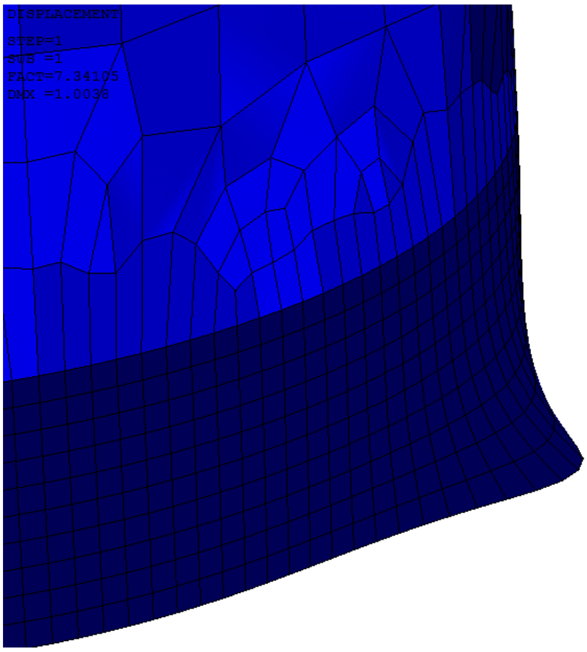

Figure 5.6: Buckled shape of unstiffened cylinder

***** INDEX OF DATA SETS ON RESULTS FILE *****

SET	TIME/FREQ	LOAD STEP	SUBSTEP	CUMULATIVE
1	7.3411	1	1	1

Table 9: Theoretical buckling load unstiffened cylinder

With a support width of 400 mm and a wall thickness of 55 mm, the force at which local yielding occurs equals 7823 kN.

If a conservative factor of 1/6 is used on the theoretical buckling value of the unstiffened cylinder, a fraction of 1/6*7.4311=1.22 remains. So, 1.22 multiplied with the applied load in the model results in a conservative buckling force of 1.22*6574=8020 kN. This is indeed higher than the load at which local yielding occurs, as was concluded from the hand calculation of Rotter & Teng.

5.7 Parameter analysis

Now that there is confidence in the correctness of the model, a parameter analysis is conducted to get insight into the parameters and their influence. This is done so it will be easier to asses other TP's. It's a small scale parameter analysis, so only one parameter at the time will be changed and its influence reviewed. It is likely that combinations of different parameter will give more information on the workings, but those will not be considered here.

In table 10 is indicated in green the parameter that is changed. Above those are the parameter that stay the same. t1 is the thickness parameter of the flange, t2 is the thickness of the first 1000 mm of h 1 of the wall, t3 is the thickness of the wall from 1000 mm up, h1 is the height of the TP wall with thickness t2. TIME/FREQ is the factor with which the applied load is multiplied to reach the theoretical buckling strength.

Some interesting insights are gained. The influence of the flange thickness is significant, especially for low values. Once it passes a thickness of about 30 mm, its influence decreases.

The influence of the lower part of the wall is the greatest, as would be expected when viewing the buckling shape in figure 5.5.

The influence of the upper wall thickness is only significant up to the point where is reaches the same thickness as the part of the wall below it. After that almost no increase in the buckling strength can be observed.

Remarkable is the little influence the height of the lower part of the wall has. Furthermore, the buckling shape also changes several times.

															t1=	40		
t3=	85				t3=	85				t1=	40				t2=	55		
t2=	55				t1=	40				t2=	55				t3=	85		
			TIME/FREQ					TIME/FREQ					TIME/FREQ					TIME/FREC
t1=	10		-2,066		t2=	20		2,278		t3=	20		8,063		h 1	500		21,442
	20		-11,831			30		6,096			30		16,956			750		20,059
	30		18,132			40		10,494			40		18,896			1000		19,484
	40		19,484			50		16,156			50		19,072			1250		19,415
	50		20,876			55		19,484			55		19,141			1500		19,542
	55		21,589			60		23,123			60		19,206			1750		19,718
	60		22,309			70		31,199			70		19,325			2000		19,789
	70		23,749			80		40,086			80		19,434			2250		19,730
																2500		20,014

Table 10: Parameter analysis

5.7 Conclusion

This chapter investigated the buckling capacity of the TP wall, when the entire weight and dynamic load effect are applied to an area of the width of a grillage beam. This analysis is necessary to justify the assumed rotation point used by the model in chapter 3. Buckling of the TP wall will not occur with the load that was calculated in chapter 3. Nor will local yielding occur. If the load were increased even more, local yielding would be the first limiting factor.

The calculation was done using an eigenvalue bucking analysis in ANSYS. A hand calculation according to the design rules proposed by Rotter & Teng [12][17] also showed that local yielding is the limiting factor and that no buckling prior will occur.

Therefore, it is concluded that the TP wall will not buckle when subjected to high acceleration induced forces and standing on only one grillage beam.

6 Load application on cylinder

In this chapter the pretension force will be applied to a part of the cylinder that represents the TP. Since the maximum force exerted by the heaviest loaded hydraulic cylinders when the TP is accelerated is 1.24 times pretension force, this will result in an increase of the local stress by 1.24. Therefore it is not necessary to calculate the maximum occurring stresses with accelerations, but only with the static situation, and then multiply the maximum occurring stress from that static situation with 1.24.

6.1 Build-up of the model

The model is build-up using shell181 elements. Only 6 m of TP length is modeled. As shown in Appendix E, the stresses reduce quickly beyond the area of application, and thus will the effect of modeling a longer cylinder be negligible.

The radius of the cylinder in this model is 2500 mm. It is constrained at the left hand side in axial direction around the entire circumference. It is further constrained in vertical (y) direction on two keypoints in the horizontal (x-z) plane, to prevent the model from rotating. In z-direction it is constrained on only one keypoint, so that the model can deform freely in radial direction.

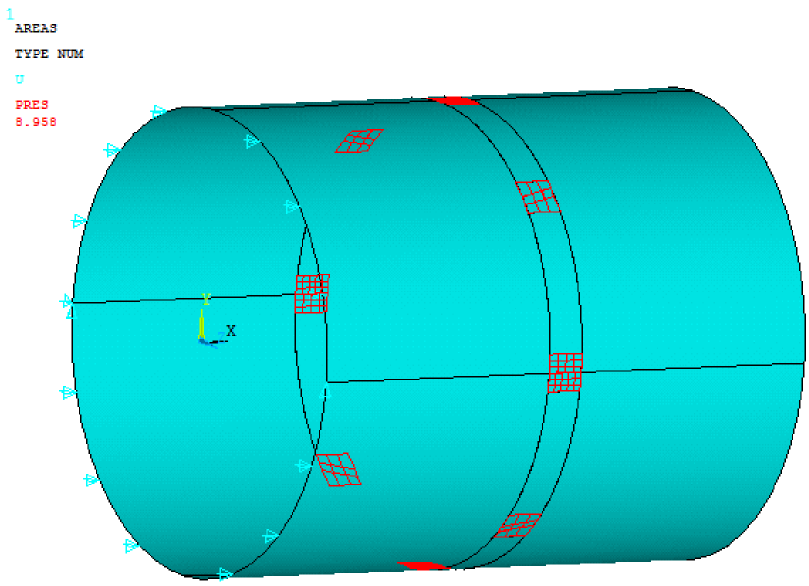

Figure 6.1: Build-up of the model

The load of 1433 kN is first applied to an area of 300x300 mm with equal distance between them, as displayed in figure 6.2 The load is applied on the inside of the cylinder facing outward, and so works perpendicular to the longitudinal axis.

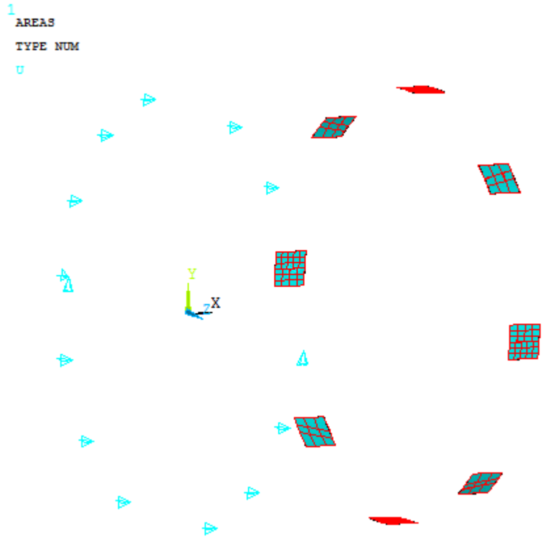

Figure 6.2: Areas of load application

After the load application and the model is constrained, the areas can be meshed. As can be seen in figure 6.3, the mesh looks regular and no out of shape elements are detected. The mesh size can be of influence on the result. A sensitivity analysis must be done to ensure a proper solution.

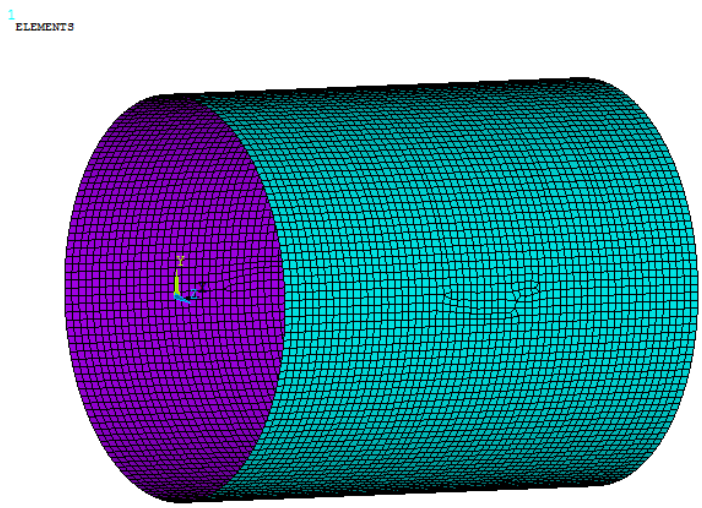

Figure 6.3: Meshed area

ANSYS calculates the stress and in figure 6.4 the Von Mises stresses are shown resulting from the pretension force.

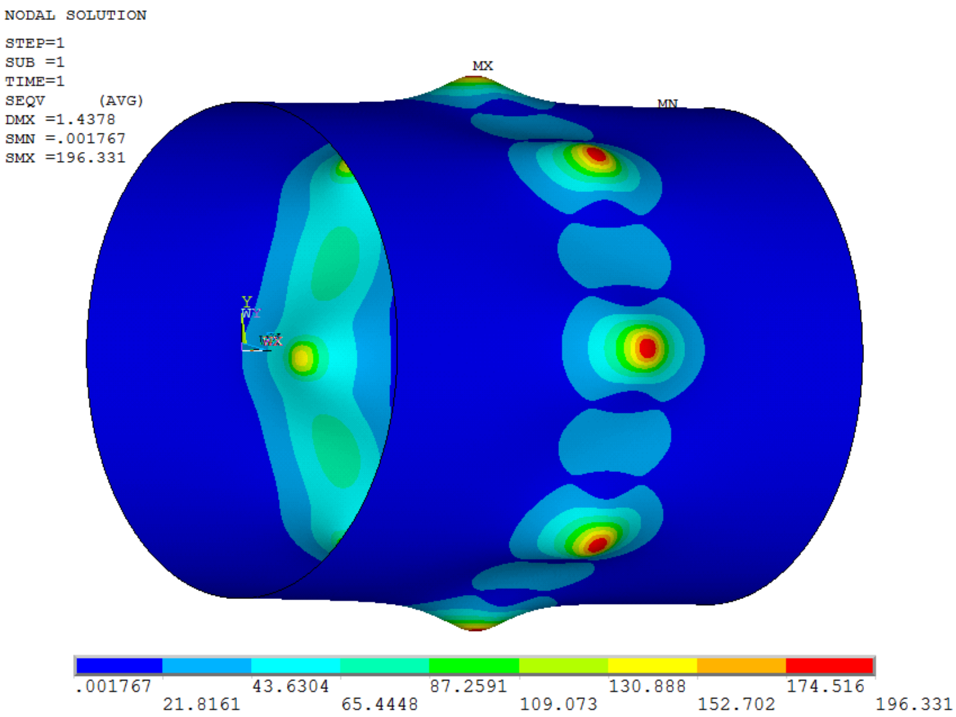

Figure 6.4: Stresses due to pretensioning force

6.1.2 Sensitivity analysis

A sensitivity analysis has been carried out to see if the used mesh size is fine enough. So different mesh sizes will be used and the result noted in the table below. When decreasing the mesh size will not be accompanied by a significant increase in stress, then the right mesh size is reached. Furthermore, a commonly accepted rule states that the difference in result of the last step with the previous step can be added to the last step as a conservative approach to obtaining the maximum stress.

mesh size		σ-max		n elements
150	mm²	174.5	N/mm²	4594
100	mm²	179.4	N/mm²	10087
50	mm²	194.4	N/mm²	39088
25	mm²	196.3	N/mm²	153219
100/25	mm²	191.6	N/mm²	11599
150/25	mm²	192.2	N/mm²	5834

Table 11: Sensitivity analysis

So, the difference between the last two steps is 2,3 N/mm^2. This is added to the result of the last step, i.e., 196.3 + 2.3 = 198.6 N/mm^2. This is assumed a safe approach.

Also a mesh refinement can be made in areas of stress concentration, and elsewhere a course mesh used. This saves computation time while still achieving high accuracy. In table 11 this is the row where it says mesh size 100/25, meaning a mesh size of 25 only in the narrow band where the load is applied, and a mesh size of 100 in the rest of the model, see figure 6.5.

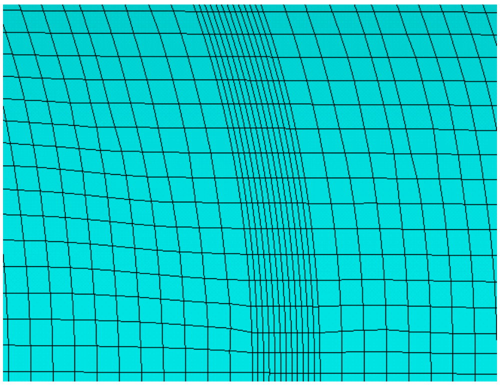

Figure 6.5: Mesh refinement at load application

Judging the values in table 10, the most accurate results are produced if a small mesh size of 25 mm is used in a regular distribution.

6.1.3 Allowable stresses

It is common in the offshore industry to use the design guides from the American Petroleum Institute (API) and the American Institute for Steel Construction (AISC). These specify maximum values for stresses, see table 12. Although it is not obligatory to use these guidelines, clients or marine warranty surveyors often do require contractors to abide by these guides and limiting values. In this thesis the following limiting value for bending stress in the TP will be used: 0.6*315 N/mm^2 = 189 N/mm^2. The maximum stress found in the analysis is 198.6 N/mm^2. This is already higher that allowed and are only the stresses due to pretensioning forces. Accelerating the TP will increase these stresses. Therefore the following sections will describe ways to reduce the peak stresses.

Plate thickness [mm]	Yield stress Fy [N/mm^2]
t ≤ 16	355
16 ≤ t ≤ 40	345
40 ≤ t ≤ 63	335
63 ≤ t ≤ 80	325
80 ≤ t ≤ 100	315

Tension	0.60 Fy
Bearing	0.90 Fy
Compression	0.60 Fy
Shear	0.66 Fy
Equivalent	0.75 Fy

Table 12: Allowable stresses [14][15]

6.2 Contact elements

To reduce the peak stresses, it has been attempted to use contact elements to achieve a different load introduction and influence the local curvature. This has been partially successful, in the sense that the aimed stress reduction was achieved, but also created a few side effects that could not be explained nor mitigated. Since there does not seem to be a straight forward way of validating these results, they will not be used.

The model has the same built-up as the model described in section 6.1. But now with pads with slightly larger radius as the TP modeled on the inside of the cylinder, “floating” in space, i.e., they are not constrained. When left there in that condition, the model will not solve due to rigid body motion, i.e. non convergence. This can be resolved in two ways. The first method is to attach the parts of the cylinder representing the pads to so-called “weak springs”. These are called weak springs because they have a stiffness high enough to prevent the parts from floating away, and weak enough to have a negligible influence on the solution. The second method is to use so-called “bonded contact”. This method has the advantage of over the first that a significant part of the iteration process can be skipped, because ANSYS doesn’t have to search where it is going to find contact.

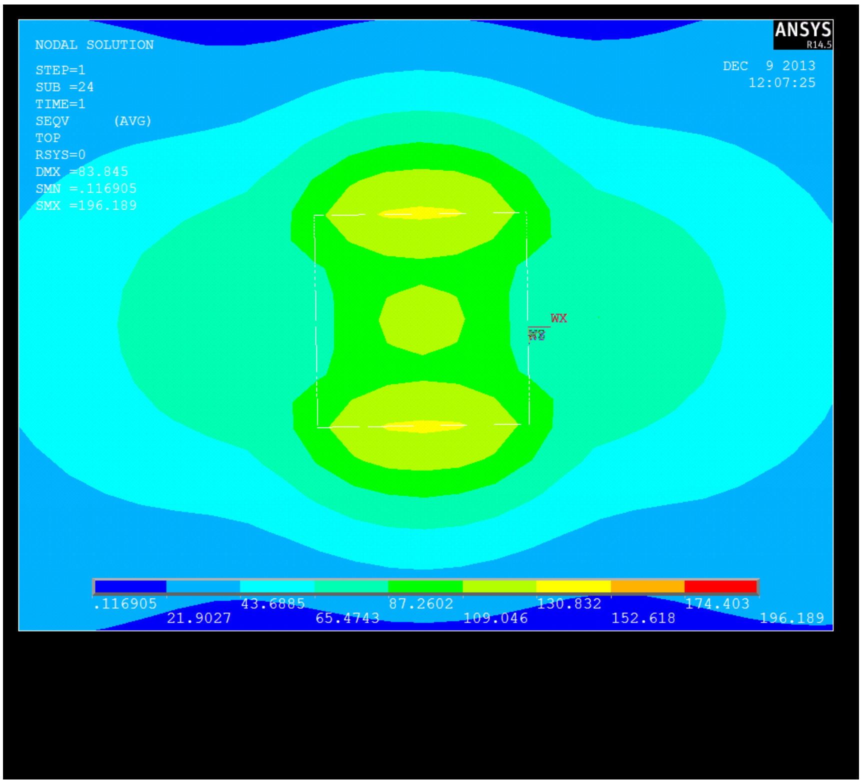

Figure 6.6: Stresses due to load applied via contact elements

The size of the pads can be changed to find more optimal forms. In particular the radius is of interest. If the radius is smaller than that of the cylinder, it will find contact mostly in the central part of the pad and thus a more concentrated load. If the radius of the pad is a bit larger than that of cylinder, the outer parts will find first contact and exert more pressure via these edges.

A beam analogy could illustrate this effect more clearly.

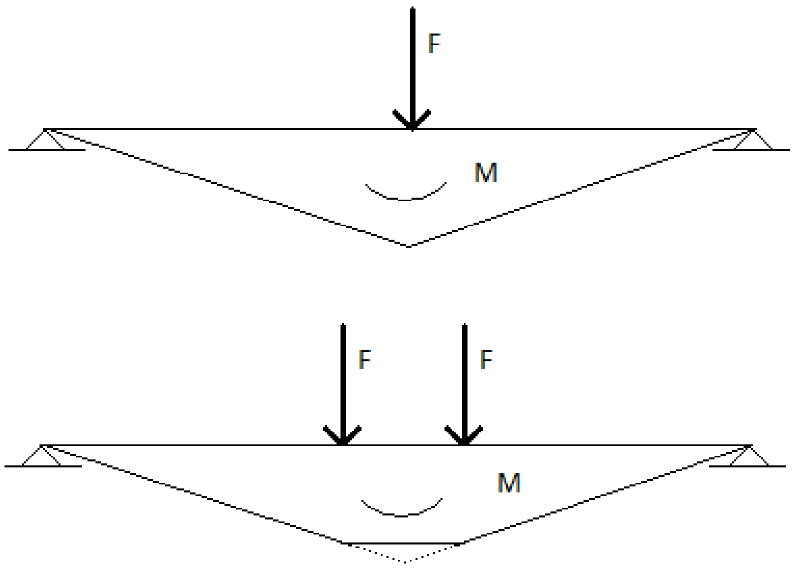

Figure 6.7: Beam analogy

By changing the way the load is applied, the curvature can be influenced, and thus the stresses reduced.

This effect is clearly visible in figure 6.6. In the upper and lower edge the stress is higher than the rest of the contact area. The peak stress however is lower than when the load is simply applied as a distributed load.

The stress reduction is not due to a locally increased thickness of the cylinder. This is because the coefficient of friction is set to zero, and thus only normal forces are transferred from the pad to the cylinder. This can be checked as well by applying a high load to the cylinder in axial direction. This creates a high and uniform stress in the cylinder. If the pad acted as if it were part of the geometry, i.e., increased thickness of the cylinder, due to the bonded contact, then it too would be stressed by the high axial load. This is not the case, as can be seen in figure 6.8.

As a check, the same analysis is run without any load applied. The result shows significant stresses in both the pad and the cylinder, see figure 6.9. No explanation could be found.

A second check resulted in a second anomaly. This occurred when the initial distance between the pad and the cylinder was changed manually. This change was accompanied by a change in stresses. This should not occur, since the curvature of the geometries and load itself did not change. Here also no explanation was found.

For these reasons contact elements will not be used further in this thesis.

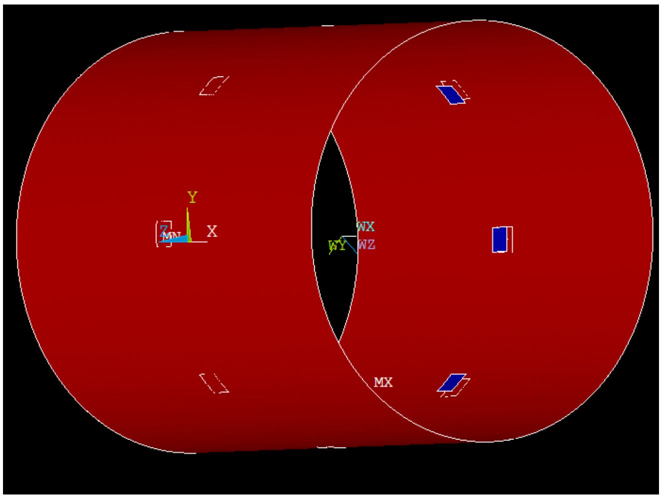

Figure 6.8: The contact pads are unaffected by high axial load in the cylinder

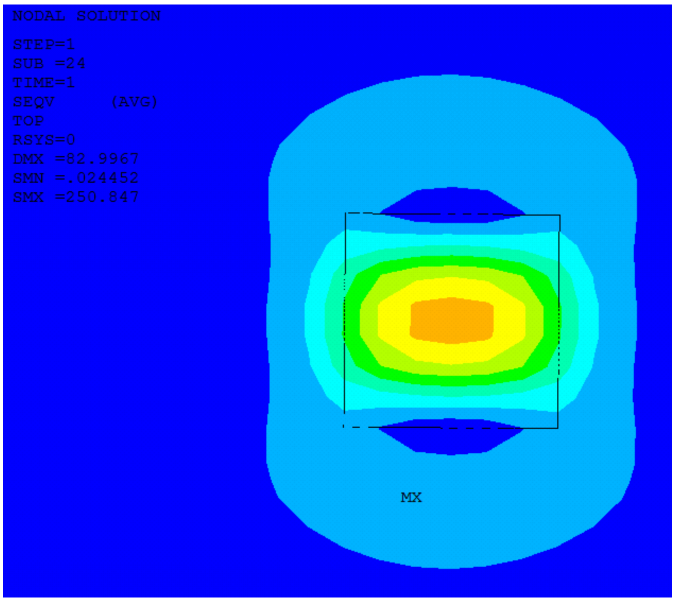

Figure 6.9: Stresses in the cylinder while zero load applied

6.3 Increase area of load application

Another way to reduce the peak stresses is to increase the area of load application. The same model as in section 6.1 is used, with the only difference that now instead of 300x300 mm^2, areas of 400x400, 500x500 and 600x600 are used.

Both the local peak stress as well as the local deformation decrease.

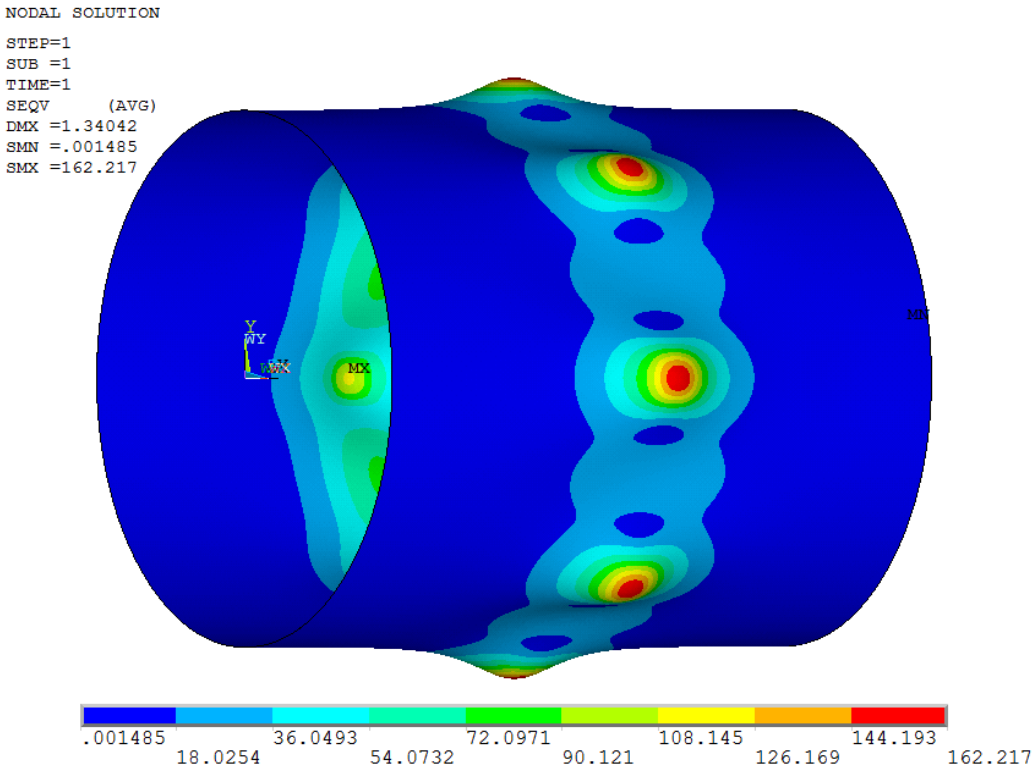

Figure 6.10: Peak stresses due to load applied on 400x400 area

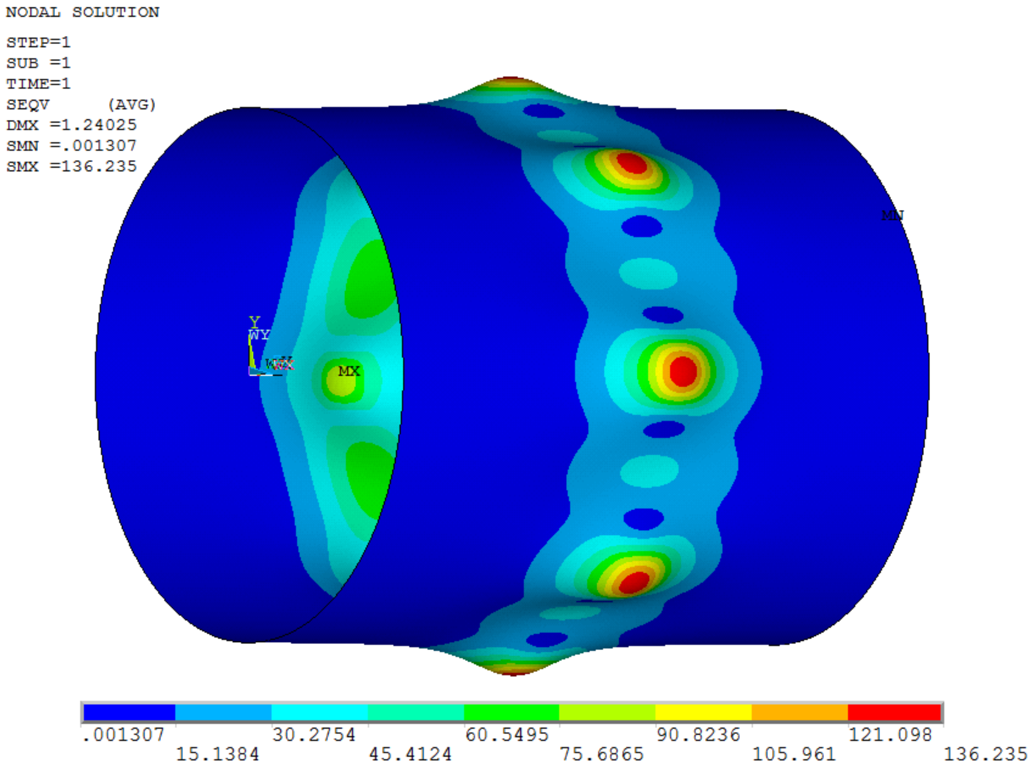

Figure 6.11: Peak stresses due to load applied on 500x500 area

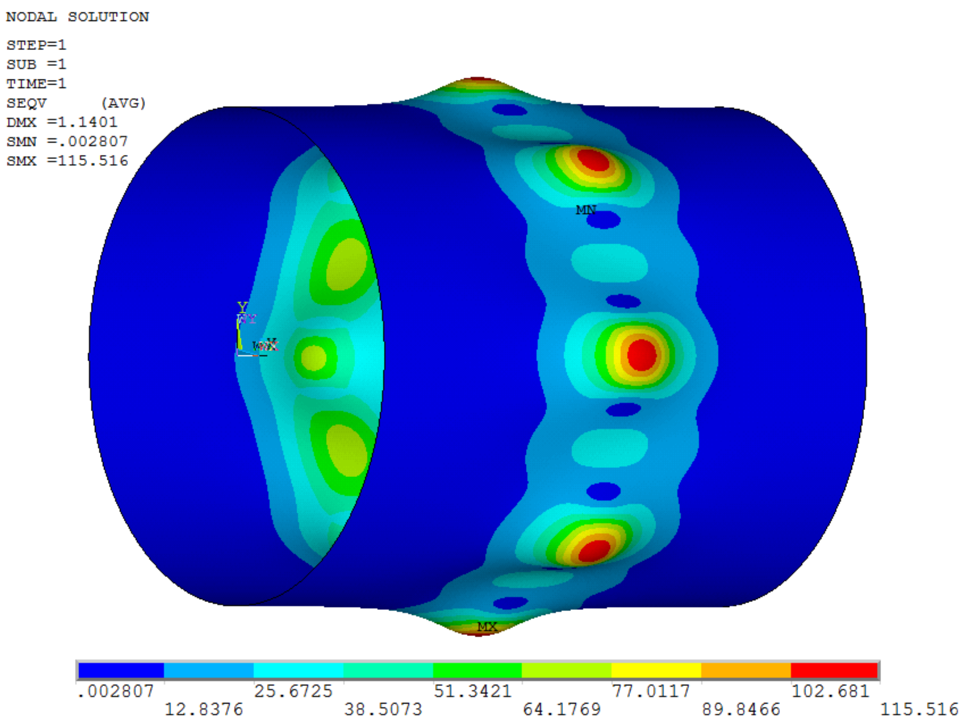

Figure 6.12: Peak stresses due to load applied on 600x600 area

In the table below the values of the different analysis are summarized. From the sensitivity analysis done in section 6.2.1 it is concluded that the results obtained using a mesh size of 25 mm is an underestimation of 1% and therefore accurate enough.

area of load application	mesh size	σ-max	
300x300	25	196.3	N/mm²
400x400	25	162.2	N/mm²
500x500	25	136.2	N/mm²
600x600	25	115.5	N/mm²

Table 13: Peak stresses depending on area of application

So, increasing the area of load application significantly reduced the stresses. A stress of 115 N/mm^2 due to pretension will result in a maximum stress of 143 N/mm^2 when the TP is accelerated. This is within the acceptable range.

6.4 Modular system

Up until now the design has assumed a fixed height of the tubular element, namely 6 m above the grillage. The reason for this 6 m are the heights of the internal platform inside the TP. In table 1 these values are summarized in row *height lower platform*. The lowest platform was 6.70 m and therefore 6 m is a sensible design height. However, if the stresses turn out to be too high, a modular system could be used, in which the height of the tubular element can be raised via a bolted connection and an additional part of tube. Making the system adjustable allows for optimizing the seafastening to the particular TP to be transported.

Increasing the height of the tubular element to just below the internal platform, the jacks will make contact with the TP wall at 8 m high. The force distribution from the model displayed in figure 3.4 will be positively affected. The closer R1 is to the CoG of the TP, the lower it will need to be.

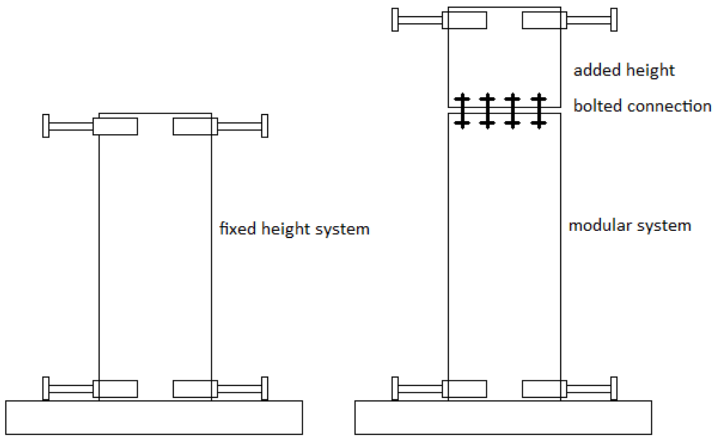

Figure 6.13: Modular system

A further benefit from this modular system is the guarantee that the jacks will make contact with the TP wall above the shear keys. These shear keys are located about halfway the height of the grouted area. This follows from a known line of reasoning, namely that the upper and lower part of the grouted connection provide resistance against the moment and the middle part, which contributes little resistance against the moment, is reserved for taking up the shear forces. Therefore, these shear keys are often located only in the middle part of the grouted connection.

The forces from chapter 3 are calculated for the new height and compared with the “old” values.

Forces needed for fixed height of 6 m.

R1	1349	kN
R2	-957	kN
R3	3181	kN
R4	6574	kN

Table 14: Governing values for height of 6 m.

Forces needed for modular height of 8 m.

R1	1212	kN
R2	-1061	kN
R3	2859	kN
R4	6328	kN

Table 15: Governing values for height of 8 m.

The maximum transverse force at the heaviest loaded hydraulic cylinder now becomes 967 kN.

With these new forces the same ANSYS model is run. Now the stresses due to pretensioning forces are even lower, with a value of 95 N/mm^2.

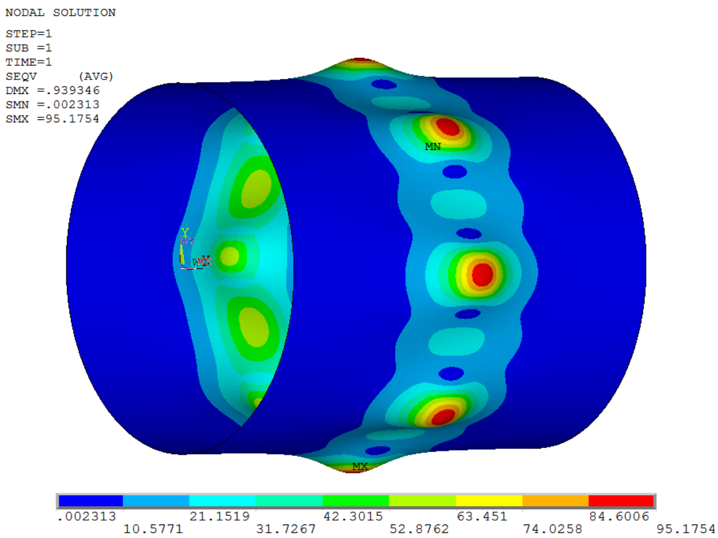

Figure 6.15: Stresses with new modular height.

However, a further stress reduction is not necessary for the Gwynt y Mor project. This modular system should be considered optional only if a stress reduction is required or to avoid contacting the TP wall at the locations of the shear keys.

6.5 Lower flange ring

Also the load application to the lower part of the TP needs to be checked.

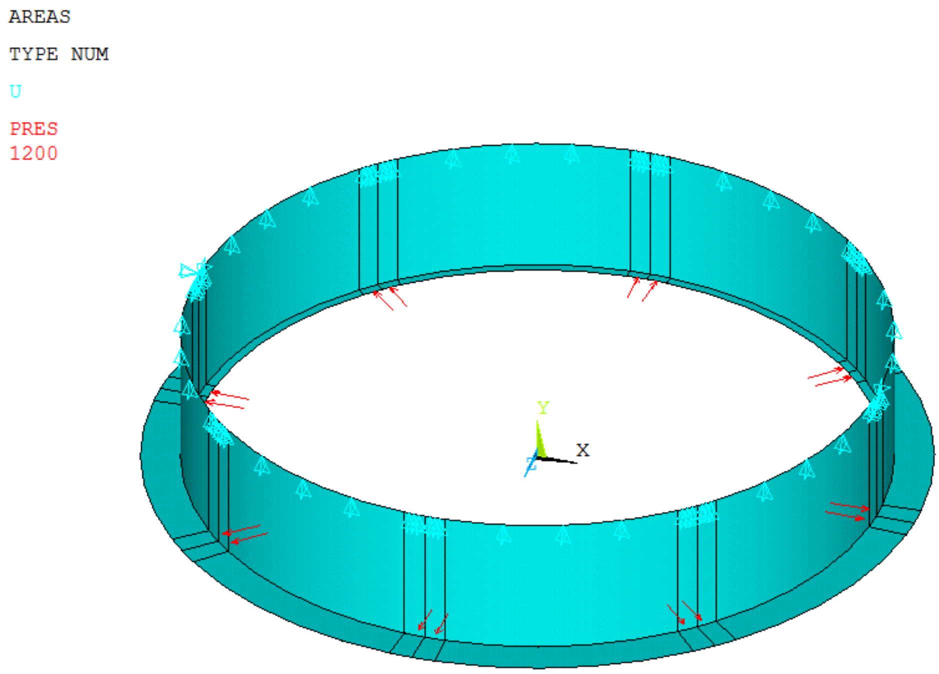

Figure 6.16: Load application to lower flange

A much lower force is introduced here. Only a minimum pretension force of 240 kN is needed, if the least loaded jack is set to zero. Here too a margin is needed, so a pretension force of 360 kN is used. The flange is also more efficient in resisting forces working in its plane. With a thickness of 40 mm and a height of 350 mm it can withstand much of the load. Part of the load will be transferred to the TP wall, therefore also the lower 1000 mm is modeled.

The model is constrained at the upper edge along the entire circumference in vertical direction. On two locations the model is constrained in z-direction and only on one location constrained in x-direction. This makes the model constrained in all directions, while still being able to freely deform in radial direction.

The load is applied over a length of 300 mm.

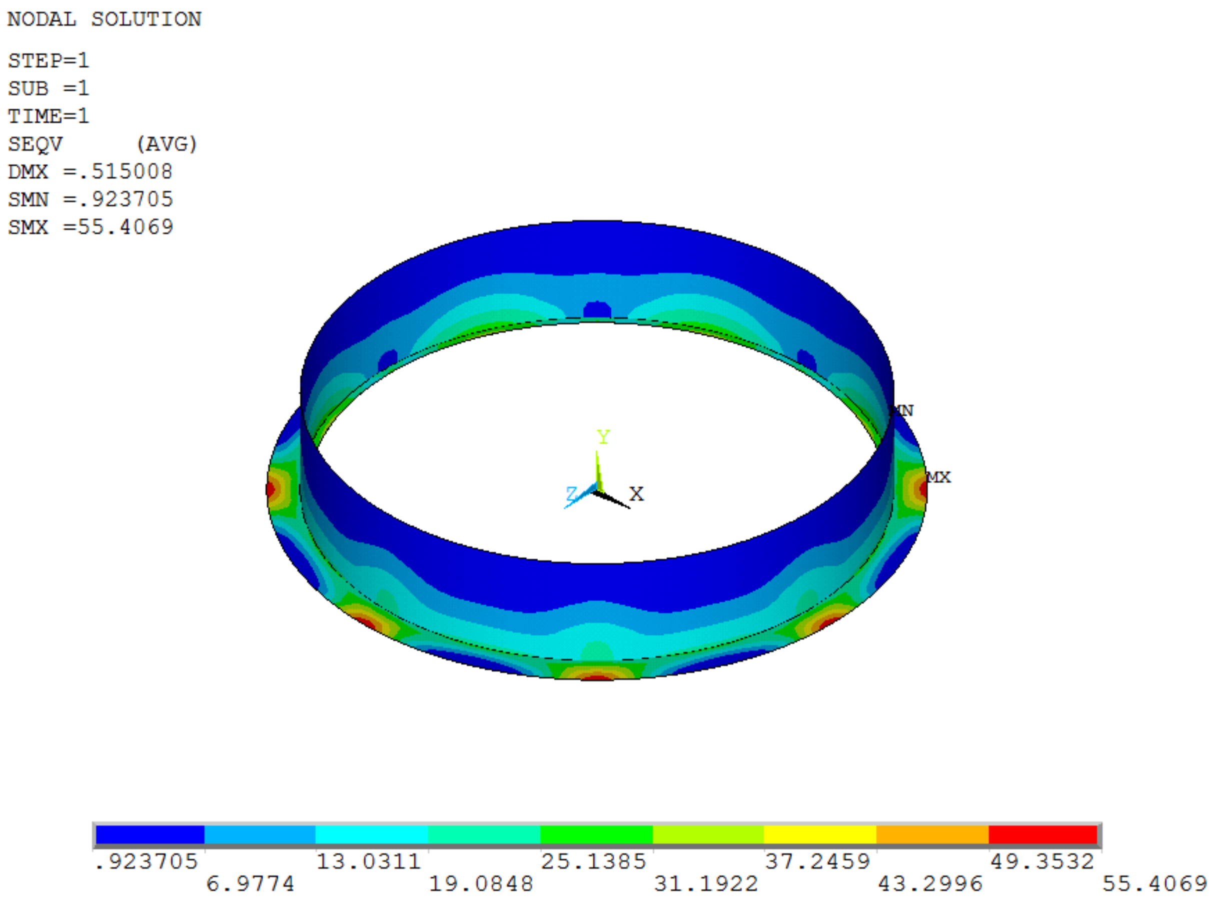

Figure 6.17: Peak stresses in lower flange

The stresses remain within the set boundaries.

6.6 Attachments on outside of TP

On the outside of the TP various kinds of attachments are found. Here it is checked what the influence will be of the stresses and deformations of the TP on the attachments.

For the Gwynt y Mor TP, a boat landing consisting of a ladder and fenders on either side of the ladder is connected to the TP approximately in the area where the pads of the hydraulic cylinders make contact with the TP. Here the peak stresses and deformation could cause stresses in the ladder connection.

A model is built in ANSYS with the load application directly below the ladder connection.

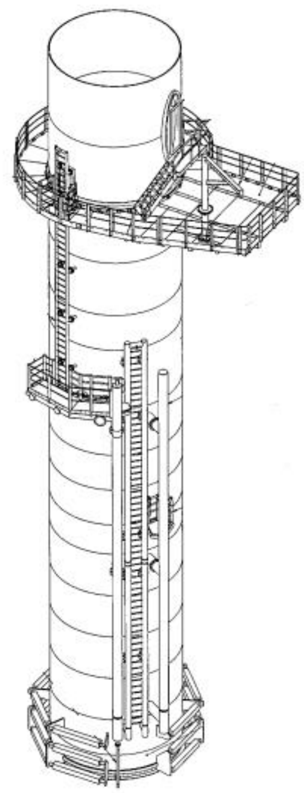

Figure 6.18: Attachments on outside of TP

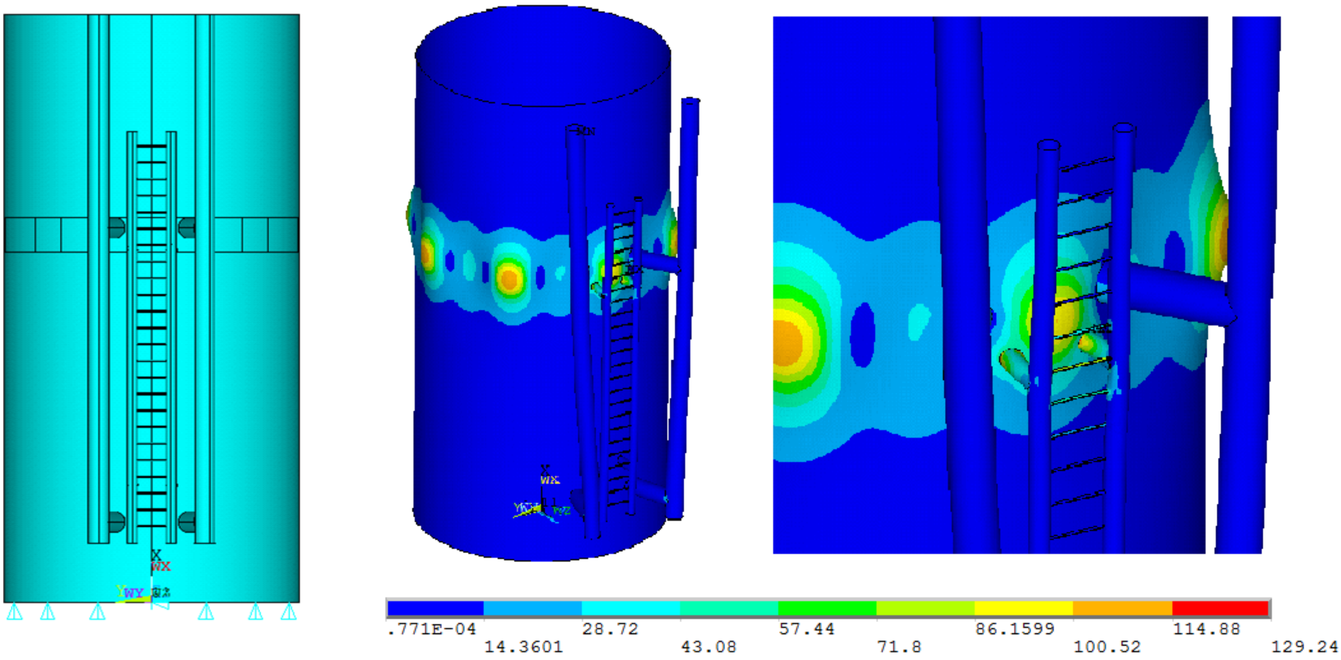

Figure 6.19: Stresses in connection attachment

In above figure the deformation is exaggerated. The peak stress is found in the connection of ladder to the TP. Multiplying this value with 1.24 a maximum stress is found of 160 N/mm^2. However, the allowable stress is also higher, with a maximum of 213 N/mm^2.

6.7 Range of prestressing

The maximum stress that occurs due to acceleration if no attachments are located near the load application equals 115x1.24=143 N/mm^2. For this situation the allowable stress is 189 N/mm^2. This means an extra capacity exists of 46 N/mm^2. This extra capacity can be used to increase the prestressing force if necessary. The maximum prestressing force equals 2019 kN, so that after acceleration a peak force of 2356 kN will produce a stress of 189 N/mm^2.

The maximum stress that occurs due to accelerations if the attachments are located near the load application equals 160 N/mm^2. For this connection the allowable stress equals 0.6 x 355 = 213 N/mm^2 , because of the much smaller thickness. So also here an extra capacity exist that can be used to increase the presstressing force, of which the maximum value is 2029 kN.

Of above two maximums, 2019 kN is the limiting maximum prestressing force. In chapter four the minimum prestressing force was calculated to be 337 kN. Then was chosen for a value of 1433 kN. In chapter eight the pads and potential friction will be calculated. From this it might prove necessary to increase the prestressing force.

6.8 Conclusion

This chapter was mainly concerned with the application of the load exerted by the hydraulic cylinders to the Transition Piece. Only the static situation was calculated, because the stresses occurring when the TP is accelerated would simply be increased by a factor of 1.24 of those of the static situation. This makes for much simpler analysis.

The stresses resulting from the load application turned out to be higher than allowed. Attempts have been made to reduce these stresses. First the use of contact element was tried. This was partially successful. The stresses were reduced but some unexplained side effect were observed. From this it is concluded

Further attempts to reduce the stresses were successful by simply increasing the area of load application. This was done for several different areas and proved effective. However, there are limits to the size of the pads that can be used. Because increasing the area of the pad also means increasing the thickness necessarily and inside the TP space is limited. Here, the arbitrary limit was set at 600x600 mm.

Optionally , a modular system can positively influence the force distribution, in which the height of the tubular element can be increased to as high as possibly fits inside the TP. This makes it better suitable for different TP's and also for future, possibly higher TP's. Due to this new height, the axial jack forces can be reduced by 10%.

Also, this modular system ensures that the pads will make contact with the TP wall above the shear keys. These are located only over a relative small band in the middle of the grouted connection. The modular system can be such that the jacks will be close to the internal platform as thus do not conflict with the shear keys.

Attachments on the outside of the TP are not limiting for the stress design.

The maximum prestressing force equals 2019 kN.

7 Model seafastening

In this chapter the seafastening structure itself will be explained, modeled and calculated. This is done in ANSYS, as it provides the necessary insights into the maximum stresses and the stresses located at the connection between the tubular element and the grillage. Furthermore, it is interesting to view the stiffness relation between the seafastening and the TP itself, especially the deformation of the whole system.

For is thesis, the seafastening structure is modeled upon the existing grillage of the Gwynt y Mor project. This was one of the secondary requests by SHL. This existing grillage can then be reused, with some slight modifications.

7.1 Build-up of the model

The original grillage is displayed in figure 7.2. The new grillage with the necessary adaptations is displayed in figure 7.1. The purpose of the grillage is to spread the load and guide these to strong points in the ship . The dimensions of the grillage thus stem from the distance between the frames and bulkheads. The I-beams that make up the grillage are laid on bearing plates that are positioned above the crossings of frames and/or bulkheads. At these location also wingplates are welded to the beams and deck.

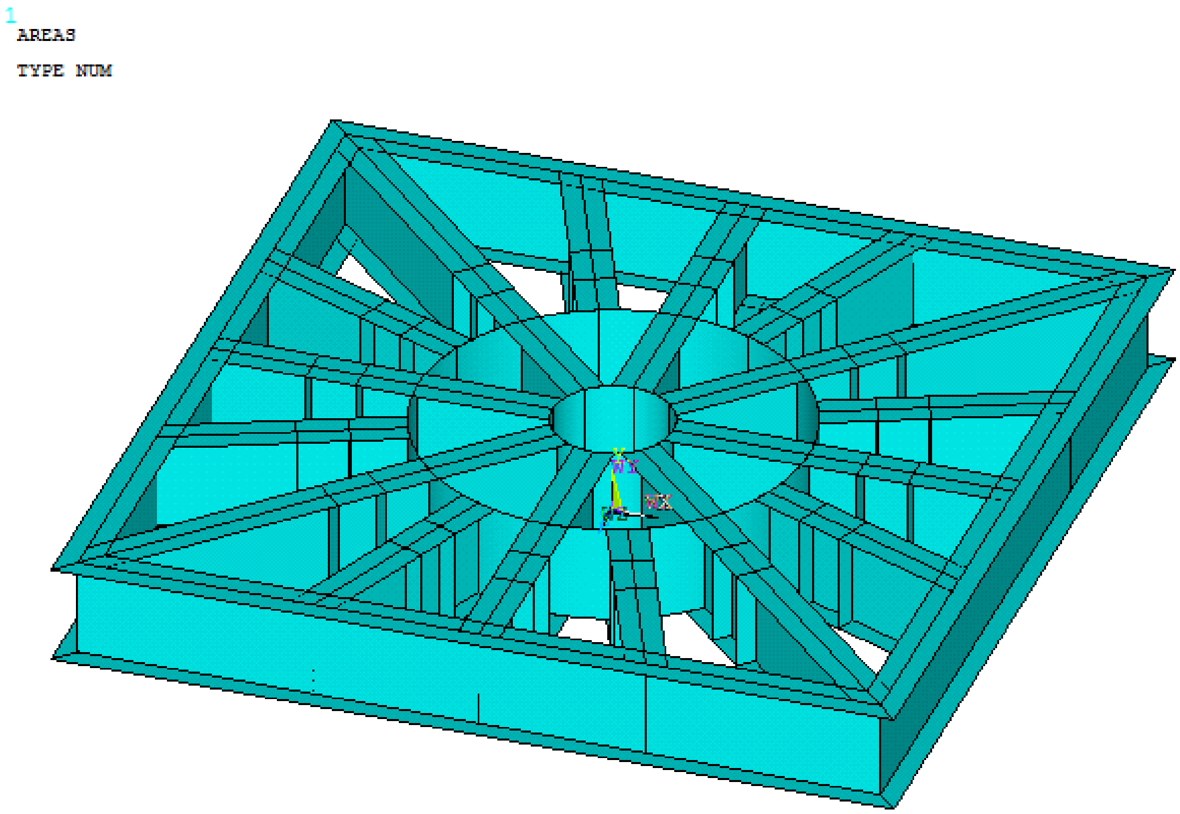

Figure 7.1: Build-up of the model seafastening including grillage modifications

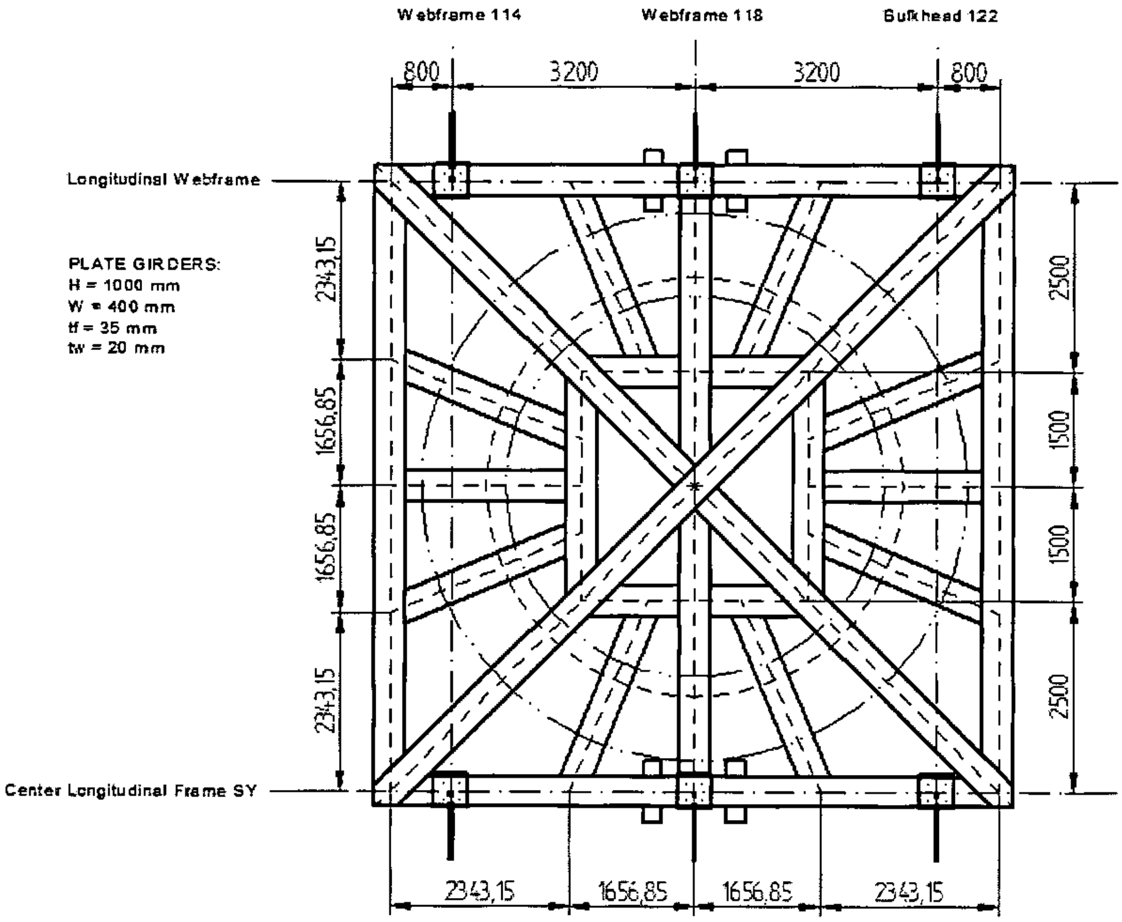

Figure 7.2: Existing grillage Gwynt y Mor

The beams are build-up out of plates and resemble a HE 1000 beam. The flanges are 400 mm wide with a thickness of 36 mm, the webs are 20 mm thick and 1000 mm high, the plate stiffeners are 20 mm thick, and the wingplates are 30 mm thick. These dimension apply to both the radial beams and the outer beams.

In the ANSYS model the same dimensions are used.

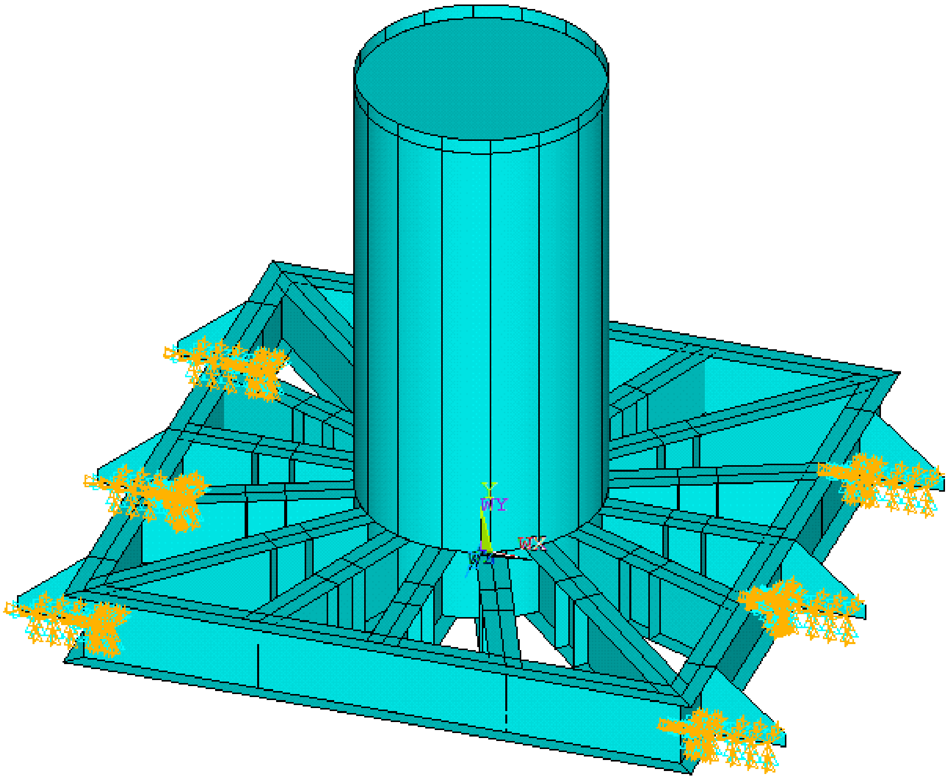

Figure 7.3: Complete model of seafastening

The model is constrained below the wingplates and the parts of the outer beams where the wingplates attach.

The load is applied to the top of the tubular element, both roll and pitch forces. In the most extreme situation, it could be that the entire TP stands on only one grillage beam, as was assumed in the derivation of the forces and the buckling analysis.

Figure 7.4 shows the result where both maximum roll and pitch forces are applied to the top of the tubular element and all the vertical downward force is introduced into the shortest grillage beam. This produces extremely high stresses. The maximum of which is 729 N/mm^2. Large part of the beam shows stresses above the yield limit, see figure 7.5. From this it is concluded that the current grillage is not fit for purpose.

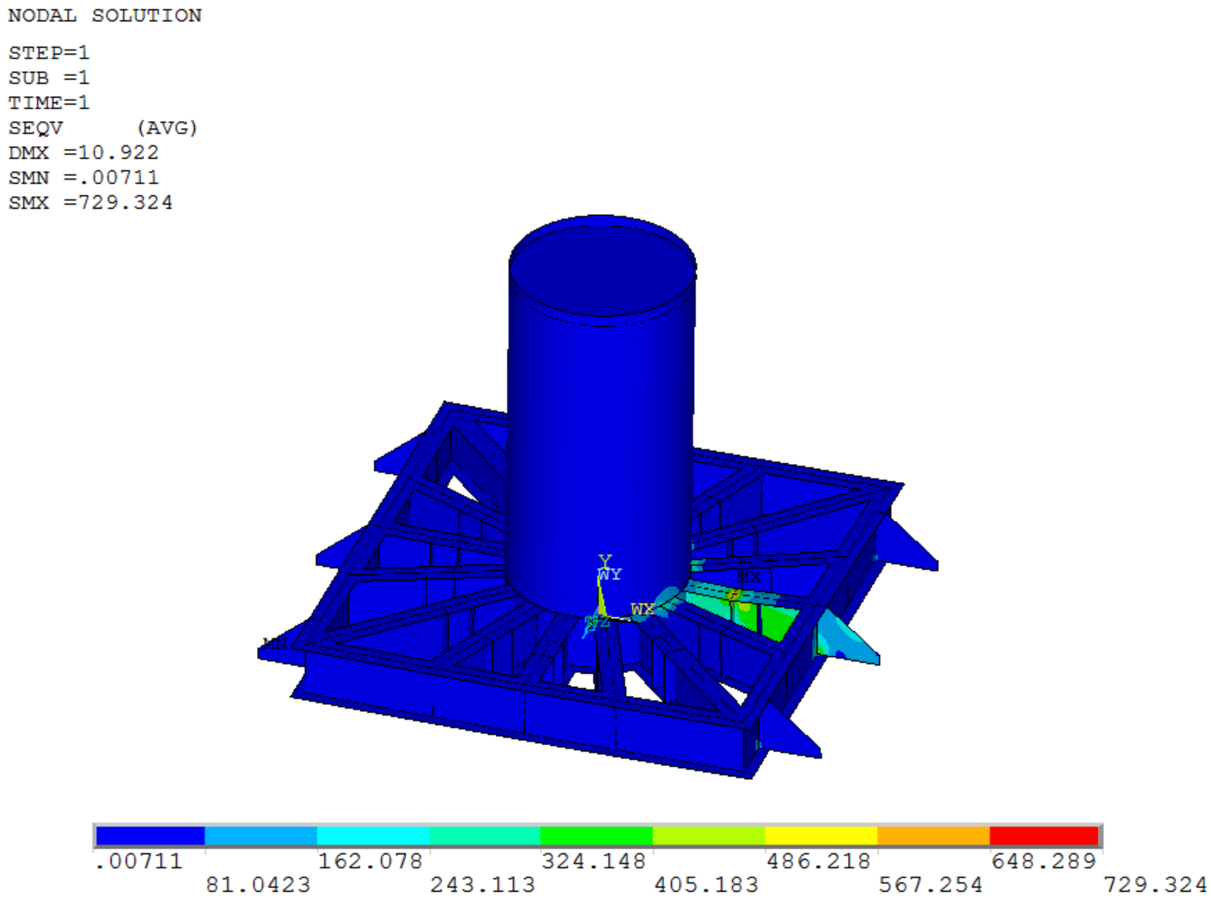

Figure 7.4: Model seafastening, 6 m high, max roll + max pitch + all vertical load on one beam

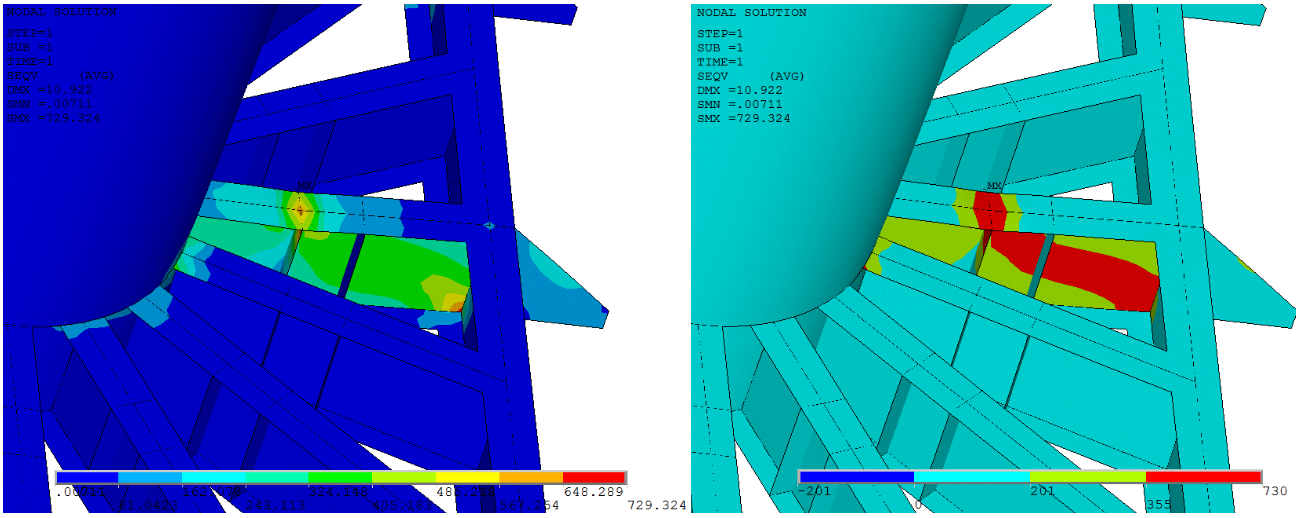

Figure 7.5: Peak stress, all vertical force down on one beam

It could be argued that the TP might stand on more than one grillage beam, due to deformation of the beam. From the spring model in chapter four, the displacement of the TP was relatively small, with a value of 3.77 mm. The displacement of the seafastening structure as calculated in above model is 10.92 mm at the top of the tubular element.

Given that the TP will rotate rigidly and not deform, the rotational angle is only $\tan^{-1}(2.45/1000)=0.14$ deg. When all the vertical load stands on only one grillage beam, it will deflect enough, so the two beam beside it will also start carrying the load. Figure 7.6 shows the stresses when three beams carry the load. The stresses are lower, now 530 N/mm^2, but still above allowable limits.

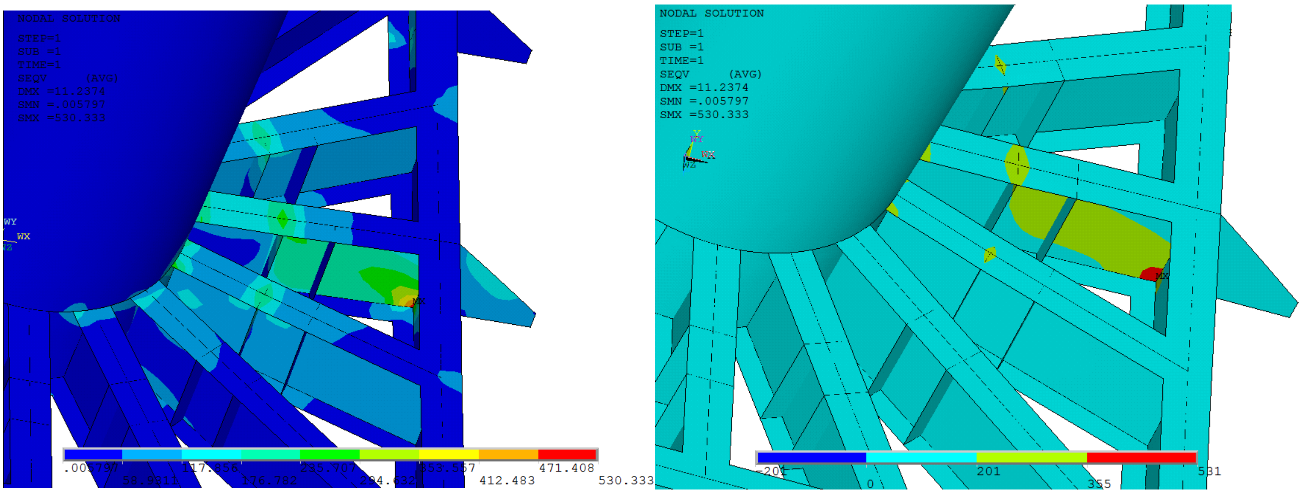

Figure 7.6: Peak stress, all vertical force on 3 beam; peak stresses are locally above yield

However, the angular rotations, displacements and deflections are so small that they fall in the order of the fabrication tolerances. Therefore it cannot be sure that more than one beam will carry load and it is not recommended to assume the TP will stand on 3 beams.

7.2 Modification

Simple modifications are recommended to lower the stresses in the grillage. In this case, the simplest ways would be to weld plates to the webs and flanges of the grillage beams. Increasing the thickness of the plate stiffeners to 40 mm, the flange from 35 to 45 mm, and the webs from 20 to 40 mm. These values make sense because the accelerations are also a factor 2 to 2.5 higher. Furthermore, applying the forces to the tube 6 m above the grillage creates a large moment that was previously spread over multiple beams.

Figure 7.7 shows the stresses after the thicknesses are increased. The peak stresses are still higher than allowed. However, these are very local at the transitions between beam and tube and partly due to the sharp edges in the model.

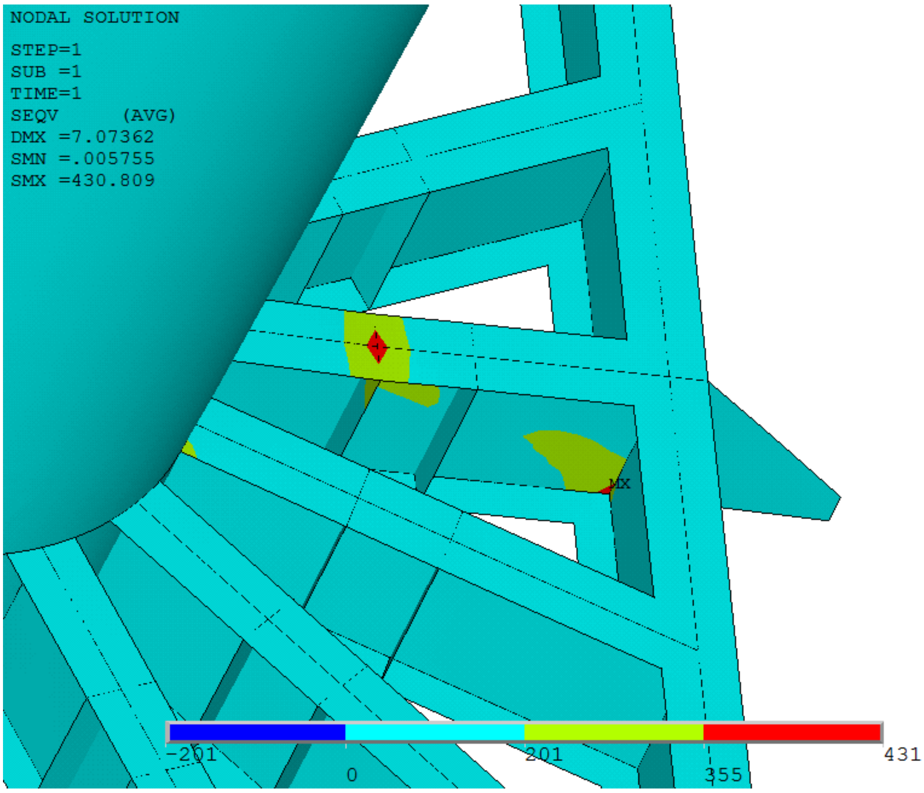

Figure 7.7: Stresses after modifications

7.3 Conclusion

This chapter has been about the seafastening structure itself, on a global scale, and to check if it could be possible to use it on the existing grillage of the Gwynt y Mor project. The grillage required a priori modification to accommodate the tubular structure. Figures 7.4, 7.5 and 7.6 showed that for the maximum accelerations the grillage is not sufficient.

Modifications to the existing grillage are most effective by welding plates to the webs and beams. The stresses are reduced, however local yielding still occurs.

It is recommend to make additional small modification at these highly stressed locations. Alternatively, a new grillage could be designed to better resist the high concentrated forces this method of seafastening produces.

8 Pads

Pads at the end of the cylinder piston rod make contact with the TP wall. These pads spread the load. In chapter 4 the force distribution on the TP was calculated. These were described by R1, R2, R3 and R4 in figure 3.4. In the model R1 and R3 were coupled. In reality they share the same hinging point between the pad, the diagonal rod and tip of the hydraulic piston. R1 is the force that goes into the hydraulic cylinder. R3 is the force that flows through the pad into the diagonal rod. Since the pad is not physically connected to the TP wall, a method of transferring this force is necessary.

8.1 Toothed grippers

The first method of transferring the force is the use of toothed grippers. These grippers are little hardened ridges on the outside of the pad. They are meant to penetrate the surface of the TP wall for one or two millimeters to physically interlock with the steel. This creates a very strong bond and is capable of transferring high shear forces

These grippers are already used to lift piles and plates and are very effective. Also, serrated wedges are sometimes used to grip test specimen in tensile tests set-ups.

Figure 8.1: Various uses of toothed grippers

Tabor [13] describes the workings of hardness tests. Indentation devices are used to press into a material specimen. The force used, the shape and size of the indenter and the indentation made provide information about the material properties.

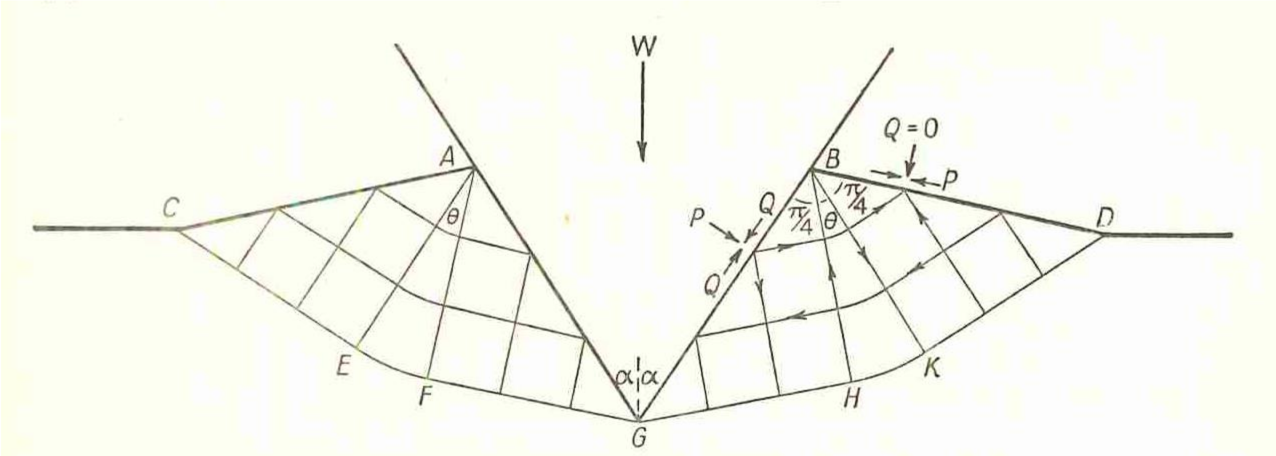

Figure 8.2: 2D model of indenter [13]

Figure 8.2 shows a 2D wedge shaped indenter. The shape of the indentation is similar for every length of the wedge. This analysis takes the displacement of the deformed material into account, as can be seen by the “piling up” of material next to the wedge.

The angles θ and α are related trough the following:

$$\cos(2\alpha - \theta) = \frac{\cos(\theta)}{1 + \sin(\theta)}$$

The pressure normal to the wedge shaped indenter is given by:

$$P = 2k \cdot (1 + \theta)$$

In which:

$$2k = 1.15\,Yield$$

The above relations can be used calculate the necessary force to press a hardened steel wedge into softer steel. This is done for an example load of 1000 N.

Table 16 shows for various values of α the indentation depth D.

α is the semi-angle of the wedge and can be freely chosen.

θ follows from the choice of α.

P is the pressure normal to the wedge.

L1 is the length of the leg of the indentation

L3 is the thickness of the wedge, here chosen as 1 mm.

D is the indentation depth for the given load and angle.

P/2k is the variation of the P with α and is also shown in figure 8.3

W= 1000 [N] 1 [kN]

α [DEG]	θ [DEG]	θ [RAD]	Yield	P [N/mm²]	L1 [mm]	L3 [mm]	D [mm]	P/2k
5	0,8	0,01	355	414	13,87	1,00	13,82	1,01
10	2,7	0,05	355	427	6,74	1,00	6,64	1,05
15	5,4	0,09	355	447	4,32	1,00	4,17	1,09
20	8,9	0,16	355	472	3,10	1,00	2,91	1,16
25	12,9	0,22	355	500	2,37	1,00	2,14	1,22
30	17,3	0,30	355	532	1,88	1,00	1,63	1,30
35	22,2	0,39	355	566	1,54	1,00	1,26	1,39
40	27,4	0,48	355	604	1,29	1,00	0,99	1,48
45	32,9	0,57	355	643	1,10	1,00	0,78	1,57
50	38,7	0,68	355	684	0,95	1,00	0,61	1,68
55	44,7	0,78	355	727	0,84	1,00	0,48	1,78
60	50,8	0,89	355	770	0,75	1,00	0,37	1,89
65	57,2	1,00	355	816	0,68	1,00	0,29	2,00
70	63,6	1,11	355	861	0,62	1,00	0,21	2,11
75	70,1	1,22	355	908	0,57	1,00	0,15	2,22
80	76,7	1,34	355	955	0,53	1,00	0,09	2,34
85	83,3	1,45	355	1002	0,50	1,00	0,04	2,45
90	90,0	1,57	355	1050	0,48	1,00	0,00	2,57

Table 16: Indentation depth D for various angles α

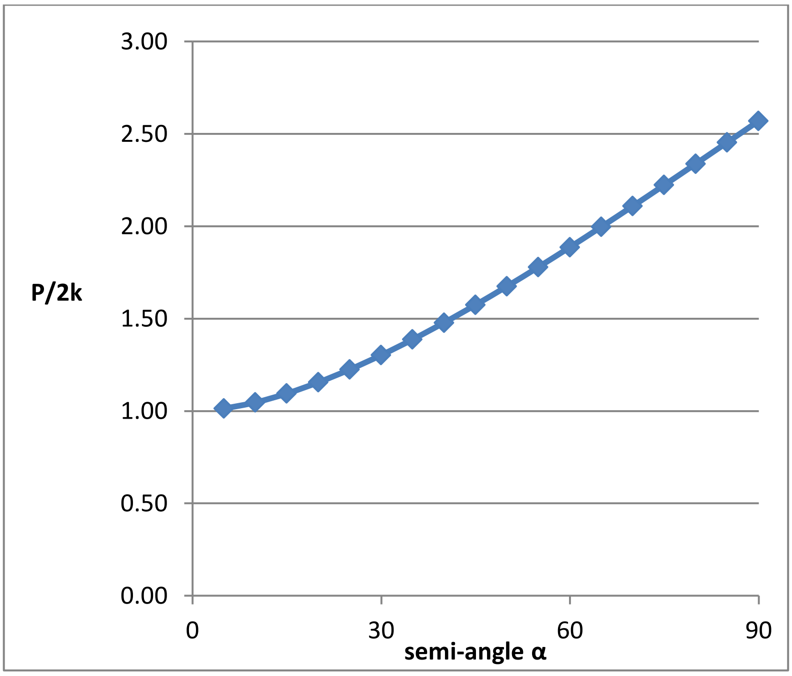

Figure 8.3: Variation of P with semi-angle α

So, for a wedge of 1 mm thick and an angle 2α of 60° and a load of 1 kN, the wedge can be pressed 1.63 mm into the steel.

The next step is to choose an angle α. If the angle is small, little force is needed to press into the metal, but the cross section of the wedge is also small and could thus easily break when a transverse force is applied. If a large angle is chosen, it requires a high force to penetrate the steel. The penetration will be relatively shallow, and little force can be resisted in transverse direction because the softer steel of the indented metal will shear off.

Moderate values for α are most likely best, and here is chosen for an angle α of 30°. This makes the complete angle 60° and is the same as the thread angle used for bolts.

A critical aspect here is that the wedge should never be the limiting factor, i.e., it should never fail before the indented materials fails. If the indented material is partly sheared off, it keeps resisting because there is enough material along the surface. If the wedge were to fail, there is nothing more left and then the system fails.

For the wedges a hardened material is used. 34CrNiMo6 has a ultimate strength of 1200 – 1400 N/mm^2, when the plate thickness is less than 16 mm. The design strength is 1000 N/mm^2. It is checked if the wedge will fail through shear at the plane that is just outside the indentation.

Rp(0,2) is material properties from 34CrNiMo6

τ allowed is Rp(0,2) /√3

α [DEG]	F-max [N]	F/W	Rp(0,2)	τ allowed [N/mm²]	shear plane wedge [mm^2]	shear strength wedge [N/mm^w]	U.C.
5	5693	5,693	1000	577	2,42	1396	4,08
10	2793	2,793	1000	577	2,34	1351	2,07
15	1802	1,802	1000	577	2,24	1292	1,40
20	1291	1,291	1000	577	2,12	1224	1,05
25	972	0,972	1000	577	2,00	1154	0,84
30	750	0,750	1000	577	1,88	1086	0,69
35	585	0,585	1000	577	1,77	1019	0,57
40	456	0,456	1000	577	1,66	956	0,48
45	354	0,354	1000	577	1,56	898	0,39
50	270	0,270	1000	577	1,46	844	0,32
55	201	0,201	1000	577	1,38	795	0,25
60	144	0,144	1000	577	1,30	749	0,19
65	99	0,099	1000	577	1,23	708	0,14
70	62	0,062	1000	577	1,16	670	0,09
75	35	0,035	1000	577	1,10	636	0,05
80	15	0,015	1000	577	1,05	605	0,03
85	4	0,004	1000	577	1,00	576	0,01
90	0	0,000	1000	577	0,95	550	0,00

Table 17: Unity check shearing off wedge

In which F-max is the maximum potential shear force. This follows from the load W and the angle α. F is the horizontal component of the normal pressure P, multiplied with the indentation depth D. This is assumed a maximum, because up to this point, the shear force applied by the wedge will simply take over the horizontal component from the other side of the wedge, and after this point the indented material will further fail through shear, and thus the pressure cannot increase.

F/W is the fraction between the normally applied load and the shear force, and can be seen as the coefficient of friction.

Rp(0.2) is the design value of the hardened wedge material.

τ allowed is the maximum allowed shear stress.

Shear plane wedge refers to the cross sectional area of the wedge at the location that is not penetrating the TP wall.

Shear plane strength is the shear plane area multiplied with the allowable shear stress.

U.C. is F-max/shear strength wedge.

As can be seen in table 17, for low values of α the wedge is the most critical part and should thus be avoided. High values of α do not provide enough friction (F/W). For angle α equals 30° the unity check is 0.69.

The total length of the wedges per pad should be determined next. A minimum and a maximum length can be calculated. The minimum value follows from the maximum shear force per pad divided by the maximum shear capacity per 1 mm thickness of wedge.

So, for α=30° a F-max is found of 750 N. The maximum shear force of the heaviest loaded pad equals 1070 kN. From this a total length of 1427 mm of wedge follows per pad as a minimum length.

The maximum length is governed by the maximum force normal to the pad, in this case 1770 kN. If there is too much length of wedge, the force is not sufficient to press it completely into the TP wall. If 1 kN can be used to press this particular wedge with a width of 1 mm into the steel, than 1770 kN can press a wedge with a width of 1770 mm into the steel. So, this is a maximum value.

L wedge min. = 1427 mm

L wedge max. = 1770 mm

It is recommended to use the maximum length of wedge. Given this length and maximum normal force, it has a capacity of 1.24 the occurring shear force. Using the maximum prestressing of 2019 kN as described in chapter 6, and accompanying total wedge length of 2356 mm, the capacity increases to 1.65 of the maximum occurring shear force. It is further recommend to use this maximum prestress.

The use of small wedges pressed into the metal could raise question, because they could be initiation points for fatigue cracks. Although this is true, the monopile on which the TP stands once on location are lifted using so called Internal Lifting Tools, which grip the steel in a similar manner. These monopiles are subject to the same loads as the TP. So, if it seems to be no problem for monopiles, it may be also no problem for TP's. Furthermore, the inside of the TP is also provided with shear keys, also known as welt beats. These are then also initiation points for fatigue. And finally, the inside of the TP, at least where these grippers leave their indentation, is grouted. So these indentations are also grouted and would thus provide with more grip for the grout.

8.2 Friction pads

Alternatives for the wedge shaped indenters could be friction pads. These do not penetrate the surface of the TP wall and leave no marks.

A high coefficient of friction (CoF) is needed. The normal force equals 1770 kN, but could be as much as 2356 kN. The transverse force equals 1070 kN. The fraction is 0.60. There are materials that would provide high coefficients of friction. Especially the softer polymers. Table 18 shows various polymers that have high coefficients of friction against bearing steel at room temperature.

Polyamide 66	$\mu = 0.57$
Polyoxymethylene	$\mu = 0.45$
Polyether ether ketone	$\mu = 0.49$
Polyethylene terepthalate	$\mu = 0.68$
Polyphenylene sulfide	$\mu = 0.70$
Polyetherimide	$\mu = 0.43$

Table 18: Overview various high friction materials[16]

There are two main problems with these materials and their CoF's.

The first is that although they provide high friction, they often don't have high resistance against shearing. This means the material on the pad could deform quite substantially, which is undesirable, because that would require the TP wall to displace a significant amount before the required transverse resistance is reached.

The second problem is that these CoF's are often measured in laboratories under carefully controlled circumstances. Scientists want to know the CoF for a particular material and thus make sure the specimen is not contaminated. In reality, outside in normal operating conditions, on the TP wall surface there is rust, dust and maybe grease. The same applies to the surface of the friction pad.

One industry that might prove interesting for solving above problems is the automotive industry. Brake pad technology has been developed extensively and would also be suitable for this application. Several benefits of brake pads linings are that they usually operate in outdoor conditions, meaning wet, rusty, dusty and in general exposed to the elements. Furthermore, they are designed to resist high normal forces and high shear forces. Both occur also in this situation.

Friction coefficients of brake pad lining used in race cars can be up to 0.55 to 0.62. For normal cars this is 0.35 to 0.42. Although it is difficult to capture the complex workings of interactive surfaces into one single numerical value. Friction depends on many different factors, such as temperature, sliding speeds, different materials used, surface cleanness and contact pressure. These are called tribosystem related variables, named after the science tribology.

It is difficult to know the composition of these brake pad linings. It has an inherently secretive nature for competitive reasons and are rarely mentioned in open literature. On the upside, the number of different compositions are nearly endless, and so it is likely that a suitable composition exists for this specific application. Brake pad linings are designed for high friction, but also for a constant CoF during braking, high temperatures and low wear. These tradeoffs naturally come at a cost, namely lower CoF's. Since these attributes need not be present in the current application, there will be compositions that provide higher CoF's.

The weakness of this option is the uncertainty of the amount of friction produced, due to surface contaminations such as dust and grease.

Figure 8.4: Typical brake pad linings

8.3 Conclusion

The pads that make contact with the TP wall not only transfer high axial forces, but also relatively high transverse forces. Since the pads are not physically connected to the TP wall, this transverse force needs to be carried over via friction. Several high friction materials have been mentioned that would provide high enough friction coefficients. However, these materials do not perform well under high normal and shear forces. Typical friction materials and technology that does perform well under these condition are brake pad linings from the automotive industry. Although it cannot be certain that these brake pads provide the required frictional force for the high accelerations that are used for this design.

It is proposed to use toothed grippers or little wedge shape ridges to make small penetrations into the metal of the TP wall. It has been shown that this can be done with the axial force exerted by the hydraulic cylinders and this would provide enough frictional resistance.

Two changes would make the brake pad linings option more attractive. One: accept lower design accelerations. If this is done, the same axial force exerted by the hydraulic cylinders can be used, which would provide the same fiction force. The required friction force however needs to lower. Two: if the stiffness of the hydraulic cylinders were to increase, they would contribute more to resisting the overturning moment and less transverse force on the pad would be required. The effect is twofold. Namely, the reduced required transverse force and the higher normal force produces a higher frictional force.

9 Final detailing

This chapter will show a few details that are crucial for this design to work. First a top view is shown. Eight hydraulic cylinders including the pad that make contact with the TP. The dashed lines shows the smallest diameter of the groutskirt. A clearance of 150 mm is used.

The hydraulic cylinders used are those of Enerpac, model RR-30024. Enerpac produces cylinders that are shorter than those of Vremac, but with the same stroke. The collapsed height of the cylinder equals 943 mm. The diameter of the housing equals 311 mm. The stroke equals 609 mm. With these dimensions, it is possible, when the pistons are retracted, to lower the TP and groutskirt past the cylinders safely. The cylinder have a stroke long enough to bridge the distance.

The cylinders are supported at the back with a ball joint. This allows for (small) rotations of the cylinder that are necessary, both in vertical and horizontal direction. Vertical rotations are due to the diagonal steel rod, that has a fixed length and is also hinged at the pad. This makes the system hinged at three points.

Horizontal movement is due the fact that the TP will translate, although only slightly. If the cylinders were connected rigidly, high stresses would result.

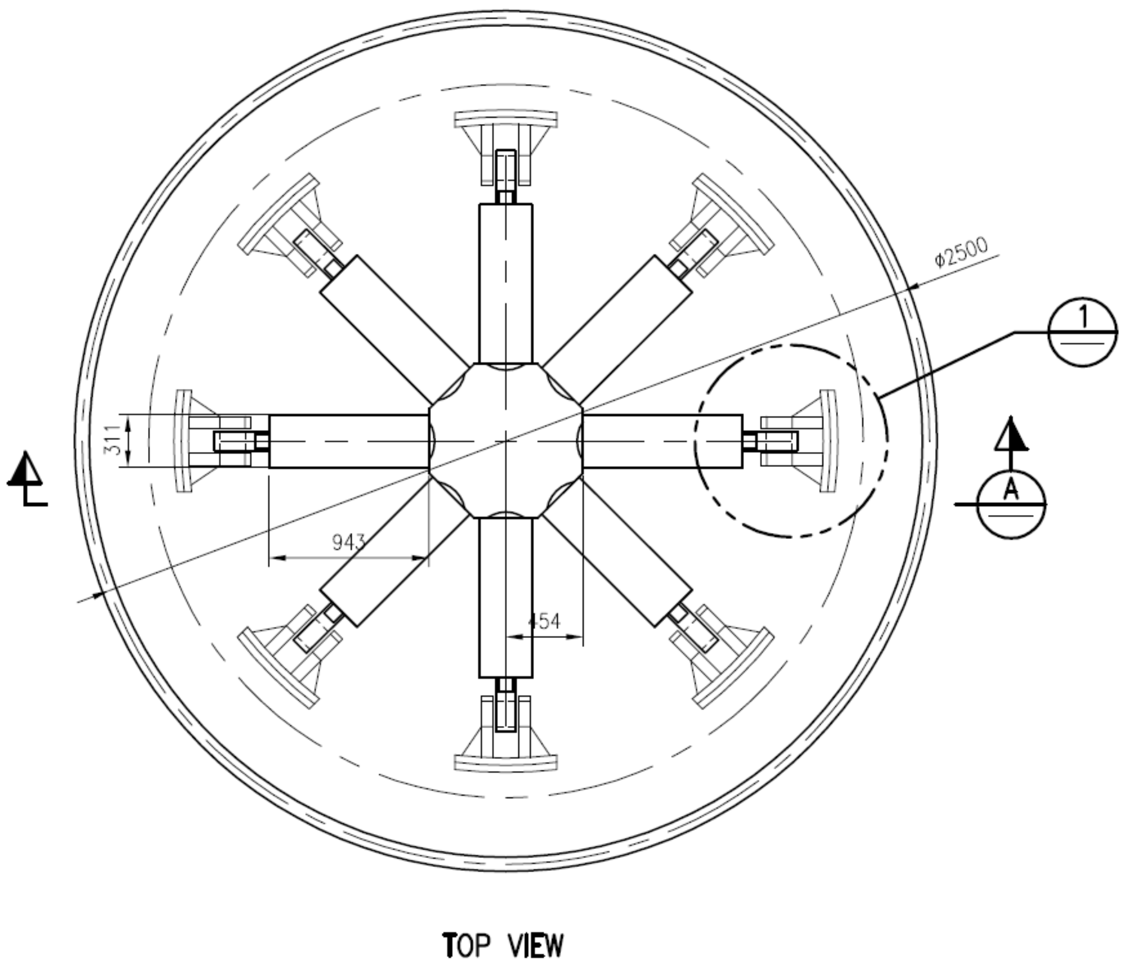

Figure 9.1: Top view of cylinder configuration

Figure 9.2 shows the side view of a cross section. Here the clearance between the pads and the groutskirt can be observed better. Note that the height of the cylinders in the figure is not corresponding with the real value. At the bottom, cylinders are positioned under an angle against the lower flange. The angle is such that the centerline of the piston crosses the middle of the flange face. This prevents a moment from occurring in the piston rod. Furthermore, since this cylinder is also supported such that it allows small rotations, the pad can slide over the grillage beam and thus “find” the TP flange.

The lower cylinders are located outside the tubular, and use the tubular as an abutment. This can be done because less stroke is required than for the upper cylinders. Less stroke is necessary because the groutskirt need not pass here and the pad can already start much closer to its final position. Also important is that this prevents the need for holes through the tube at the bottom, where it is most stressed and connected to the grillage beams.

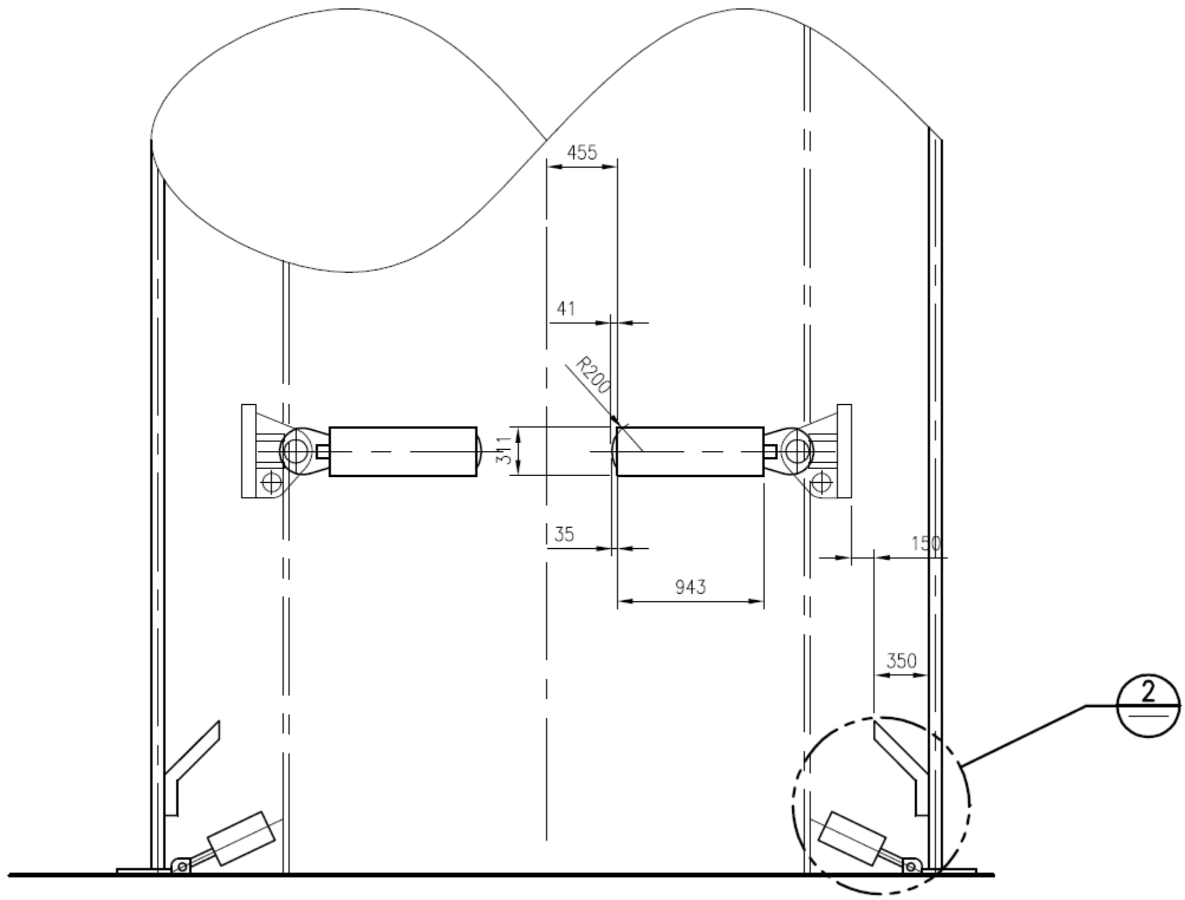

Figure 9.2: Side view of cross section

Figure 9.3 shows a more detailed illustration of the pads and their connection to the piston rod. The pad and piston rod are connected via a bearing that allows for small rotations of the pin. This gives the pad the ability to move slightly relative to the hydraulic cylinder. Notice also that the bearing is not centered in the plate. It is specifically designed to be eccentric. This is uncommon but for this case very suitable, because the piston rod will never have to pull on the pad, and therefore the thickness doesn't have to be equal all around the bearing. The advantage this offers is reduced length of the pad and cylinder combination. In the setup displayed in figure 9.1 it can be seen that space is scarce and approaching critical values. That justifies using an eccentric design.

In the side view, elevation B, a second bearing is located in the pad. Here the steel diagonal rod is connected to the pad.

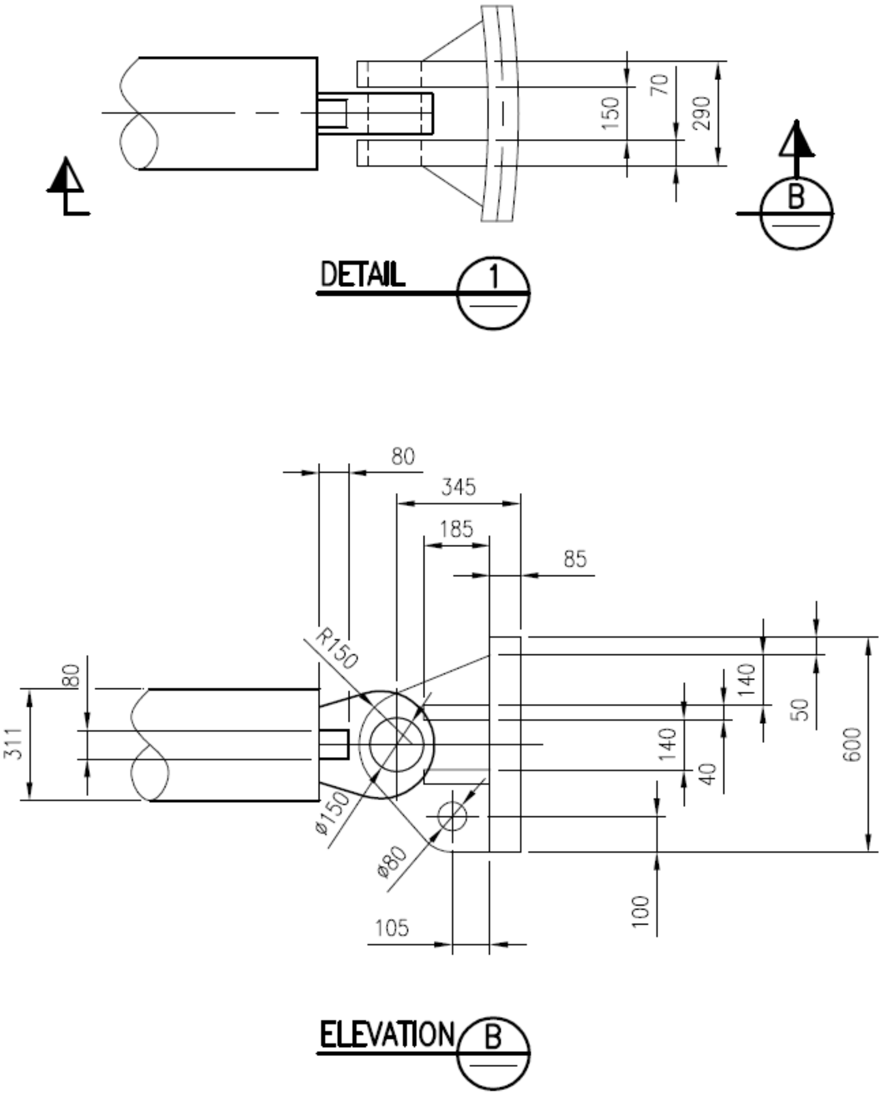

Figure 9.3: Details of pad and pad connection

Figure 9.4 shows the principle solution of supporting the hydraulic cylinders. At the top of the figure, the central horizontal abutment is shown. Eight cylinders transfer their forces trough a saddle or sphere like structure. Behind these saddles, a plated structure transfers the forces, in large part towards the other cylinders, and a small part to the tubular element of the seafastening. In the middle of the figure, the side view of the horizontal abutments is shown. At the bottom of the figure the vertical support is shown. This is a fork like structure with rubber blocks in them. Both the saddle, shaped as a bowl, and the rubber block accommodate small horizontal and vertical movements of the cylinders. This is necessary to prevent high bending forces in the cylinders.

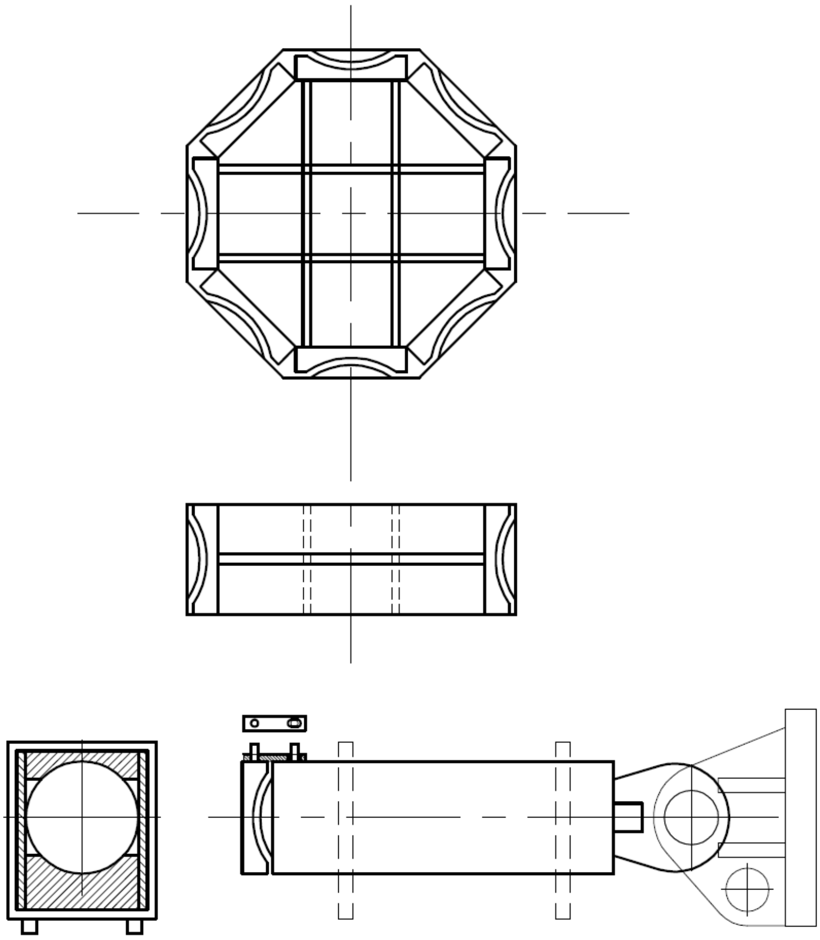

Figure 9.4: Principle solution of cylinder support

Figure 9.5 shows a more detailed view of the lower hydraulic cylinder securing the lower flange. It can be clearly observed that the groutskirt doesn't need to pass het cylinder and thus the clearance can be reduced. Furthermore, the angle of the cylinder is such that the centerline crosses the flange halfway through, and therefore no moment occurs. The support is similar to the cylinders at the top, which allow for small rotations.

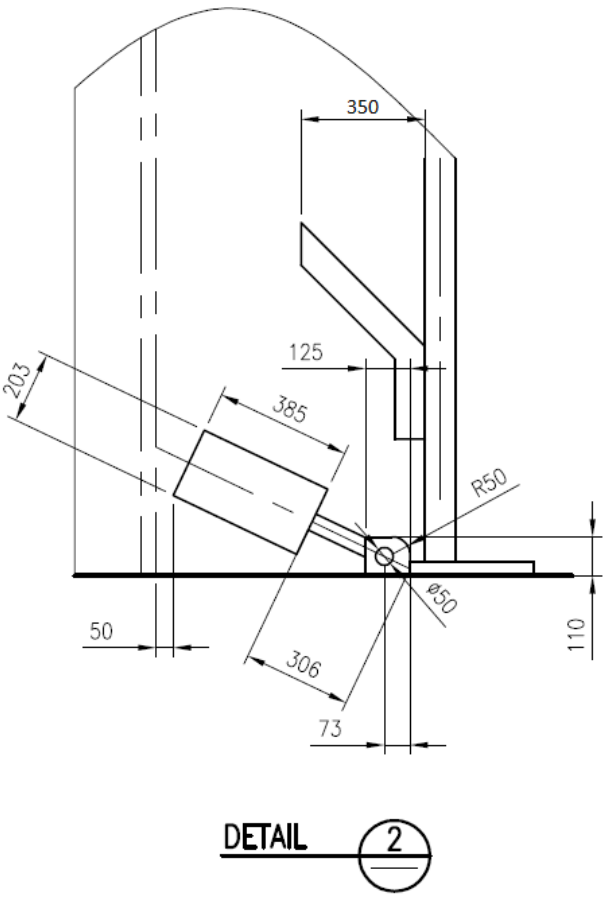

Figure 9.5: Detail of lower hydraulic cylinder pressing against lower flange

Figure 9.6 shows the top view of the bolted connection. This makes the seafastening modular, so it can be adapted to TP's having different heights of internal platforms. Future TP's may also be higher. By making the system modular, the cylinders can located as close as possible to the CoG of the TP. This positively influences the force distribution. Maybe the most ideal situation would be if the cylinders could be located in the CoG. Then no overturning moment would occur and thus no transverse force on the pad. Although still a large moment would occur in the grillage.

The bolted flange is located at the inside of the tubular at a height of 5 m.

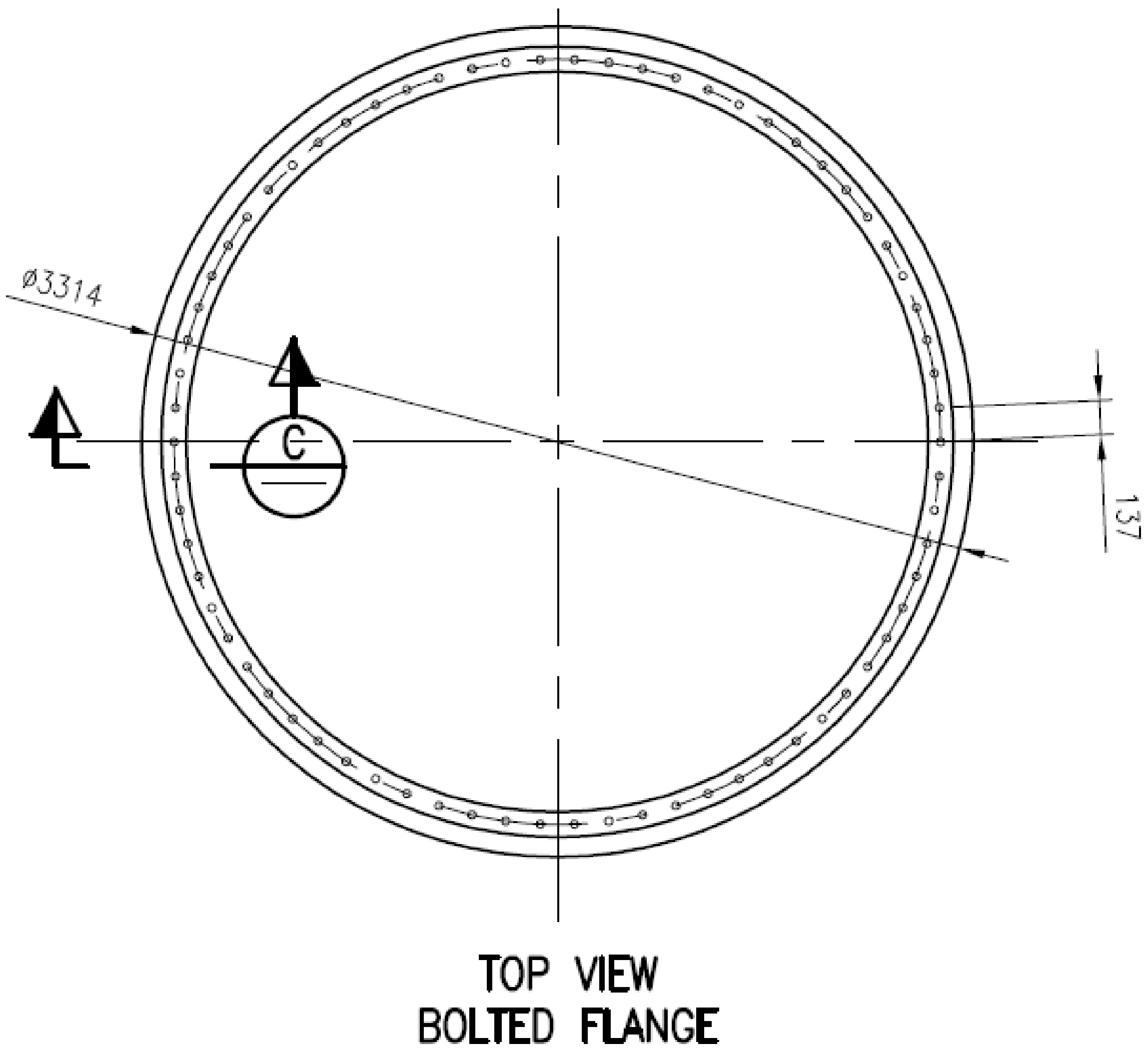

Figure 9.6: Top view of bolted connection used to make the seafastening modular.

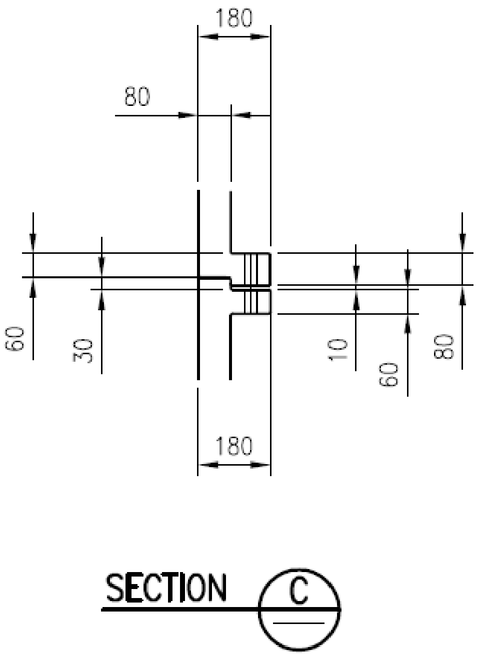

Figure 9.7: Dimensions of bolted flange

Figure 9.7 shows a cross section of the bolted flange. A space of 10 mm is left between the flanges where to bolts go through, so that when the pretension bolts are tightened, the wall of the tubular is pressed against the other part. This increases the stiffness and reduces the fatigue sensitivity.

In figure 9.8 the parametric view of the seafastening is sketched. As in figure 9.9, where the sliding guides are displayed. The guides slides trough a casing or sleeves and needs to be counterweighted. This ensures that is will be at the top of the tube, until the TP is placed on it and presses it down. On the guide a catcher and edge are placed. This prevents the TP from moving towards the seafastening tubular. Thus both the seafastening and TP cannot collide with each other.

When the TP is completely lowered and stands on the grillage, the guides are located in between the grillage beams. Alternatively, the guides can also have one sleeve on either side of one grillage beam where no cylinders are located. This would alter the design of the guides slightly. An upside down U shaped guide would slide down over one of the grillage beams. This option is better if the space between the grillage beams is too small.

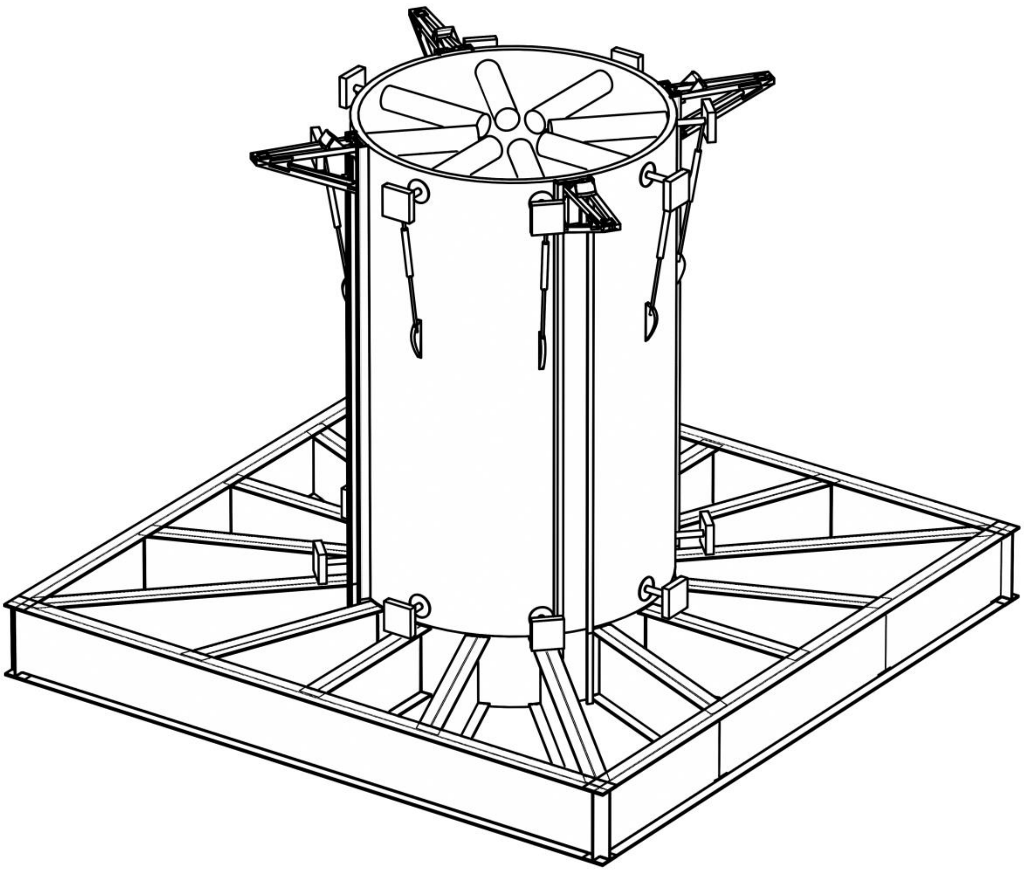

Figure 9.8: Parametric view of seafastening

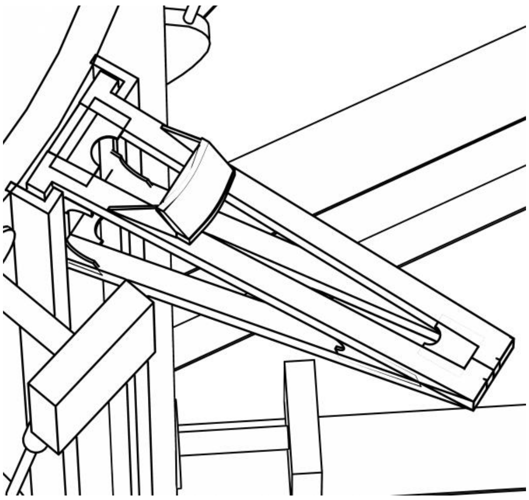

Figure 9.9: Sketch of sliding guide

10 Conclusion

The objective of this thesis was to invent a new method for seafastening offshore wind turbine Transition Pieces. This new method was supposed to provide several improvements over the current method, such as to be capable of withstanding higher accelerations, to require less time for activation and deactivation, and be safer.

A new method has been proposed. The method consists of a tube in upright position welded onto a grillage. The Transition Piece is lifted and lowered over the tube onto the grillage. At the top and bottom of the tube hydraulic cylinders are placed, which extends outwards toward the inner TP wall surface. This effectively fixates the TP in horizontal direction.

- Overall calculations have shown it to be capable of withstanding high accelerations. Nearly twice as high as the current methods. The accelerations are the highest for the vessel the Stanislav Yudin, in a seastate of 7.5 m significant wave height.

- Due to the use of hydraulic cylinders, the new method requires less time to be activated and deactivated. The crane lifts the TP when all seafastening is removed. When using bolts, there is a moment of time when the TP is not seafastened or only on a few bolts that are not sufficient enough to prevent it from tipping over. This moment where it stands unsecured on the deck is hazardous. Because the new method is faster, it reduces the time of an unsecured TP to a minimum, thus making it safer.

- The new method requires no manual labour at all, thus removing the potential for injuries.

- The force distribution exerted by the hydraulic cylinders is not significantly altered due to deformations of the TP. Therefore, when calculating the force distribution the hydraulic cylinders exert on the TP due to pretensioning and accelerations, it can be assumed that the TP is infinitely stiff. The hydraulic cylinders in between can be modeled as springs. The force distribution is now geometrically determined.

- An ANSYS buckling analysis showed that buckling of the TP wall will not occur for the maximum acceleration. Also a hand calculation was done to check the conclusion from the numerical model, as proposed by Rotter en Teng. This calculation also concluded that local yielding of the material will occur before buckling, and that local yielding does not occur under the given load.

- The area of load application needs to be sufficiently large to keep stresses below the set criteria. In this case an area of 600x600 mm per pad is needed. A smaller pad introduces the load in a more concentrated way and results in higher than allowed stresses.

- In ANSYS, modeling with contact elements can effectively influence the distribution of the load on the TP wall, thus reducing stresses. However, several side effects could not be explained. And in combination with the lack of validation, the results of the contact analysis are not used.

- A modular system must be used if further reduction of the stresses are required or to avoid conflict with the shear keys.

- Strength calculations have shown that the existing grillage of the Gwynt y Mor project is not sufficient enough to withstand the acting forces resulting from the high accelerations. Roll and pitch forces were applied to the top of the tube. High stresses resulted in the grillage beams and from this it is concluded that the existing grillage is not sufficient and needs modifications. The most obvious and effective modifications are to increase the thickness of the material by welding plated to the beams.

- Toothed grippers are capable of transferring the high transverse forces acting on the contact surface between the pad and the TP inner wall. The grippers are small wedge shaped indenters that penetrate the TP wall surface one or several millimeters to create an interlock effect and allows for the transfer of high forces. The alternative of toothed grippers are brake pad linings and could also provide enough frictional resistance but with much less certainty.

11 Recommendations

Several recommendations can be made to potentially improve the design further.

- Design for lower accelerations. The method used for the Gwynt y Mor project allowed a maximum acceleration of 3.57 m/s^2 in roll direction. The new method proposed in this thesis is designed for a maximum acceleration of 6.4 m/s^2 in roll direction. This allows SHL to sail unrestricted but also comes at a cost of a heavy seafastening structure. Reviewing the design accelerations could provide a value in between 3.57- and 6.4 m/s^2 which is more optimal.

- Alternative designs for the pads should be considered. In this thesis square pads were used to introduce the force into the TP. Pads that would be very wide and somehow connected to each other, forming sort of a ring, could prove very effective in securing the TP without causing high stresses.

- Also a closer look at the “grippers” on the pads is recommended. Questions remain, such as how much force will the rest of the pad introduce in the TP wall? What are the tolerances on these wedge shape grippers. When will they lose their “sharpness”? Can it be trusted to always have enough penetration?

- The seafastening has not been checked for fatigue. Ship motions causes loading that varies by nature, which cause stress fluctuations in the tension-compression range. This could make the seafastening prone to suffer from fatigue.

- An analysis of the repetitive loading on the hydraulic cylinders is required. This is a vital part of the seafastening. A thorough failure analysis provides valuable insights into the failure modes, maintenance needs and signs of wear.

- Lock nut cylinders are an interesting addition to the current system. The most important improvement this would provide is the reduced failure probability. A hydraulic system has many components, such as seals and valves, that could fail. Whereas a locknut cylinder would only have one failure mode, of which the workings are well understood.
  Tough, the use of locknut cylinders does change the stiffness of the system and thus the force distribution. In this case the axial force in the cylinders would increase significantly, resulting in higher stresses in the TP wall. Therefore, it was chosen not to use these in this design. However, for lower accelerations or in combinations with further stress reducing measures, this could be a further improvement of the system. Although it would require manual labour to tighten and secured the locknut bolts, and release them when on location.

- Research different configurations of hydraulic cylinders. Here was chosen for 8 symmetrically positioned cylinders. This is the only configuration that fits if they lay in one plane. Multiple planes could be imagined offering more space and different configurations. Also, for TP’s with a diameter larger than 5 m additional options become available. Adding hydraulic cylinders or deviating from the symmetrical layout towards a configuration where more cylinders are applied in roll direction than in pitch direction.

- The grillage from chapter 7 can be modified in more refined ways than simply making the plates thicker. Maybe even a completely new grillage needs to be designed.

- The curvature of the pads probably can influence the curvature of the TP wall. In chapter 6 it has been attempted to model such an effect with contact elements in ANSYS. If however, a properly working model could be build and also be validated with confidence, then some interesting gains can be made here. A stress reduction of 15% should be possible.

- This method of gripping an upright tube could also be integrated into the ships structure. In chapter 7 it was shown that large forces are introduced into the grillage and needed to be heavily reinforced. This is because that grillage was originally not designed for this type of loading. Integrating this method into the ship, e.g., several meters below deck, has the advantage that the CoG of the TP is closer to the centre of rotation of the ship, and therefore would experience lower accelerations. Furthermore, large horizontal forces can be transferred directly to strong points in the ship, e.g., frames, bulkheads and the deck. These can be transferred in the plane where the force works, instead of transferring large horizontal force via a long arm causing bending moments.

- The need for hydraulic cylinders against the lower flange should be reviewed. Alternatives that would make hydraulics superfluous attractive, because then, half of all the hydraulics can be removed. This saves maintenance and decreases the amount of components that could fail.

- The indentations from the toothed grippers could be fatigue initiation points. Further study is required to find out if this could be critical.

- No specific safety factors were used to calculate the capacity of the toothed grippers and the amount of friction they can produce. Since the indentation depth of the grippers is well within the range of fabrication tolerances of the structure, it requires further study to how high the safety factor should be.

List of references

[1] EWEA: European Wind Energy Association; http://www.ewea.org/statistics/offshore/
[2] Shell global solutions
[3] NREAP's: National Renewable Energy Action plans
[4] Sheringham Shoal Design Brief
[5] Meerwind Design Brief
[6] Riffgat Design Brief
[7] Gwynt y Mor Design Brief
[8] Roark's formulas for stress and strain; 7^{th} edition (2002) p.319
[9] Theory of elasticity, Timoshenko, 1934
[10] Theory of elastic stability, Timoshenko, 1961
[11] Hydraulic fluids, Hodges 1996
[12] Buckling of thin metal shells, J.G. Teng & J.M. Rotter, 2004
[13] Hardness of metals, Tabor, 1951
[14] AISC; American Institute for Steel Construction
[15] API; American Petroleum Institute
[16] Friction science and technology, P.J. Blau, 2009
[17] Economic design of circular metal silos, J.M. Rotter, 2001
[18] Engineering Analysis with ANSYS Software, Stolarski, Nakasone, Yoshimoto, 2006
[19] ANSYS Help
[20] DNV-RP-C205; Environmental condition and environmental loads, 2010

Appendix A: Clamps used in current method

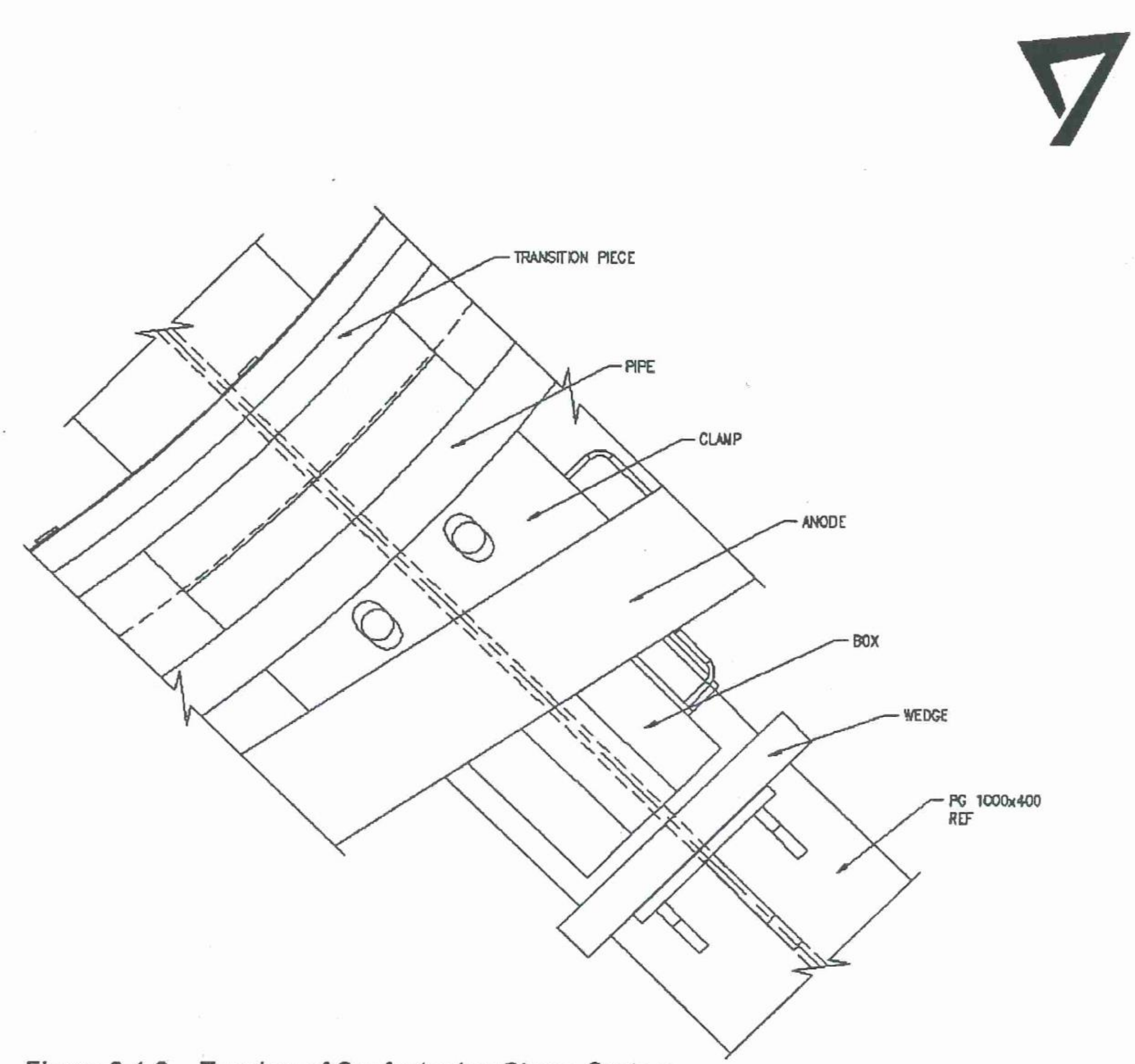

Figure 2.1.3 – Topview of Seafastening Clamp System

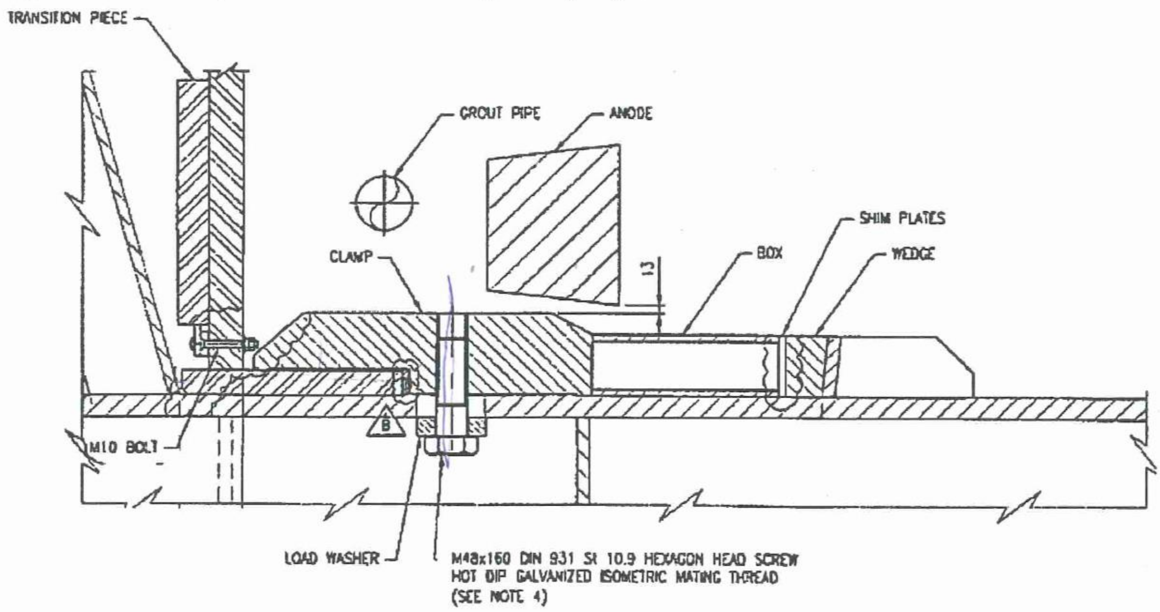

Appendix B: part of contract OWP Riffgat specifying accelerations

Specifications: Logistics for monopiles and transition pieces OWP RIFFGAT

1.8.2 Installation tolerances for the transition pieces

The following tolerances are to be adhered to in the erection of the transition pieces:

<u>Alignment / orientation of the transition pieces</u>

As the TP fittings are pre-installed and the installation of the TP is independent of the achieved installation tolerance of the monopiles, the transition pieces are to be erected respecting the following tolerances.

The permissible tolerance for the orientation of the installed transition pieces is therefore:

For all TPs ± 10° relative to true north.

Maximum acceleration values for the electrical components of the transition pieces when setting the TP on the MP:

- For static accelerations (gravity) the limits are set at 0.5 g vertical, 0.3 g lateral and 1.0 g longitudinal. All electrical components within the TPs are to be situated within the same alignment. The alignment of the TPs on board the HLV for optimal transport is to be established by the Contractor such that the abovementioned acceleration values can be adhered to.
- Dynamic accelerations (vibrations) in the millisecond range are set at 2.0 g vertical, 1.5 g lateral and 1.5 g longitudinal. These values may not be exceeded during installation of the TP.

<u>Height of the upper edge of the TP flange</u>

The tolerance allowance for each transition piece is calculated over the tolerance allowance for the installation height of the monopiles.

In addition, the lower edge of the TP support, after completion of the alignment of the TP using hydraulic presses at the narrowest point, must have a height distance from the upper edge of the MP of at least 20 mm.

<u>Inclination of the transition pieces</u>

While allowing for the possibility of adjustments in the grout connections when erecting the TPs, a maximum inclination of the transition pieces after alignment and grouting of 0.10° must not be exceeded.

The inclination is to be measured at the TP reference plate.

Appendix C1: Thickness primary steel Sheringham Shoal Transition Piece

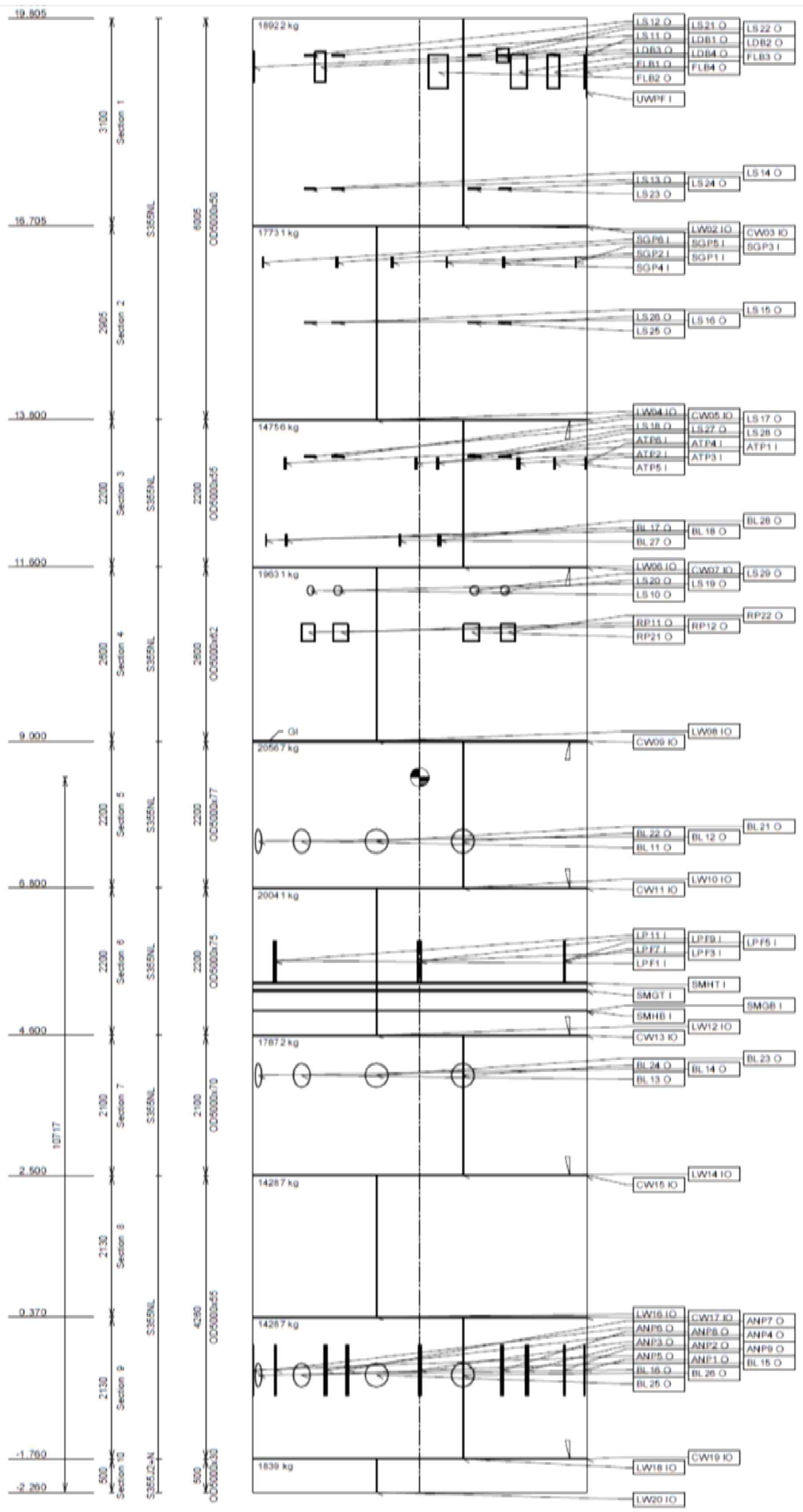

Appendix C2: Thickness primary steel MeerWind Transition Piece

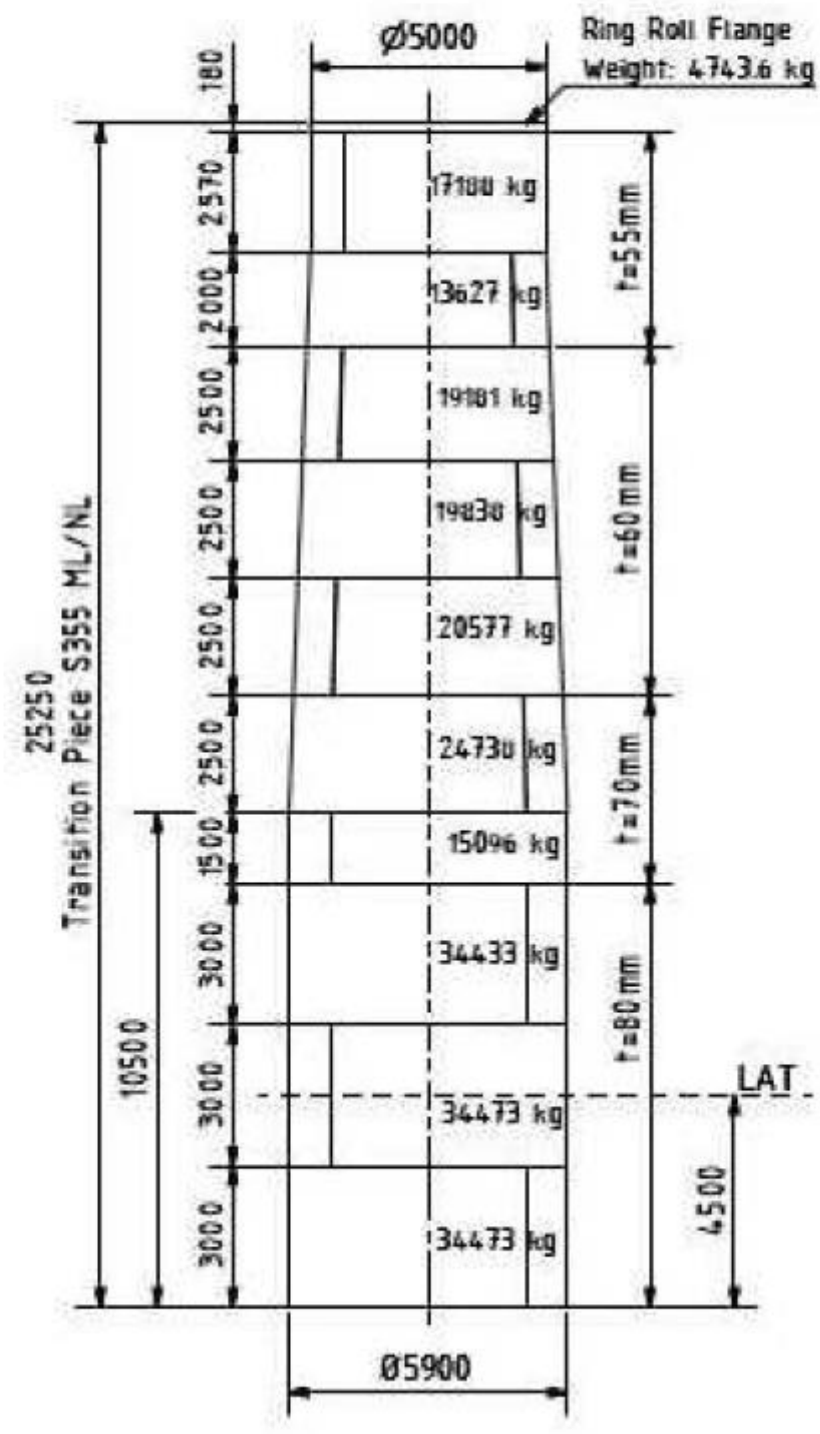

Appendix C3: Thickness primary steel Gwynt y Môr Transition Piece

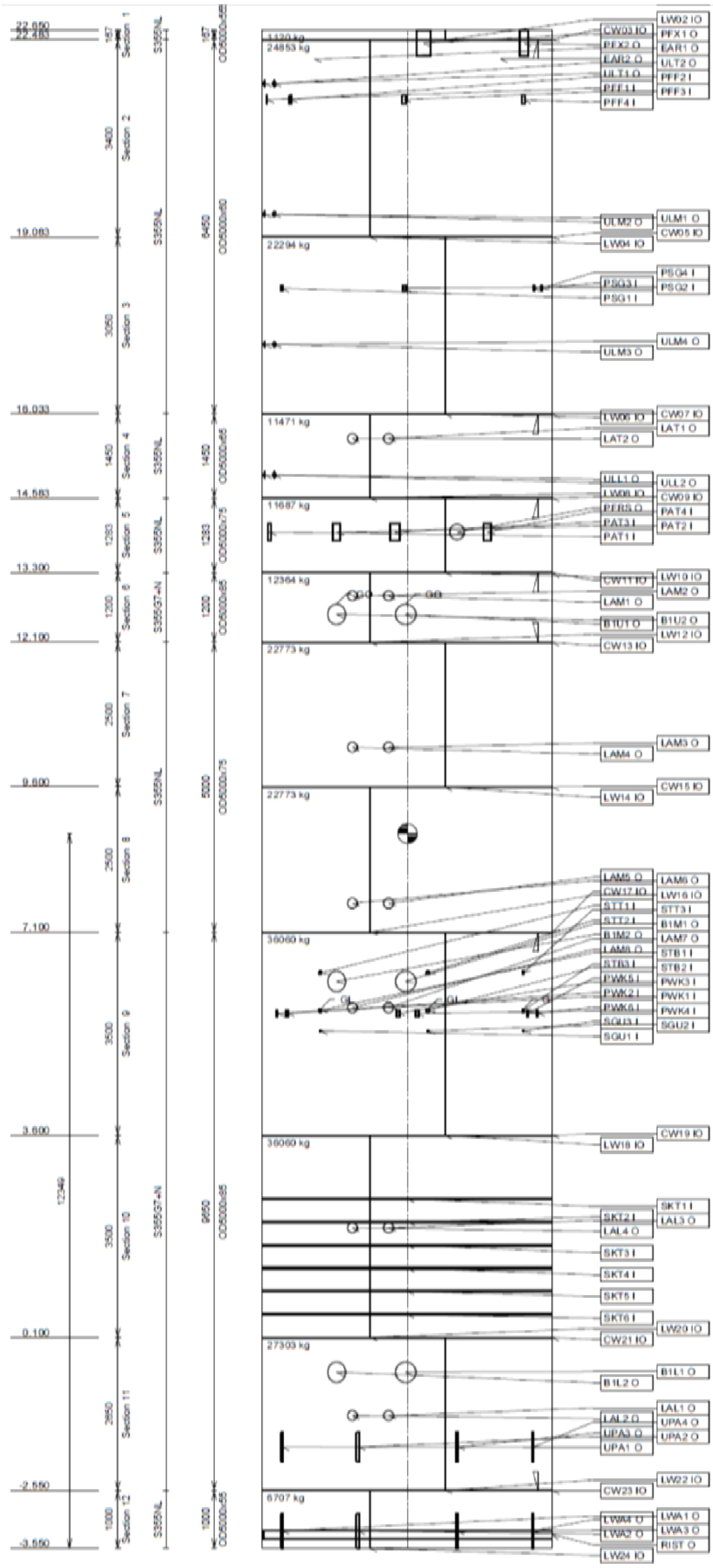

Appendix D: Roark's formula

7. Ring under any number of equal radial forces equally spaced

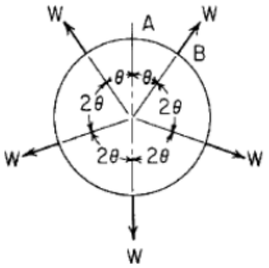

For $0 < x < \theta$ $\quad M = \dfrac{WR(u/s - k_2/\theta)}{2} \quad N = \dfrac{Wu}{2s} \quad V = \dfrac{-Wz}{2s}$

$\text{Max} + M = M_A = \dfrac{WR(1/s - k_2/\theta)}{2} \quad \text{Max} - M = \dfrac{-WR}{2}\left(\dfrac{k_2}{\theta} - \dfrac{c}{s}\right)$ at each load position

Radial displacement at each load point $= \Delta R_B = \dfrac{WR^3}{EI}\left[\dfrac{k_1(\theta - sc)}{4s^2} + \dfrac{k_2 c}{2s} - \dfrac{k_2^2}{2\theta}\right]$

Radial displacement at $x = 0, 2\theta, \ldots = \Delta R_A = \dfrac{-WR^3}{EI}\left[\dfrac{k_1(s - \theta c)}{4s^2} - \dfrac{k_2}{2s} + \dfrac{k_2^2}{2\theta}\right]$

If $\alpha = \beta = 0$, $M = K_M WR$, $\Delta R = K_{\Delta R} WR^3/EI$

θ	15°	30°	45°	60°	90°
K_{M_A}	0.02199	0.04507	0.07049	0.09989	0.18169
K_{M_B}	−0.04383	−0.08890	−0.13662	−0.18879	−0.31831
$K_{\Delta R_B}$	0.00020	0.00168	0.00608	0.01594	0.07439
$K_{\Delta R_A}$	−0.00018	−0.00148	−0.00539	−0.01426	−0.06831

TABLE 9.2 Formulas for circular rings

NOTATION: W = load (force); w and v = unit loads (force per unit of circumferential length); ρ = unit weight of contained liquid (force per unit volume); M_o = applied couple (force-length). M_A, M_B, M_C, and M are internal moments at A, B, C, and x, respectively, positive as shown. N_A, N, V_A, and V are internal forces, positive as shown. E = modulus of elasticity (force per unit area); ν = Poisson's ratio; A = cross-sectional area (length squared); R = radius to the centroid of the cross section (length); I = area moment of inertia of ring cross section about the principal axis perpendicular to the plane of the ring (length^4). [Note that for a pipe or cylinder, a representative segment of

TABLE 9.2 Formulas for circular rings

NOTATION: W = load (force); w and v = unit loads (force per unit of circumferential length); ρ = unit weight of contained liquid (force per unit volume); M_o = applied couple (force-length). M_A, M_B, M_C, and M are internal moments at A, B, C, and x, respectively, positive as shown. N_A, N, V_A, and V are internal forces, positive as shown. E = modulus of elasticity (force per unit area); ν = Poisson's ratio; A = cross-sectional area (length squared); R = radius to the centroid of the cross section (length); I = area moment of inertia of ring cross section about the principal axis perpendicular to the plane of the ring (length^4). [Note that for a pipe or cylinder, a representative segment of unit axial length may be used by replacing EI by $Et^3/12(1-\nu^2)$.] e = positive distance measured radially inward from the centroidal axis of the cross section to the neutral axis of pure bending (see Sec. 9.1). θ, x, and ϕ are angles (radians) and are limited to the range zero to π for all cases except 18 and 19; $s = \sin\theta$, $c = \cos\theta$, $z = \sin x$, $u = \cos x$, $n = \sin\phi$, and $m = \cos\phi$.

ΔD_V and ΔD_H are changes in the vertical and horizontal diameters, respectively, and an increase is positive. ΔL is the change in the lower half of the vertical diameter or the vertical motion relative to point C of a line connecting points B and D on the ring. Similarly ΔL_W is the vertical motion relative to point C of a horizontal line connecting the load points on the ring. ΔL_{WH} is the change in length of a horizontal line connecting the load points on the ring. ψ is the angular rotation (radians) of the load point in the plane of the ring and is positive in the direction of positive θ. For the distributed loadings the load points just referred to are the points where the distributed loading starts, i.e., the position located by the angle θ. The reference to points A, B, and C and to the diameters refer to positions on a circle of radius R passing through the centroids of the several sections; i.e., diameter = $2R$. It is important to consider this when dealing with thick rings. Similarly, all concentrated and distributed loadings are assumed to be applied at the radial position of the centroid with the exception of the cases where the ring is loaded by its own weight or by dynamic loading, cases 15 and 21. In these two cases the actual radial distribution of load is considered. If the loading is on the outer or inner surfaces of thick rings, an equivalent loading at the centroidal radius R must be used. See the examples to determine how this might be accomplished.

The hoop-stress deformation factor is $\alpha = I/AR^2$ for thin rings or $\alpha = e/R$ for thick rings. The transverse (radial) shear deformation factor is $\beta = FEI/GAR^2$ for thin rings or $\beta = 2F(1+\nu)e/R$ for thick rings, where G is the shear modulus of elasticity and F is a shape factor for the cross section (see Sec. 8.10). The following constants are defined to simplify the expressions whcih follow. Note that these constants are unity if no correction for hoop stress or shear stress is necessary or desired for use with thin rings. $k_1 = 1 - \alpha + \beta$, $k_2 = 1 - \alpha$.

Appendix E: Effective width

E1: Effective width

For the convenience of engineering future projects, it's practical to do calculations assuming an effective width instead of doing detailed calculations of the entire TP. The concept of effective width assumes that a certain distance is completely effective in transmitting forces and stress, and beyond this distance the stresses become zero immediately. The force can then be spread over this width and only a beam analysis has to be done. This section establishes the effective width of the cylinder.

Also, the effective width must be known to calculate a spring stiffness of the rotational spring beneath the concentrated force.

E2: ANSYS model

To this end a model was created in ANSYS. Because it is expected that the influence of the point load will decrease to negligible levels, only a part of the cylinder need to be modeled. In this case 6 meters is modeled. The concentrated forces are applied halfway and spread over an area of 300x300mm.

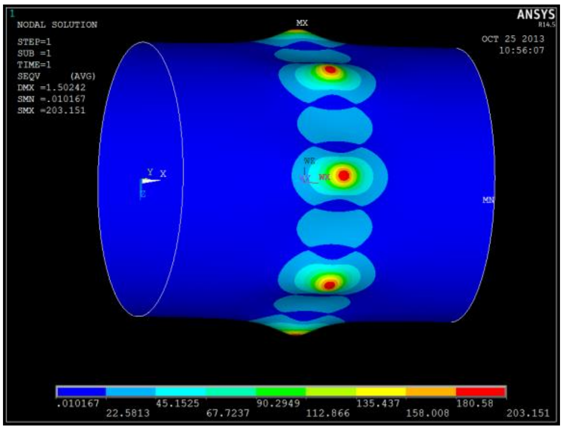

Peak Von Mises stresses are rather high at 203 N/mm^2. A path is created beneath concentrated force, over the full length of the cylinder, along which the stresses are plotted. This gives more insight in the stress distribution from which an effective width can be determined.

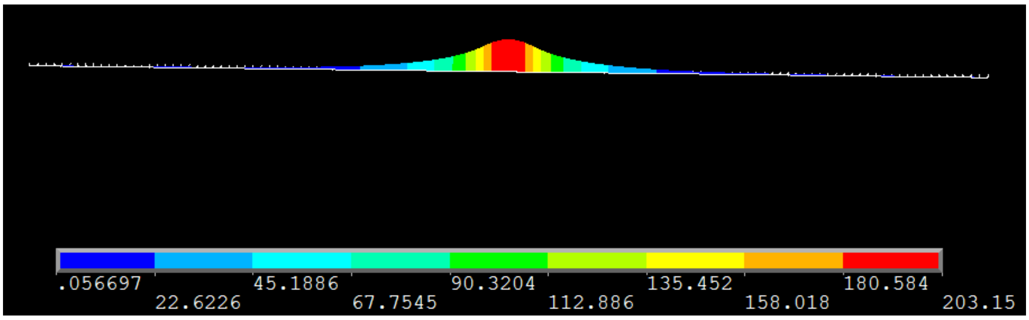

This stress distribution is expected. Using the nodal solution list the stress of every individual node along the path is given. These values are plotted in a graph. The area below the graph (blue markers) can be imagined as concentrated in the rectangular area (red box). If both cover the same area and have the same peak stress, the width of the red box is the sought after effective width.

The nodal solutions are listed below.

1	0.4697	21	2.8486	41	19.161	61	203.15	81	19.168	101	2.7123
2	0.49096	22	3.1054	42	21.458	62	198.08	82	17.138	102	2.455
3	0.54299	23	3.3846	43	24.054	63	182.97	83	15.346	103	2.2145
4	0.6059	24	3.6886	44	26.986	64	160.46	84	13.765	104	1.9892
5	0.67276	25	4.0202	45	30.293	65	137.26	85	12.372	105	1.7782
6	0.74301	26	4.383	46	34.02	66	117.91	86	11.143	106	1.5805
7	0.81744	27	4.7811	47	38.227	67	102.31	87	10.059	107	1.3954
8	0.89691	28	5.2193	48	42.979	68	89.49	88	9.0997	108	1.2225
9	0.98266	29	5.7036	49	48.345	69	78.667	89	8.2498	109	1.0616
10	1.0757	30	6.2409	50	54.447	70	69.363	90	7.4941	110	0.91253
11	1.1769	31	6.8394	51	61.448	71	61.374	91	6.8198	111	0.77563
12	1.2872	32	7.5088	52	69.477	72	54.439	92	6.2154	112	0.65128
13	1.4077	33	8.2603	53	78.663	73	48.353	93	5.6714	113	0.54005

14	1.5392	34	9.1067	54	89.388	74	42.985	94	5.1792	114	0.44294
15	1.6827	35	10.063	55	102.27	75	38.235	95	4.7319	115	0.36042
16	1.8388	36	11.145	56	117.96	76	34.032	96	4.3235	116	0.29177
17	2.0088	37	12.371	57	137.33	77	30.303	97	3.9487	117	0.23559
18	2.1936	38	13.763	58	160.5	78	26.997	98	3.6036	118	0.18818
19	2.3943	39	15.342	59	182.99	79	24.064	99	3.2843	119	0.14396
20	2.6121	40	17.132	60	198.08	80	21.466	100	2.9881	120	0.089636
										121	0.056697

The nodal solutions are plotted in a graph. To find the area below the graph a Trapezoidal numerical integration is used.

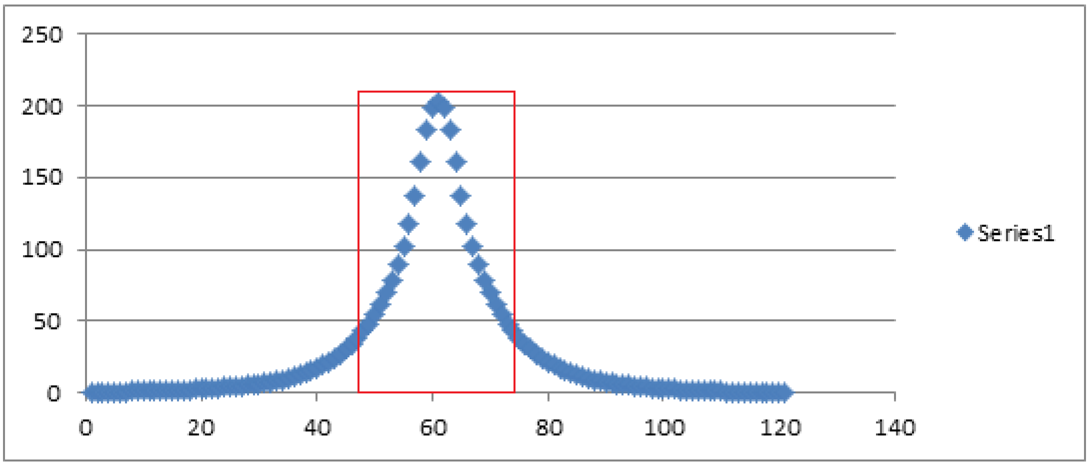

This amounts to an area of 3632. The peak stress is 203 N/mm^2. The element size is 50 mm. The effective width can now be calculated: (3632/203)*50=894 mm. This is less than initially assumed.

This effective width will be used in the analytical model.

E3: Assessment of numerical model

When one makes a numerical model, one needs be confident that de results it produces are a good approximation of reality. This is an important step and can be done in several ways. Here, three checks are employed.

1 - Comparing nodal solution with element solution.

The nodal solution is the average of adjacent elements solution. E.g., if the nodal solution equals 250, and this is the average of 245 and 255 then it's OK. If this is the average of 200 and 300 then it is not OK. For a graphical rendering, see Appendix F.

In this case the nodal solution and element solution are very close.

The nodal solution produces a stress of 203.151 N/mm^2

The element solution produces a stress of 203.796 N/mm^2

2 – Increasing mesh density without significantly increasing results.

Several mesh densities have been tried. Increasing the density should produce more accurate results, though also taking more computational time. A mesh size of 50 mm. is considered fine enough, given the following results:

mesh size	Von mises stress	number of elements
150	182	4188
100	188	9424
50	203	37699
25	205	150796

3 – Comparing with a known analytical result [. Here Roark's formula is used, see Appendix D. The stress according to Roark amounts to 230 N/mm^2 under the concentrated load. The difference is about 12% and can be explained by the fact that in the numerical model the force was spread over an area of 300x300mm, which reduce the peak stress.

Appendix F: Nodal solution vs. element solution

Below are two graphical renderings of the nodal solution and the element solution. As can be seen, the difference is marginal, suggesting the numerical model is good enough.

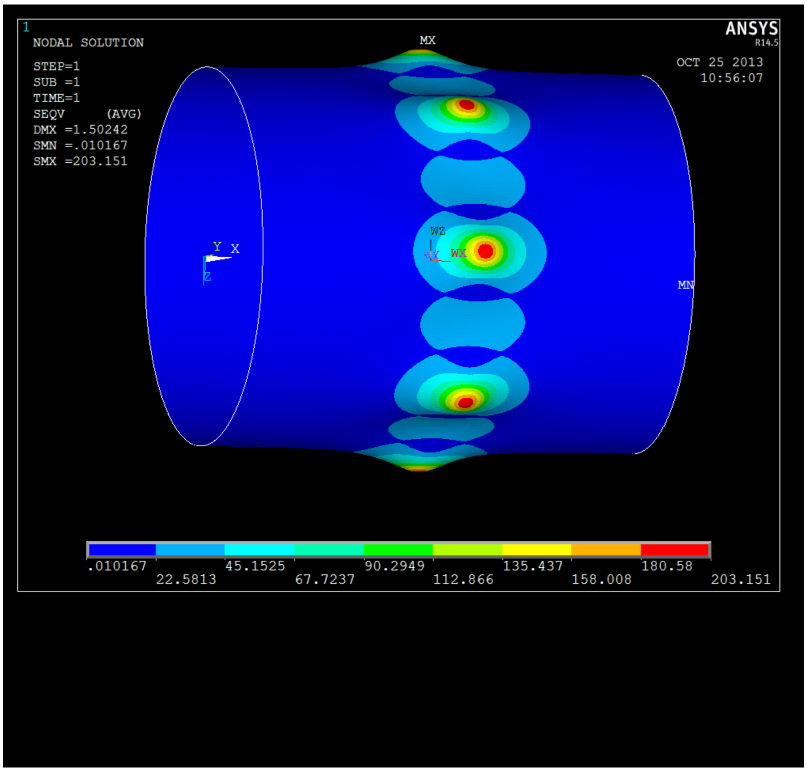

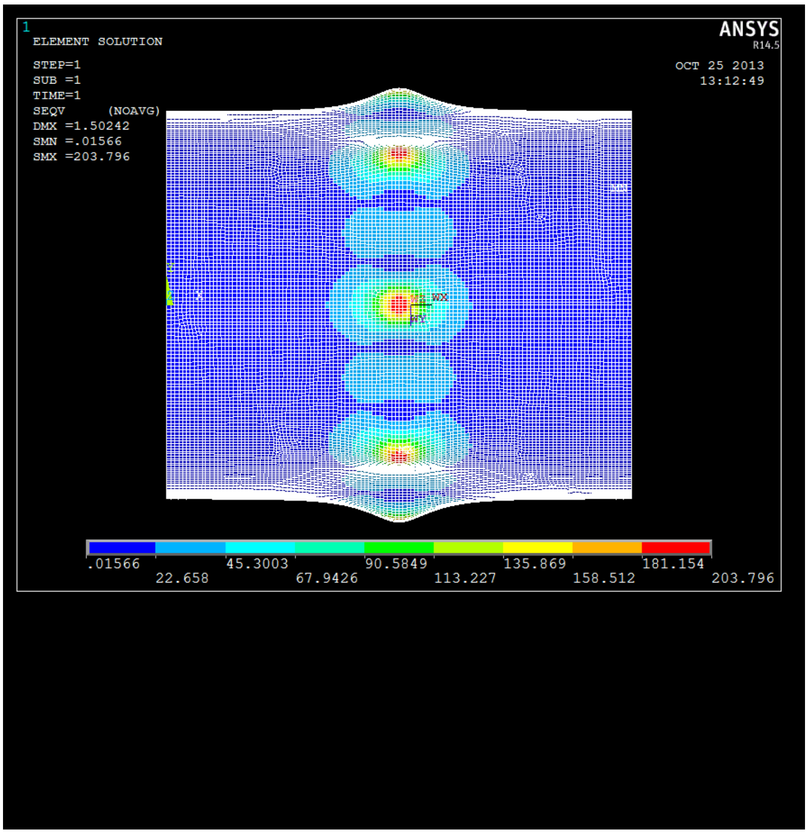

Appendix G: Bulk modulus of hydraulic fluid

For the calculation of the stiffness of the hydraulic cylinders, an average modulus of elasticity is useful. When working with hydraulic fluids, it is common to use the term Bulk Modulus. This is because the bulk modulus is not a fixed value but instead dependent on several different factors.

Factors that influence the compressibility are the type of oil, operating temperature, pressure and entrained air. In every case it is important to keep the oil free of entrained air, as it has a devastating effect on the compressibility of the oil. E.g., if 2% of free air is entrained in the oil, its compressibility reduces to about 10% of its air free compressibility.

Furthermore, the method of measuring the bulk modulus also has an effect on the resulting value. There are two ways of measuring, the Secant method and the Tangent method.

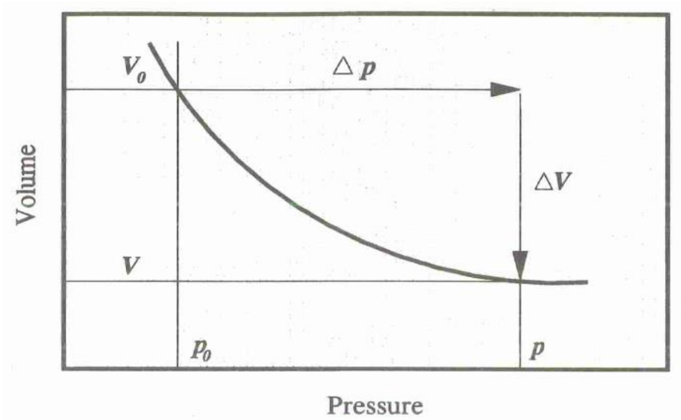

In the figure above the Secant method is displayed. This provides a more average value of the bulk modulus and is the preferred parameter when changes is pressure are expected. This is the case for the method of seafastening in this thesis. As can be seen the compressibility decreases with increasing pressure.

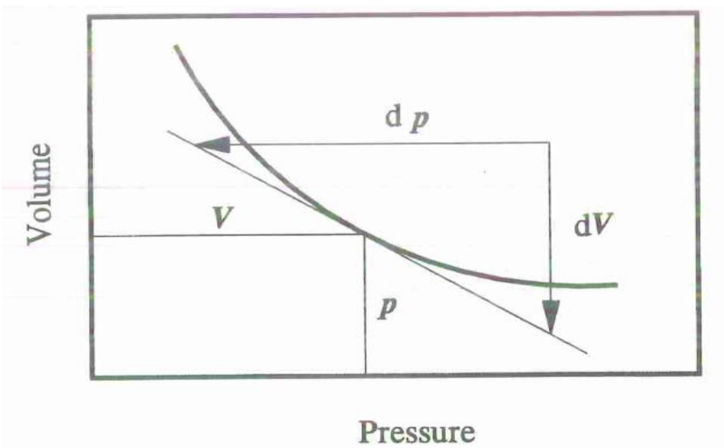

In the figure above the Tangent method is displayed. This is the scientifically correct bulk modulus if the temperature is constant.

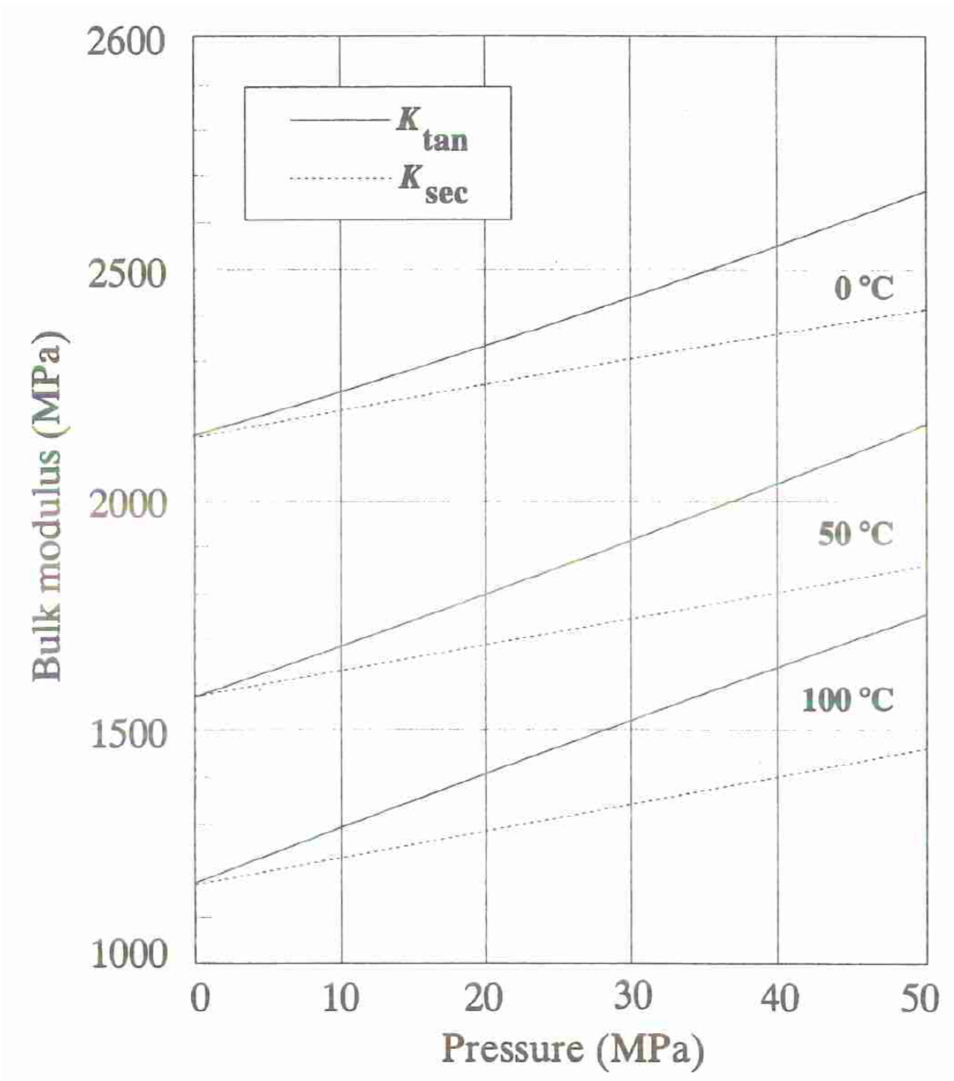

In the figure above the Bulk modulus is displayed on the vertical axis. The horizontal axis displays the pressure. The bulk modulus is increased with increasing pressure but decreased with increasing temperature. The figure above shows the graph for the commonly used ISO VG32 oil.

Throughout this thesis, use is made of a spring stiffness of about 250.000 psi or 1750 N/mm^2. This was based upon an average operating force the hydraulic cylinders needs to supply, i.e., about 1400 kN pretension. It is expected that the temperature of the oil will be above that of its environment because due to ship motions it will be compressed and decompressed, causing friction and thus heat.

The Secant bulk modulus is used because it provides a more average values, useful for oils subject to pressure changes.

The 1400 kN pretension force in the hydraulic cylinders is that used for the extreme case. In normal operating conditions the pretension will be lower. 1400*10^3 N / 45730 mm^2 = 30.68 N/mm^2. At a bit lower that 50 degrees this relates to 1750 N/mm^2

This is the modulus of Elasticity used for modeling the spring stiffness that represents the hydraulic cylinders.

Appendix H: Stiffness relation hydraulic cylinder and steel diagonal rod

In chapter 3 the force distribution on the seafastening is calculated. To do this, the stiffness relation should be known between R1 and R3 because they make contact with the TP at the same location.

First, there is a geometric relation dependent on the width of the TP and the height of the jacks. If the TP will rotate around the Rotational Centre at the corner of the TP, the displacement of both the axial direction of the jacks and the transverse direction of the steel diagonal rod depends on above mentioned height and width.

For a height of 6 m. where the jacks make contact with the TP wall and a width of the TP, the relation is R1:R3 = 1: 5/6. So, for every millimeter the jacks are pushed inwards, the diagonal rod in extended upward. Herein the angle of the diagonal rod is very small and its effect neglected.

For the stiffness's themselves, some reasonable values for the dimensions must be assumed. In case of the cylinder, an Enerpac model RR-30024 is used. This has an maximum operating force of 3201 kN. For the steel diagonal rod, as an indication, a force of 1900 kN divided by 0.6*355 provides an area of 8920 mm^2.

Now from Hooke's law follow the stiffness's for a test load of, say, 1000 kN, a column of oil of 500 mm, a bulk modulus of elasticity described in Appendix G.

If the geometrical relation and the physical relation are combined, a total relation between R1 and R3 amounts:

R1 = 0.43*R3 (for a jack height of 6 m.)

R1 = 0.57*R3 (for a jack height of 8 m.)

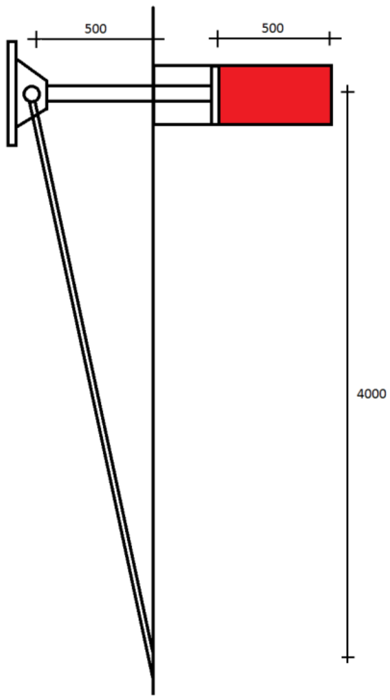

Appendix I: Results spring model

Below the results from the spring model are shown. First a test was done with zero acceleration and two infinite stiff rings to check if the model is correctly build. Given the spring stiffness in ANSYS in combination with the initial length should provide the right force, i.e., 1433 kN. This is in fact the case.

As can be seen, the local deformation is practically zero, as expected. On the next page the force per element are shown. The top of the list shows the upper spring. From there the list goes clockwise to the rest of the springs. ANSYS maintains the global coordinates system for displaying the forces. As such the second, fourth, sixth and eighth forces listed are the x- and y- components of the radial force.

The spring force is the product of the spring stiffness multiplied by its displacement, i.e., the initial length minus its force free length.

Acceleration = 0

Ring stiffness = 2e14 → infinite; k,spring=160055; ILength=508.953

Linear analysis

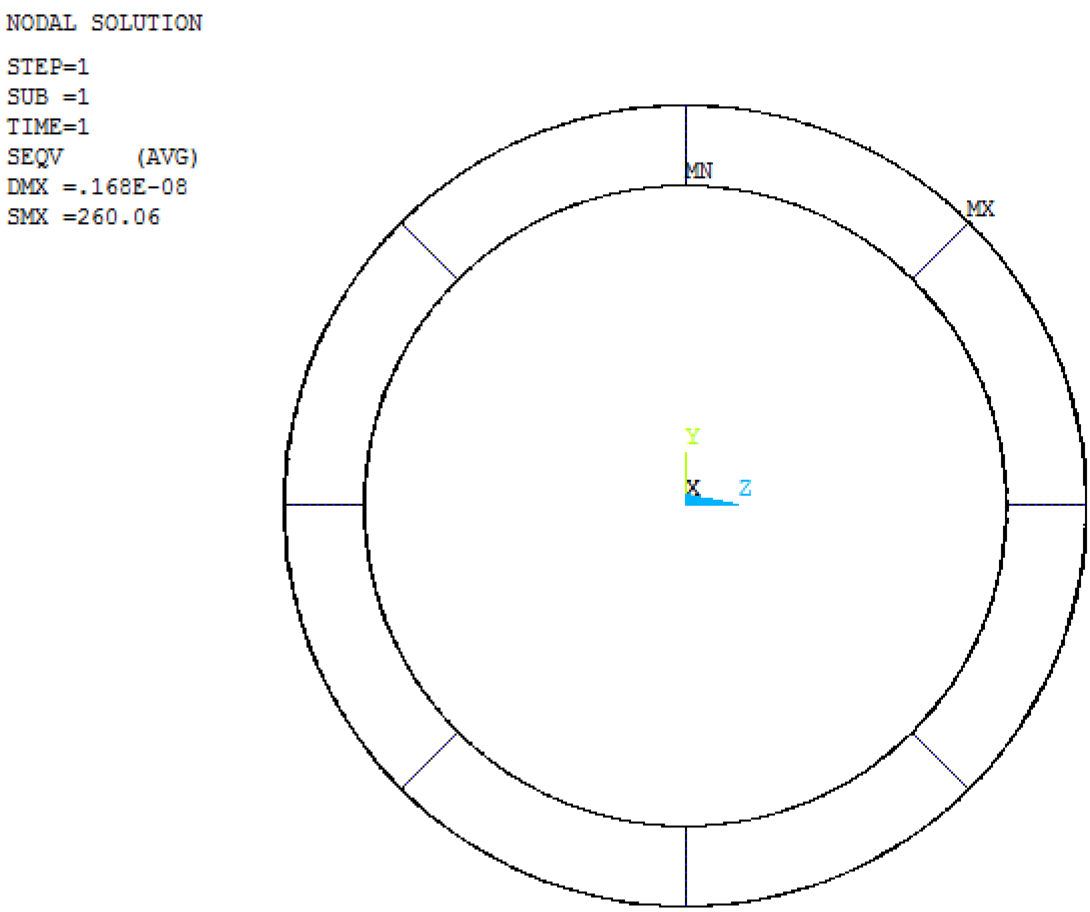

```
PRINT F    ELEMENT SOLUTION PER ELEMENT

***** POST1 ELEMENT NODE TOTAL FORCE LISTING *****

 LOAD STEP=     1  SUBSTEP=     1
  TIME=    1.0000      LOAD CASE=   0

 THE FOLLOWING X,Y,Z FORCES ARE IN GLOBAL COORDINATES


 ELEM=   17281  FX          FY          FZ
   9808   0.0000    -0.14330E+07  0.0000
     52   0.0000     0.14330E+07  0.0000

 ELEM=   17282  FX          FY          FZ
   9778   0.0000    -0.10133E+07-0.10133E+07
     22   0.0000     0.10133E+07 0.10133E+07

 ELEM=   17283  FX          FY          FZ
  10814   0.0000      0.0000    -0.14330E+07
   1302   0.0000      0.0000     0.14330E+07

 ELEM=   17284  FX          FY          FZ
  11790   0.0000     0.10133E+07-0.10133E+07
   2522   0.0000    -0.10133E+07 0.10133E+07

 ELEM=   17285  FX          FY          FZ
  12766   0.0000     0.14330E+07  0.0000
   3742   0.0000    -0.14330E+07  0.0000

 ELEM=   17286  FX          FY          FZ
  13742   0.0000     0.10133E+07 0.10133E+07
   4962   0.0000    -0.10133E+07-0.10133E+07

 ELEM=   17287  FX          FY          FZ
  14718   0.0000      0.0000     0.14330E+07
   6182   0.0000      0.0000    -0.14330E+07

 ELEM=   17288  FX          FY          FZ
  15694   0.0000    -0.10133E+07 0.10133E+07
   7402   0.0000     0.10133E+07-0.10133E+07
```

The same analysis is done with an acceleration of 6.457 m/s^2. These results are exactly what is predicted from the spring model proposed in chapter 3.

Acceleration = 6.457 m/s^2

Ring stiffness = 2e14 → infinite; k,spring=160055; lLength=508.953

Linear analysis

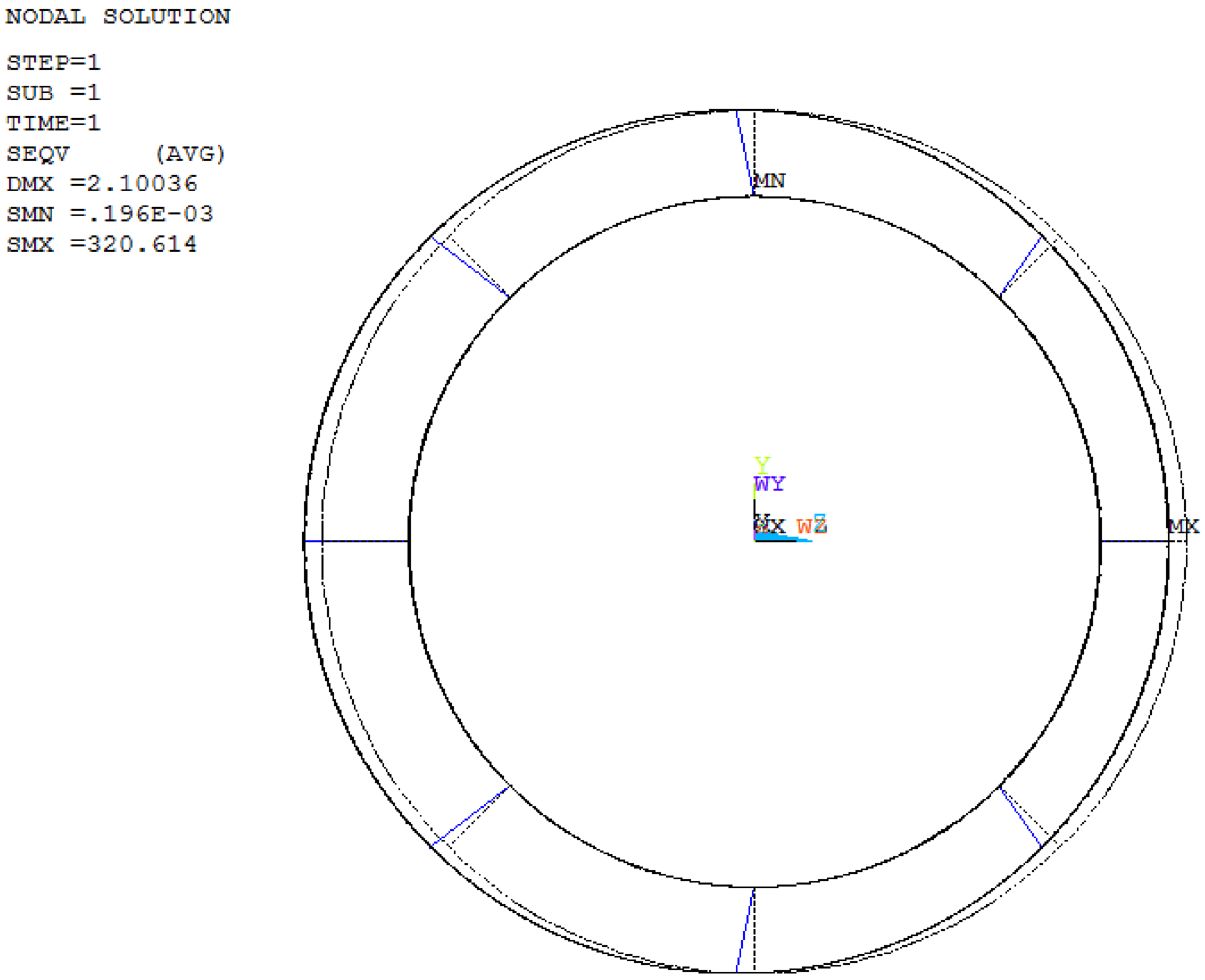

```
PRINT F    ELEMENT SOLUTION PER ELEMENT

 ***** POST1 ELEMENT NODE TOTAL FORCE LISTING *****

  LOAD STEP=     1  SUBSTEP=     1
   TIME=    1.0000      LOAD CASE=   0

  THE FOLLOWING X,Y,Z FORCES ARE IN GLOBAL COORDINATES


  ELEM=   17281  FX          FY          FZ
    9808   0.0000    -0.14330E+07  0.0000
      52   0.0000     0.14330E+07  0.0000

  ELEM=   17282  FX          FY          FZ
    9778   0.0000    -0.11813E+07-0.11813E+07
      22   0.0000     0.11813E+07 0.11813E+07

  ELEM=   17283  FX          FY          FZ
   10814   0.0000      0.0000    -0.17691E+07
    1302   0.0000      0.0000     0.17691E+07

  ELEM=   17284  FX          FY          FZ
   11790   0.0000     0.11813E+07-0.11813E+07
    2522   0.0000    -0.11813E+07 0.11813E+07

  ELEM=   17285  FX          FY          FZ
   12766   0.0000     0.14330E+07  0.0000
    3742   0.0000    -0.14330E+07  0.0000

  ELEM=   17286  FX          FY          FZ
   13742   0.0000     0.84518E+06 0.84518E+06
    4962   0.0000    -0.84518E+06-0.84518E+06

  ELEM=   17287  FX          FY          FZ
   14718   0.0000      0.0000     0.10968E+07
    6182   0.0000      0.0000    -0.10968E+07

  ELEM=   17288  FX          FY          FZ
   15694   0.0000    -0.84518E+06 0.84518E+06
    7402   0.0000     0.84518E+06-0.84518E+06
```

Now the analysis is run with a realistic value of the stiffness of the ring. First with zero acceleration, so the local deformation due to the spring force is known. In this case it is 1.40676 mm. This means the springs lose part of their initial force, as can be seen on the next page. DMX is the displacement, in this case only the local deformation and corresponds precisely with the loss in spring force. The initial length (this is the force free length, also called ILength) is 508.953 mm. The length or distance between the cylinders equals 500 mm. The initial force was 1433 kN

160055 * (8.953-1.40676) = 1207.800 N

In reality this loss of initial spring force doesn't exist, therefore in the next analysis the initial spring force is compensated for, so that after local deformation the required pretension force remains.

Acceleration = 0

Ring stiffness = 2e5 → realistic value ; k,spring=160055; ILength=508.953

Linear analysis

DMX = deformation = 1.40676

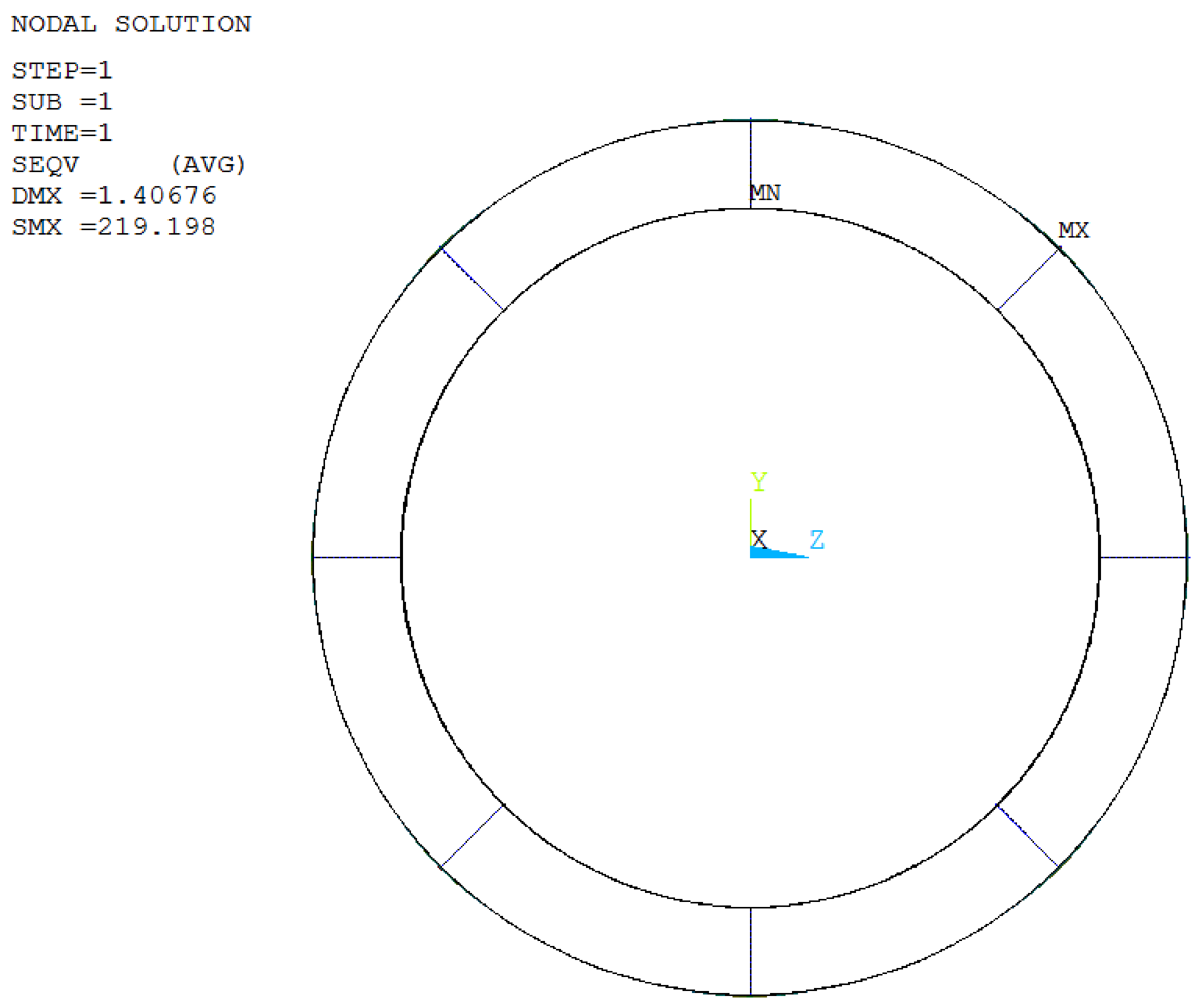

```
 PRINT F    ELEMENT SOLUTION PER ELEMENT

  ***** POST1 ELEMENT NODE TOTAL FORCE LISTING *****

   LOAD STEP=     1  SUBSTEP=     1
    TIME=    1.0000      LOAD CASE=   0

   THE FOLLOWING X,Y,Z FORCES ARE IN GLOBAL COORDINATES


   ELEM=   17281  FX          FY          FZ
     9808   0.0000    -0.12078E+07  0.0000
       52   0.0000     0.12078E+07  0.0000

   ELEM=   17282  FX          FY          FZ
     9778   0.0000    -0.85405E+06-0.85405E+06
       22   0.0000     0.85405E+06 0.85405E+06

   ELEM=   17283  FX          FY          FZ
    10814   0.0000      0.0000     -0.12078E+07
     1302   0.0000      0.0000      0.12078E+07

   ELEM=   17284  FX          FY          FZ
    11790   0.0000     0.85405E+06-0.85405E+06
     2522   0.0000    -0.85405E+06 0.85405E+06

   ELEM=   17285  FX          FY          FZ
    12766   0.0000     0.12078E+07  0.0000
     3742   0.0000    -0.12078E+07  0.0000

   ELEM=   17286  FX          FY          FZ
    13742   0.0000     0.85405E+06 0.85405E+06
     4962   0.0000    -0.85405E+06-0.85405E+06

   ELEM=   17287  FX          FY          FZ
    14718   0.0000      0.0000      0.12078E+07
     6182   0.0000      0.0000     -0.12078E+07

   ELEM=   17288  FX          FY          FZ
    15694   0.0000    -0.85405E+06 0.85405E+06
     7402   0.0000     0.85405E+06-0.85405E+06
```

The initial length is increased to ILength = 510.623 so that after local deformation the spring force equals 1433 kN.

Acceleration = 0

Ring stiffness = 2e5 → realistic value

Linear analysis

DMX = deformation = 1.66916

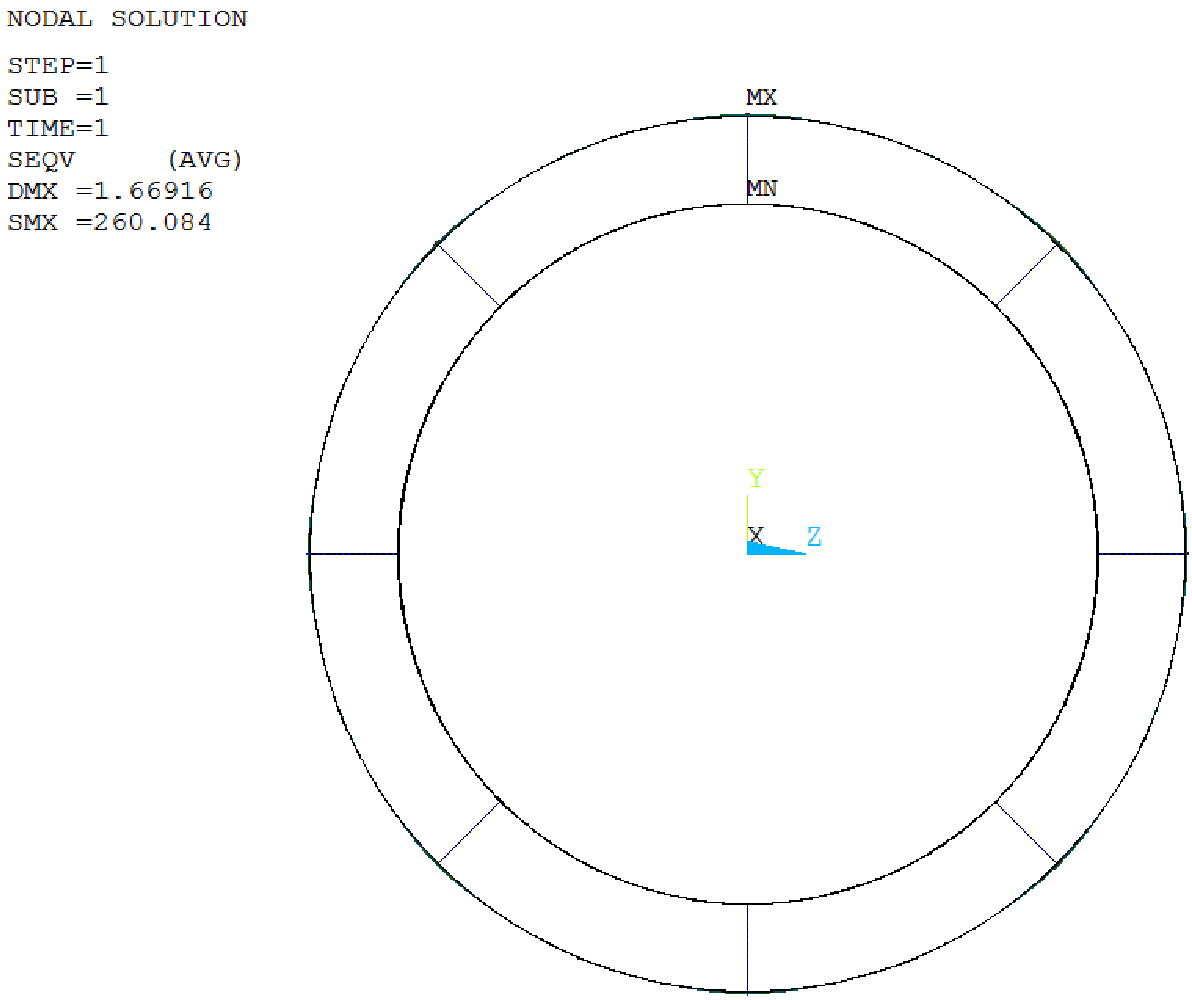

```
PRINT F    ELEMENT SOLUTION PER ELEMENT

***** POST1 ELEMENT NODE TOTAL FORCE LISTING *****

 LOAD STEP=     1  SUBSTEP=     1
  TIME=    1.0000      LOAD CASE=   0

 THE FOLLOWING X,Y,Z FORCES ARE IN GLOBAL COORDINATES


 ELEM=   17281  FX          FY          FZ
   9808   0.0000    -0.14331E+07  0.0000
     52   0.0000     0.14331E+07  0.0000

 ELEM=   17282  FX          FY          FZ
   9778   0.0000    -0.10134E+07-0.10134E+07
     22   0.0000     0.10134E+07 0.10134E+07

 ELEM=   17283  FX          FY          FZ
  10814   0.0000      0.0000    -0.14331E+07
   1302   0.0000      0.0000     0.14331E+07

 ELEM=   17284  FX          FY          FZ
  11790   0.0000     0.10134E+07-0.10134E+07
   2522   0.0000    -0.10134E+07 0.10134E+07

 ELEM=   17285  FX          FY          FZ
  12766   0.0000     0.14331E+07  0.0000
   3742   0.0000    -0.14331E+07  0.0000

 ELEM=   17286  FX          FY          FZ
  13742   0.0000     0.10134E+07 0.10134E+07
   4962   0.0000    -0.10134E+07-0.10134E+07

 ELEM=   17287  FX          FY          FZ
  14718   0.0000      0.0000     0.14331E+07
   6182   0.0000      0.0000    -0.14331E+07

 ELEM=   17288  FX          FY          FZ
  15694   0.0000    -0.10134E+07 0.10134E+07
   7402   0.0000     0.10134E+07-0.10134E+07
```

Now the analysis is run with the acceleration and realistic values of the TP stiffness. The heaviest loaded spring now has increased its force to 1433+337 kN = 1770 kN. This was the sought after conclusion. It appears thus that the TP will not deform substantial enough to influence the force distribution such that it needs taking account of.

Acceleration = 6.476 m/s^2

Ringstiffness = 2e5 → realistic value

Linear analysis

DMX = max. deformation = 3.77 mm

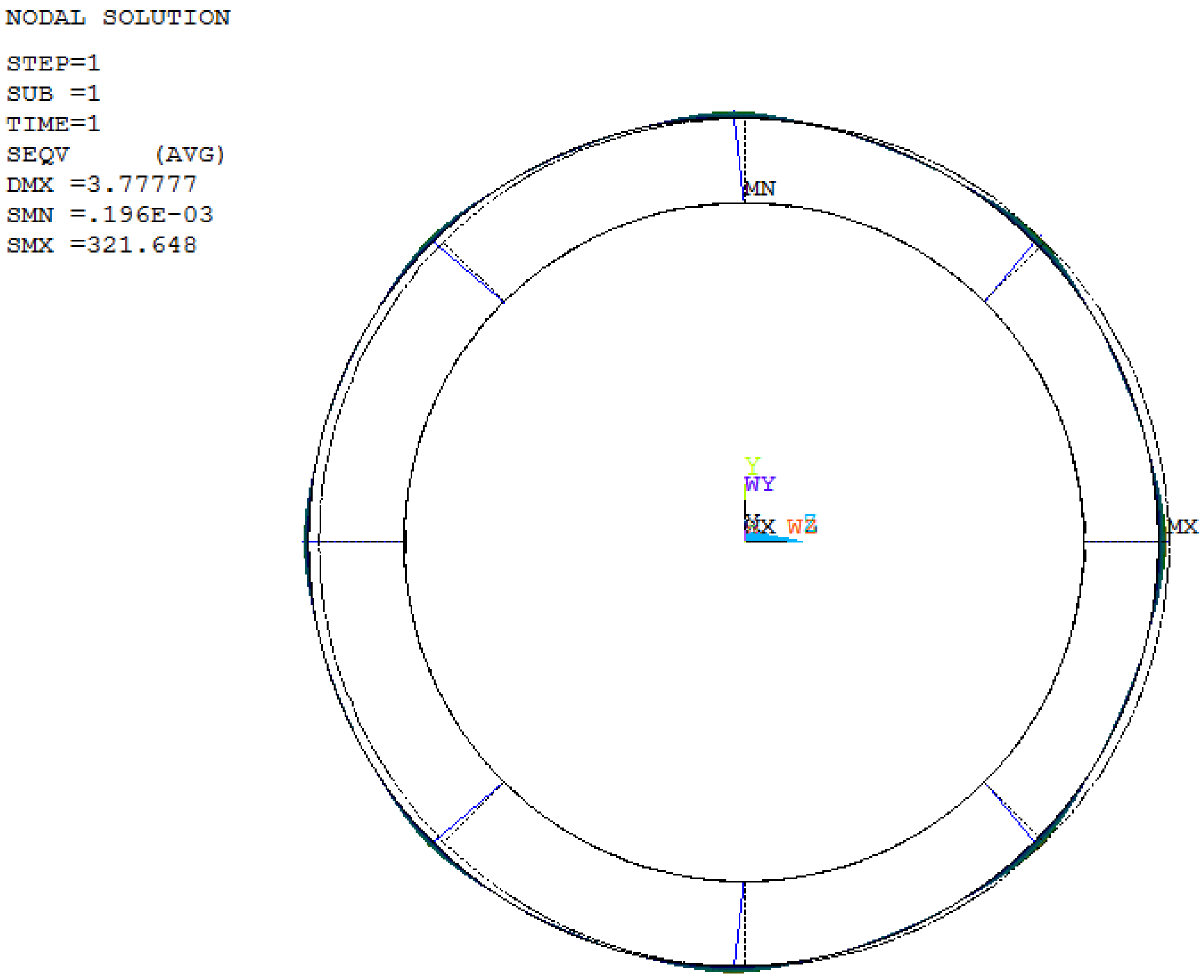

```
PRINT F    ELEMENT SOLUTION PER ELEMENT

 ***** POST1 ELEMENT NODE TOTAL FORCE LISTING *****

  LOAD STEP=     1  SUBSTEP=     1
   TIME=    1.0000      LOAD CASE=   0

  THE FOLLOWING X,Y,Z FORCES ARE IN GLOBAL COORDINATES


  ELEM=   17281  FX          FY          FZ
    9808   0.0000    -0.14331E+07  0.0000
      52   0.0000     0.14331E+07  0.0000

  ELEM=   17282  FX          FY          FZ
    9778   0.0000    -0.11821E+07-0.11821E+07
      22   0.0000     0.11821E+07 0.11821E+07

  ELEM=   17283  FX          FY          FZ
   10814   0.0000      0.0000    -0.17706E+07
    1302   0.0000      0.0000     0.17706E+07

  ELEM=   17284  FX          FY          FZ
   11790   0.0000     0.11821E+07-0.11821E+07
    2522   0.0000    -0.11821E+07 0.11821E+07

  ELEM=   17285  FX          FY          FZ
   12766   0.0000     0.14331E+07  0.0000
    3742   0.0000    -0.14331E+07  0.0000

  ELEM=   17286  FX          FY          FZ
   13742   0.0000     0.84461E+06 0.84461E+06
    4962   0.0000    -0.84461E+06-0.84461E+06

  ELEM=   17287  FX          FY          FZ
   14718   0.0000      0.0000     0.10956E+07
    6182   0.0000      0.0000    -0.10956E+07

  ELEM=   17288  FX          FY          FZ
   15694   0.0000    -0.84461E+06 0.84461E+06
    7402   0.0000     0.84461E+06-0.84461E+06
```

Also a nonlinear analysis can be done. This produces a difference of less than 1% compared with the linear analysis.

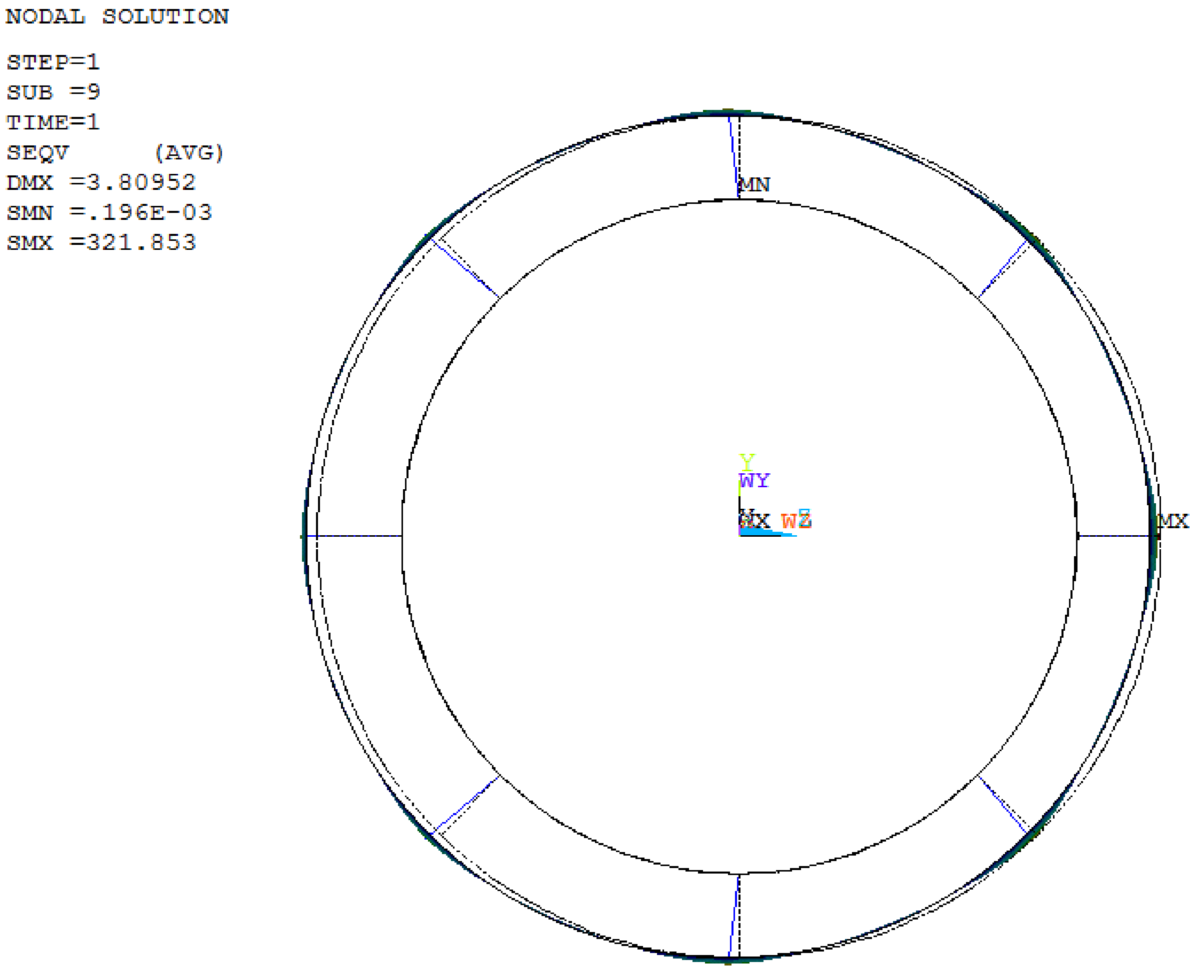

```
PRINT F    ELEMENT SOLUTION PER ELEMENT

***** POST1 ELEMENT NODE TOTAL FORCE LISTING *****

 LOAD STEP=     1  SUBSTEP=     9
  TIME=    1.0000      LOAD CASE=   0

 THE FOLLOWING X,Y,Z FORCES ARE IN GLOBAL COORDINATES


 ELEMENT=   17281  FX          FY          FZ
   9808  0.48827E-05-0.14345E+07  7367.4
     52 -0.48827E-05 0.14345E+07 -7367.4

 ELEM=   17282  FX          FY          FZ
   9778  0.55013E-05-0.11914E+07-0.11828E+07
     22 -0.55013E-05 0.11914E+07 0.11828E+07

 ELEM=   17283  FX          FY          FZ
  10814 -0.86888E-03  0.0000    -0.17803E+07
   1302  0.86888E-03  0.0000     0.17803E+07

 ELEM=   17284  FX          FY          FZ
  11790  0.10548E-05 0.11914E+07-0.11828E+07
   2522 -0.10548E-05-0.11914E+07 0.11828E+07

 ELEM=   17285  FX          FY          FZ
  12766 -0.48112E-07 0.14345E+07  7367.4
   3742  0.48112E-07-0.14345E+07 -7367.4

 ELEM=   17286  FX          FY          FZ
  13742  0.96018E-06 0.83916E+06 0.84526E+06
   4962 -0.96018E-06-0.83916E+06-0.84526E+06

 ELEM=   17287  FX          FY          FZ
  14718 -0.22476E-03  0.0000     0.10905E+07
   6182  0.22476E-03  0.0000    -0.10905E+07

 ELEM=   17288  FX          FY          FZ
  15694  0.14166E-05-0.83916E+06 0.84526E+06
   7402 -0.14166E-05 0.83916E+06-0.84526E+06
```

Appendix J1: ANSYS script spring model

```
finish                          ! stops processes
/clear                          ! clears database
/prep7                          ! enter preprocessor
k,1                             ! defines keypoints
k,2,6000
k,3,,2500
k,4,6000,2500
k,5,,2000
k,6,6000,2000
l,3,4                           ! defines lines between keypoints
l,5,6
arota,1,,,,,,1,2,,8             ! rotates lines around keypoints
arota,2,,,,,,1,2,,8
/pnum,area,1                    ! turns on area numbering
/rep                            ! replot
wpoffs,3000                     ! offset workplane
wprota,,,90                     ! rotate workplane
asbw,all                        ! devides area's
asel,s,loc,x,3000,6000          ! select area's with x-coordinate
/rep                            ! replot
l,43,35                         ! defines line between inner and outer shells
l,44,36                         ! defines line between inner and outer shells
l,45,37                         ! defines line between inner and outer shells
l,46,38                         ! defines line between inner and outer shells
l,47,39                         ! defines line between inner and outer shells
l,48,40                         ! defines line between inner and outer shells
l,49,41                         ! defines line between inner and outer shells
l,50,42                         ! defines line between inner and outer shells
asel,all                        ! select all areas
aplot                           ! plot areas
ET,1,shell181                   ! sets element type 1 to shell 181
sectype,,shell
secdata,85,1                    ! sets element thickness
mp,ex,1,2e5                     ! defines material constants
mp,prxy,1,0.3                   ! defines Poisson's ratio
MP,DENS,1,(0.679*4.8*7.86e-6)           ! density
ET,2,shell181                   ! sets element type 2 to shell 181
sectype,,shell
secdata,85,1                    ! sets shell thickness
mp,ex,2,2e14                    ! defines material constants
mp,prxy,2,0.3                   ! defines Poisson's ratio
MP,DENS,2,0                     ! density
ET,3,combin14                   ! defines element type 3
r,3,160055,,,,,510.623,         ! sets real constant set 3, belonging to ET,3 to K=16055  and initial
force free length to 510.623
asel,all                        ! select all area's
asel,s,area,,17,32              ! select outer shell
real,1,                         ! turns on real constants set 1
aesize,all,100                  ! sets element size for area's
```

```
amesh,all                ! mesh all selected area's
asel,all                 ! select all area's
asel,s,area,,33,48       ! select inner shell
real,2,                  ! turns on real constants set 2
aesize,all,100           ! sets element size
amesh,all
lsel,s,line,,1,9         ! selects line connecting inner and outer shell
real,3,                  ! turns on real constants set 2
lesize,all,500           ! sets element size for lines
lmesh,all                ! meshes selected line
asel,all                 ! select all area's
aplot                    ! plot area's
asel,s,area,,33,48       ! select inner shell
lsla                     ! select lines from selected area's
lsel,r,loc,x,0           ! select lines with x-coordinate 0
dl,all,,ux,,1            ! constrains line DOF
dl,all,,uy,,1            ! constrains line DOF
dl,all,,uz,,1            ! constrains line DOF
asel,s,area,,33,48       ! select inner shell
lsla                     ! select lines from selected area's
lsel,r,loc,x,6000        ! select lines with x-coordinate 6000
dl,all,,ux,,1            ! constrains line DOF
dl,all,,uy,,1            ! constrains line DOF
dl,all,,uz,,1            ! constrains line DOF
asel,all                 ! select all area's
aplot                    ! plot area's
asel,s,area,,17,32       ! select outer shell
lsla                     ! select lines from selected area's
lsel,r,loc,x,0           ! select lines with x-coordinate 0
dl,all,,ux,,1            ! constrains line DOF
asel,s,area,,17,32       ! select outer shell
lsla                     ! select lines from selected area's
lsel,r,loc,x,6000        ! select lines with x-coordinate 0
dl,all,,ux,,1            ! constrains line DOF
dk,9,uy                  ! constrains keypoint DOF
dk,17,uy                 ! constrains keypoint DOF
dk,18,uy                 ! constrains keypoint DOF
dk,10,uy                 ! constrains keypoint DOF
lsel,s,line,,79          ! select line to which springs are attached
lsel,a,line,,75          ! select line to which springs are attached
lsel,a,line,,96          ! select line to which springs are attached
lsel,a,line,,94          ! select line to which springs are attached
lsel,a,line,,91          ! select line to which springs are attached
lsel,a,line,,88          ! select line to which springs are attached
lsel,a,line,,85          ! select line to which springs are attached
lsel,a,line,,82          ! select line to which springs are attached
dl,all,,ux,,1            ! constrains line DOF
dl,all,,uy,,1            ! constrains line DOF
dl,all,,uz,,1            ! constrains line DOF
asel,all                 ! select area's
aplot
allsel                   ! select all
```

```
WPCSYS,-1,0                 ! allign workplane with global cartesian
finish                      ! stop preprocessor
/solu                       ! start solution phase
antype,static               ! static analysis
! nlgeom,on                 ! turn on non-linear geometry analysis
! autots,on                 ! auto time stepping
! nsubst,50,1000,1          ! Size of first substep=1/5 of the total load, max # substeps=1000,
min # substeps=1
! outres,all,all            ! save results of all iterations
! ACEL,,,0
ACEL,,,6.476                ! sets acceleration in z-direction
! ACEL,,,1.700              ! sets acceleration in z-direction
SOLVE                       ! solve
FINISH                      ! stop solver
/POST1                      ! enter postprocessor
! /DSCALE,ALL,AUTO          ! scale deformation auto
/DSCALE,ALL,10              ! scale deformation user specified
/EFACET,1                   ! specifies number of facets per element edge for PowerGraphics
displays
PLNSOL, S,EQV, 1,1.0        ! show von mises stresses
/REPLOT,RESIZE              ! replot
/VIEW,1,-1                  ! show left view
/ANG,1
/REP,FAST
esel,s,type,,3              ! select element type 3
! eplot                     ! plot elements
! elist                     ! list selected elements
PRESOL,F                    ! show list with spring forces
! PLDISP,1                  ! show deformed shape
```

Appendix J2: ANSYS script buckling TP wall

```
finish                        ! stops all processes
/clear                        ! clears current database
/prep7                        ! enters preprocessor stage
ET,1,shell181                 ! Define element
sectype,1,shell               ! associates section type information with a section ID number
secdata,40,1                  ! set shell thickness
MP,EX,1,2e5                   ! Young's modulus
MP,PRXY,1,0.3                 ! Poisson's ratio
ET,2,shell181                 ! Define element
sectype,2,shell               ! associates section type information with a section ID number
secdata,55,2                  ! set shell thickness
MP,EX,2,2e5                   ! Young's modulus
MP,PRXY,2,0.3                 ! Poisson's ratio
ET,3,shell181                 ! Define element
sectype,3,shell               ! associates section type information with a section ID number
secdata,85,3                  ! set shell thickness
MP,EX,3,2e5                   ! Young's modulus
MP,PRXY,3,0.3                 ! Poisson's ratio
k,1,2430                      ! defines keypoints
k,2,2500
k,3,2780
k,4,2500,1000
k,5,2500,7000
k,6,0,0,0
k,7,0,7000,0
l,1,2                         ! defines lines between keypoints
l,2,3
l,2,4
l,4,5
arota,1,2,,,,,6,7,360,8       ! create cylindrical area by rotating lines around keypoints
arota,3,4,,,,,6,7,360,8       ! create cylindrical area by rotating lines around keypoints
asel,s,area,,17               ! select areas
asel,a,area,,2
asel,a,area,,1
wprota,,,9.167                ! rotate workplane
asbw,all                      ! devides areas
allsel                        ! select all
aplot                         ! plot areas
/pnum,area,1,                 ! turn on area numbering
/rep                          ! replot
AGLUE,ALL                     ! glue all areas together
allsel                        ! select all
lsel,s,loc,y,7000             ! select lines with specific coordinate
lplot                         ! plot lines
dl,all,,all                   ! constrain upper edge in all direction
allsel                        ! select all
aplot                         ! plot areas
lsel,s,line,,82               ! select line with specific number
SFL,all,PRES,16435,           ! apply force on line
```

```
allsel
aplot
asel,s,loc,y,-1,1            ! select lines with specific coordinate
/rep                         ! replot
type,1                       ! turn on element type 1
real,1                       ! turn on real constant set 1
mat,1                        ! turn on material properties 1
secnum,1                     ! turn on section data 1
aesize,all,100               ! set mesh size
amesh,all                    ! mesh all selected areas
allsel
aplot
asel,s,loc,y,1,1000          ! select lines with specific coordinate
/rep                         ! replot
type,2                       ! turn on element type 2
real,2                       ! turn on real constant set 2
mat,2                        ! turn on material properties 2
secnum,2                     ! turn on section data 2
aesize,all,100               ! set mesh size
amesh,all                    ! mesh all selected areas
allsel                       ! select all
aplot                        ! plot areas
asel,s,loc,y,1000,7000       ! select lines with specific coordinate
/rep                         ! replot
type,3                       ! turn on element type 3
real,3                       ! turn on real constant set 3
mat,3                        ! turn on material properties 3
secnum,3                     ! turn on section data 3
aesize,all,500               ! set mesh size
amesh,all                    ! mesh all selected areas
allsel                       ! select all
FINISH
/SOLU                        ! Enter the solution mode
ANTYPE,STATIC                ! Static analysis
PSTRES,ON                    ! Prestress on
solve
finish
/SOLU                        ! Enter the solution mode again to solve buckling
ANTYPE,BUCKLE                ! Buckling analysis
BUCOPT,LANB,1                ! Buckling options - subspace, one mode
SOLVE
FINISH
/SOLU                        ! Re-enter solution mode to expand info - necessary
EXPASS,ON                    ! An expantion pass will be performed
MXPAND,1                     ! Specifies the number of modes to expand
SOLVE
FINISH
/POST1                       ! Enter post-processor
SET,LIST                     ! List eigenvalue solution - Time/Freq
SET,LAST                     ! Read in data for the desired mode
PLDISP                       ! Plots the deflected shape
```

Appendix J3: ANSYS script load application cylinder

```
finish                          ! stops all running processors
/clear                          ! clears database
/prep7                          ! enter preprocessor
k,1                             ! create keypoints
k,2,6000
k,3,,2500
k,4,6000,2500
l,3,4                           ! create
arota,1,,,,,,1,2
et,1,shell181                   ! define element properties
sectype,,shell
secdata,85,1
mp,ex,1,2e5
mp,prxy,1,0.3
dl,5,,ux,0                      ! constrain model
dl,7,,ux,0
dl,9,,ux,0
dl,11,,ux,0
dk,5,uy,0
dk,9,uy,0
dk,9,uz,0
wpoffs,2700
wprota,,,90
asbw,all
wpoffs,,,600
asbw,all
asel,,area,,13,16
wprota,,,-90
wprota,,-6.875
asbw,all
wprota,,13.751
asbw,all
wprota,,31.250
asbw,all
wprota,,13.751
asbw,all
wprota,,31.250
asbw,all
wprota,,13.751
asbw,all
wprota,,31.250
asbw,all
wprota,,13.751
asbw,all
! A16, A15, A21, A30, A10, A17, A22, A19, A25, A29, A6, A14
! *SET,PRESS,3.981              ! for system height of 6 m
*SET,PRESS,3.28                 ! for system height of 8 m
sfa,16,,pres,PRESS
sfa,15,,pres,PRESS
```

```
sfa,21,,pres,PRESS
sfa,30,,pres,PRESS
sfa,10,,pres,PRESS
sfa,17,,pres,PRESS
sfa,22,,pres,PRESS
sfa,19,,pres,PRESS
sfa,25,,pres,PRESS
sfa,29,,pres,PRESS
sfa,6,,pres,PRESS
sfa,14,,pres,PRESS
allsel
aplot
aesize,all,25
amesh,all
WPCSYS,-1,0                 ! align workplane with global cartesian
! solve
FINISH
/SOL
/STATUS,SOLU
SOLVE
FINISH
! plot results
/POST1
! esel,all                  ! define nodes to define path
! esel,s,cent,z,2500        ! choose nodes half way through structure
! path,cutline,2,,3000      ! define a path labeled cutline
! ppath,1,,0,0,2500         ! define endpoint nodes on path
! ppath,2,,6000,0,2500
! PDEF,,S,eqv,AVG           ! calculate equivalent stress on path
                            ! nsel,all
! PLPAGM,SEQV,2000,NODE     ! show graph on plot with nodes
! nsel,all                  ! define nodes to define path
! shell,top
! nsel,s,loc,z,2500         ! choose nodes half way through structure
! nsel,r,loc,y,-150
! path,cutline,2,,3000      ! define a path labeled cutline
! ppath,1,,0,0,2500         ! define endpoint nodes on path
! ppath,2,,6000,0,2500
! PDEF,,S,eqv,AVG           ! calculate equivalent stress on path
                            ! nsel,all
! PLPAGM,SEQV,2000,NODE     ! show graph on plot with nodes
PLNSOL, S,EQV, 0,1.0        ! show von Mises stress
```

Appendix J4: ANSYS script contact elements

```
finish
/clear
/prep7
k,1,1000                             ! defines keypoints
k,2,5000
k,3,1000,2500
k,4,5000,2500
l,3,4                                ! defines lines between keypoints
arota,1,,,,,,1,2                     ! rotates lines around keypoints
asel,,area,,1,4                      ! select area's
wpoffs,2850                          ! offsets workplane
wprota,,,90
asbw,all                             ! cuts geometry in xy-plane
wpoffs,,,300
asbw,all
asel,all
asel,,area,,13,16
wprota,,,-90
wprota,,-3.44
asbw,all
wprota,,6.88
asbw,all
wprota,,38.12
asbw,all
wprota,,6.88
asbw,all
wprota,,38.12
asbw,all
wprota,,6.88
asbw,all
wprota,,38.12
asbw,all
wprota,,6.88
asbw,all
agen,2,6,,,,-83,,,0                  ! Generates addition areas from a pattern of areas
agen,2,14,,,,-83,,,0
agen,2,16,,,,-58.69,-58.69,,0
agen,2,15,,,,,-83,,0
agen,2,21,,,,,-83,,0
agen,2,30,,,,58.69,-58.69,,0
agen,2,10,,,,83,,,0
agen,2,17,,,,83,,,0
agen,2,22,,,,58.69,58.69,,0
agen,2,19,,,,,83,,0
agen,2,25,,,,,83,,0
agen,2,29,,,,-58.69,58.69,,0
/pnum,area,1
/rep
asel,all
```

```
aplot
ET,1,shell181                ! sets element type 1 to shell 181
sectype,,shell
secdata,85,1                 ! sets element thickness
ET,2,conta173
ET,3,targe170
ET,4,combin14
r,3,5,,,,,,                  ! sets real constant set 3, belonging to ET,4 to K=5
mp,ex,1,2e5                  ! defines material constants
mp,prxy,1,0.3
/pnum,area,0
/pnum,line,1
/rep
dl,5,,ux,0                   ! defines boundary conditions on lines
dl,7,,ux,0
dl,9,,ux,0
dl,11,,ux,0
dk,9,uy,0
dk,5,uy,0
dk,9,uz,0
*SET,PRESS,15.925            ! assigns to the term PRESS a value of 14.61, based on 1433 kN op
300*300 area
! *SET,PRESS,15.925
sfa,8,,pres,PRESS            ! defines load on area. Based on 1433 kN on area 300*300 of the
pads
sfa,12,,pres,PRESS
sfa,31,,pres,PRESS
sfa,32,,pres,PRESS
sfa,33,,pres,PRESS
sfa,34,,pres,PRESS
sfa,35,,pres,PRESS
sfa,36,,pres,PRESS
sfa,37,,pres,PRESS
sfa,38,,pres,PRESS
sfa,39,,pres,PRESS
sfa,40,,pres,PRESS
allsel
aplot
aesize,all,50                ! sets mesh size
amesh,all                    ! meshes all area's, defaults to Element Type 1
allsel
aplot
MP,MU,1,                     ! set coefficient of friction
MAT,1                        ! Assign this material number to subsequently defined elements
(defaults to 1)
MP,EMIS,1,7.88860905221e-031         ! Material property Emissivity
R,4
REAL,4
ET,5,170                     ! sets element type 5 to target170
ET,6,174                     ! sets element type 6 to contact174
KEYOPT,6,9,0                 ! defines keyoption for ET 6, KO (9) to 0=Include both initial
geometrical penetration or gap and offset
```

```
KEYOPT,6,10,2                    ! defines keyoption for ET 6, KO (10) to 2=Each iteration
based on current mean stress of underlying elements
R,4,
RMORE,
RMORE,,0
RMORE,0
KEYOPT,6,12,5                    ! defines keyoption fot ET 6, KO (12) to 5=Always bonded
! Generate the target surface
ASEL,S,,,6                       ! select target area's
ASEL,A,,,10                      ! adds area to selected set
ASEL,A,,,14
ASEL,A,,,15
ASEL,A,,,16
ASEL,A,,,17
ASEL,A,,,19
ASEL,A,,,21
ASEL,A,,,22
ASEL,A,,,25
ASEL,A,,,29
ASEL,A,,,30
! CM,_TARGET,AREA
TYPE,5                           ! activates this element type
NSLA,S,1                         ! select nodes associated with selected area's;
ESLN,S,0                         ! select elements attached to selected nodes;
ESLL,U                           ! select elements associated with selected lines; (u) unselect
from current set
ESEL,U,ENAME,,188,189            ! unselect element with element number ...
NSLE,A,CT2                       ! select nodes attached to selected elements
ESURF                            ! generates elements overlaid on free faces of existing
selected elements
! CMSEL,S,_ELEMCM
! Generate the contact surface
ASEL,S,,,8
ASEL,A,,,12
ASEL,A,,,31
ASEL,A,,,32
ASEL,A,,,33
ASEL,A,,,34
ASEL,A,,,35
ASEL,A,,,36
ASEL,A,,,37
ASEL,A,,,38
ASEL,A,,,39
ASEL,A,,,40
! CM,_CONTACT,AREA
TYPE,6
NSLA,S,1
ESLN,S,0
NSLE,A,CT2                       ! CZMESH patch (fsk qt-40109 8/2008)
ESURF
*SET,_REALID,4
ALLSEL
```

```
ESEL,ALL
ESEL,S,TYPE,,5
ESEL,A,TYPE,,6
ESEL,R,REAL,,4
/PSYMB,ESYS,1                ! shows various symbols on display
/PNUM,TYPE,1                 ! controls entity numbering/coloring on plots
/NUM,1
EPLOT
! Reverse target normals
ESEL,NONE
ESEL,A,TYPE,,5
ESEL,R,REAL,,4
ESURF,,REVERSE
ESEL,ALL
ESEL,S,TYPE,,5
ESEL,A,TYPE,,6
ESEL,R,REAL,,4
/PSYMB,ESYS,1
/PNUM,TYPE,1
/NUM,1
EPLOT
!
ESEL,ALL
ESEL,S,TYPE,,5
ESEL,A,TYPE,,6
ESEL,R,REAL,,4
asel,all
aplot
allsel
WPCSYS,-1,0                  ! align workplane with global cartesian
finish
/solut
antype,0                     ! specifies analysis type and restart status
time,1                       ! Sets time at end of run to 1 sec
autots,on                    ! Auto time-stepping on
nsubst,100,1000,20           ! Number of sub-steps
outres,all,all               ! Write all output
neqit,100                    ! Max number of iterations
! solve
FINISH
/SOLU
!/STATUS,SOLU
SOLVE
FINISH
/POST1                       ! enters post processor
/DSCALE,ALL,OFF              ! no scale
/EFACET,1                    ! specifies number of facets per element edge for PowerGraphics
display
PLNSOL, S,EQV, 0,1.0         ! show von Mises stress
```

Appendix J5: ANSYS script lower flange

```
finish                          ! stops running processes
/clear                          ! clears current database
/prep7                          ! enters preprocessor stage
/VIEW,1,1,1,1
/rep
ET,1,shell181                   ! Define element
sectype,1,shell                 ! associates section type information with a section ID number
secdata,40,1                    ! set shell thickness
MP,EX,1,2e5                     ! Young's modulus
MP,PRXY,1,0.3                   ! Poisson's ratio
ET,2,shell181                   ! Define element
sectype,2,shell                 ! associates section type information with a section ID number
secdata,55,2                    ! set shell thickness
MP,EX,2,2e5                     ! Young's modulus
MP,PRXY,2,0.3                   ! Poisson's ratio
k,1,2430                        ! defines keypoints
k,2,2500
k,3,2780
k,4,2500,1000
k,6,0,0,0
k,7,0,7000,0
l,1,2                           ! defines lines between keypoints
l,2,3
l,2,4
arota,1,2,,,,,6,7,360,8         ! create cylindrical area by rotating lines around keypoints
arota,3,,,,,,6,7,360,8          ! create cylindrical area by rotating lines around keypoints
/VIEW,1,,1                      ! show top view
aplot
AGLUE,ALL                       ! glue areas together
wprota,,,-3.44
asbw,all
wprota,,,6.88
asbw,all
wprota,,,38.12
asbw,all
wprota,,,6.88
asbw,all
wprota,,,38.12
asbw,all
wprota,,,6.88
asbw,all
wprota,,,38.12
asbw,all
wprota,,,6.88
asbw,all
asel,s,loc,y,-1,1
/rep
*SET,PRESS,1996
sfl,42,pres,PRESS
```

```
sfl,27,pres,PRESS
sfl,18,pres,PRESS
sfl,64,pres,PRESS
sfl,21,pres,PRESS
sfl,88,pres,PRESS
sfl,24,pres,PRESS
sfl,114,pres,PRESS
sfl,59,pres,PRESS
sfl,81,pres,PRESS
sfl,32,pres,PRESS
sfl,107,pres,PRESS
sfl,35,pres,PRESS
sfl,135,pres,PRESS
sfl,38,pres,PRESS
sfl,142,pres,PRESS
type,1
real,1
secnum,1
allsel
asel,s,loc,y,-1,1
aesize,all,100
amesh,all
allsel
asel,s,loc,y,1,1000
type,2
real,2
secnum,2
aesize,all,100
amesh,all
aplot
lsel,s,loc,y,999,1001
lplot
/rep
dl,all,,uy
dk,4,uz
dk,35,uz
dk,35,ux
allsel
aplot
allsel
WPCSYS,-1,0
FINISH
/SOL
/STATUS,SOLU
SOLVE
/post1
/DSCALE,ALL,5
/EFACET,1
PLNSOL, S,EQV, 0,1.0
/VIEW,1,1,1,1
/rep
```

Appendix J6: ANSYS script model seafastening

```
finish
/clear
/prep7
cylinder1=600
cylinder2=1618
height=9200
roll=3717
pitch=997
downone=15135/3
downall=469
/VIEW,1,1,2,3
! flanges
ET,1,shell181               ! Define element (beam flange)
sectype,1,shell             ! associates section type information with a section ID number
secdata,45,1                ! set shell thickness
MP,EX,1,2e5                 ! Young's modulus
MP,PRXY,1,0.3               ! Poisson's ratio
! webs
ET,2,shell181               ! Define element (beam web)
sectype,2,shell             ! associates section type information with a section ID number
secdata,50,2                ! set shell thickness
MP,EX,2,2e5                 ! Young's modulus
MP,PRXY,2,0.3               ! Poisson's ratio
! tubulars
ET,3,shell181               ! Define element (seafatening tube)
sectype,3,shell             ! associates section type information with a section ID number
secdata,80,3                ! set shell thickness
MP,EX,3,2e5                 ! Young's modulus
MP,PRXY,3,0.3               ! Poisson's ratio
! plate stiffeners
ET,4,shell181               ! Define element (seafatening tube)
sectype,4,shell             ! associates section type information with a section ID number
secdata,50,4                ! set shell thickness
MP,EX,4,2e5                 ! Young's modulus
MP,PRXY,4,0.3               ! Poisson's ratio
! wing plates
ET,5,shell181               ! Define element (seafatening tube)
sectype,5,shell             ! associates section type information with a section ID number
secdata,30,5                ! set shell thickness
MP,EX,5,2e5                 ! Young's modulus
MP,PRXY,5,0.3               ! Poisson's ratio
k,1,-200,,6000              ! keypoints for beams
k,2,,,6000
k,3,200,,6000
k,4,-200,1000,6000
k,5,,1000,6000
k,6,200,1000,6000
k,7,-200,,
k,8,,,
```

```
k,9,200,,
k,10,-200,1000,
k,11,,1000,
k,12,200,1000,
a,1,2,8,7                            ! areas of beams
a,2,3,9,8
a,4,5,11,10
a,5,6,12,11
a,2,8,11,5
wpoffs,,,2500                        ! devide areas for platestiffeners
asbw,all
WPCSYS,-1,0                          ! align workplane with global cartesian
a,13,14,17,16
a,14,15,18,17
wpoffs,,,3000
asbw,all
a,19,20,23,22                        ! create plate stiffeners
a,20,21,24,23                        ! create plate stiffeners
k,193,,,cylinder1
k,194,,1000,cylinder1
k,195,
k,196,,1000
l,193,194                            ! =L337
lsel,s,loc,z,cylinder1-1,cylinder1+1
arota,all,,,,,,195,196,360,8
allsel
aplot
asel,s,loc,z,0,2000
asel,r,loc,x,-250,250
/rep
aovlap,all
aglue,all
asel,all
CSYS,5
asel,s,loc,x,0,cylinder1-1
adele,all,,1
CSYS,0
asel,all
aplot
asel,s,loc,z,cylinder1,6000
/rep
WPCSYS,-1,0                          ! align workplane with global cartesian
k,215,,,cylinder2
k,216,,1000,cylinder2
l,215,216
lsel,s,loc,z,cylinder2
lsel,r,loc,x,-1,1
arota,all,,,,,,195,196,180,8
lsel,s,loc,z,-cylinder2
lsel,r,loc,x,-1,1
arota,all,,,,,,195,196,180,8
asel,all
```

```
aplot
asel,s,loc,z,cylinder1,cylinder2
asel,r,loc,x,-400,400
/rep
aovlap,all
aglue,all
asel,all
aplot
asel,s,loc,z,cylinder1,8000
asel,r,loc,x,-150,150
/rep
CSYS,5                              ! change workplane to global y cylindrical
agen,8,all,,,,45
CSYS,0                              ! change workplane to global cartesian
asel,s,loc,x,-150,150
asel,r,loc,z,cylinder2,8000
/rep
CSYS,5                              ! change workplane to global y cylindrical
agen,2,all,,,,22.5
CSYS,0
asel,r,loc,x,200,4000
/rep
CSYS,5                              ! change workplane to global y cylindrical
agen,8,all,,,,45
CSYS,0
allsel
aplot
/rep
wpoffs,,,4000                       ! cut outer perimeters
asbw,all
wpoffs,,,-8000
asbw,all
wprota,,,90
wpoffs,,,4000
asbw,all
wpoffs,,,-8000
asbw,all
WPCSYS,-1,0                         ! align workplane with global cartesian
asel,s,loc,x,4001,8000              ! select areas outside cut
asel,a,loc,x,-4001,-8000
asel,a,loc,z,4001,8000
asel,a,loc,z,-4001,-8000
adele,all,,,1                       ! delete areas outside outer perimeter
asel,all
aplot
/pnum,area,0
/pnum,kp,1
/rep
allsel
ksel,u,loc,x,-4095,4095
ksel,u,loc,z,-4095,4095
kplot
```

```
/VIEW,1,1,2,3
allsel
k,,3800,,3800                       ! create keypoints to create outer beams
k,,3800,,-3800
k,,3800,1000,-3800
k,,3800,1000,3800
k,,4200,,4200
k,,4200,,-4200
k,,4200,1000,-4200
k,,4200,1000,4200
a,492,516,519,495                   ! create web of outer beam
a,4,495,519,3                       ! create upper inner flange of outer beam
a,1,492,516,2                       ! create lower inner flange of outer beam
a,495,84,83,519                     ! create upper outer flange of outer beam
a,5,6,516,492                       ! create lower outer flange of outer beam
asel,s,loc,x,3800,4200              ! select outer beam
CSYS,5                              ! change workplane to global y cylindrical
agen,4,all,,,,90                    ! generate outer beam 4 times and rotate around origin
CSYS,0                              ! change workplane to global cartesian
/pnum,kp,0
allsel
aplot
/rep
k,600,0,height,cylinder2            ! create tubular element
l,216,600
lsel,s,loc,y,1001,height
arota,all,,,,,,195,196,180,8
lsel,r,loc,z,-cylinder2+1,-cylinder2-1
arota,all,,,,,,195,196,180,8
wpoffs,,height-200                  ! create plate on which jacks lay
wprota,,-90
asbw,all
cyl4,,,,,cylinder2                  ! create circular plate on working plane
asel,s,loc,x,3800,4200              ! select two outer beam for attaching wingplates
asel,a,loc,x,-3800,-4200
/rep
WPCSYS,-1,0
asbw,all                            ! cut beams for wingplates
wpoffs,,,3200
asbw,all
wpoffs,,,-6400
asbw,all
/rep
WPCSYS,-1,0
RECTNG,4000,4200,0,1000,            ! create wingplate part 1
RECTNG,4200,5132.5,0,200,           ! create wingplate part 2
a,621,626,625                       ! create wingplate part 3
asel,s,loc,x,4000,5200              ! select parts of wingplate
asel,r,loc,z,-1,1
aadd,all                            ! adds areas of wingplate together
aoffst,all,3200                     ! create next wingplane by offsetting first
```

```
asel,r,loc,z,-1,1
aoffst,all,-3200                  ! create next wingplane by offsetting first
asel,all
asel,s,loc,x,4150,5200
CSYS,5                            ! change to cylindrical coordinates
agen,2,all,,,,180                 ! generate wingplanes on opposite site
CSYS,0
allsel
lsel,u,loc,x,-3801,3801           ! select lines for boundary conditions
lsel,u,loc,z,-3000,-150
lsel,u,loc,z,150,3000
lsel,u,loc,z,-3350,-5000
lsel,u,loc,z,3350,5000
lsel,u,loc,y,1,1001
/rep
dl,all,,all                       ! create boundary conditions
WPCSYS,-1,0
wprota,,-90
cyl4,0,0,400,,600                 ! create extra circular plates on connection inner tube and
beams
wpoffs,,,1000
cyl4,0,0,400,,600
wpoffs,,,-1000
cyl4,0,0,cylinder2-200,,cylinder2+200
aovlap,all
aglue,all
allsel
/rep
asel,s,loc,y,1,999                ! select webs of beams
CSYS,5
asel,u,loc,x,400
asel,u,loc,x,1950
asel,u,loc,x,2500
asel,u,loc,x,3000
CSYS,0
asel,r,loc,x,-4001,4001
type,2                            ! turn on element type 2
real,2                            ! turn on real constant set 2
mat,2                             ! turn on material properties 2
secnum,2                          ! turn on section data 2
aesize,all,100                    ! set mesh size
amesh,all                         ! mesh all selected areas
asel,all
aplot
asel,u,loc,x,-4150,4150           ! select wing plates
type,5                            ! turn on element type 5
real,5                            ! turn on real constant set 5
mat,5                             ! turn on material properties 5
secnum,5                          ! turn on section data 5
aesize,all,100                    ! set mesh size
amesh,all                         ! mesh all selected areas
asel,all
```

```
aplot
asel,s,loc,y,-1,1001                    ! select flanges of beams
asel,u,loc,y,1,999
type,1                                  ! turn on element type 1
real,1                                  ! turn on real constant set 1
mat,1                                   ! turn on material properties 1
secnum,1                                ! turn on section data 1
aesize,all,100                          ! set mesh size
amesh,all                               ! mesh all selected areas
asel,all
aplot
CSYS,5
asel,s,loc,x,cylinder1                  ! select tubular elements
asel,a,loc,x,cylinder2
type,3                                  ! turn on element type 3
real,3                                  ! turn on real constant set 3
mat,3                                   ! turn on material properties 3
secnum,3                                ! turn on section data 3
aesize,all,100                          ! set mesh size
amesh,all                               ! mesh all selected areas
asel,all
asel,s,loc,x,2500                       ! select plate stiffeners
asel,a,loc,x,3000
type,4                                  ! turn on element type 4
real,4                                  ! turn on real constant set 4
mat,4                                   ! turn on material properties 4
secnum,4                                ! turn on section data 4
aesize,all,100                          ! set mesh size
amesh,all                               ! mesh all selected areas
CSYS,0
allsel
asel,s,loc,y,height-200                 ! select circular plate
type,4                                  ! turn on element type 4
real,4                                  ! turn on real constant set 4
mat,4                                   ! turn on material properties 4
secnum,4                                ! turn on section data 4
aesize,100                              ! set mesh size
amesh,all                               ! mesh all selected areas
allsel
aplot
WPCSYS,-1,0                             ! align workplane with global cartesian
lsel,s,loc,y,height-201,height-199      ! select lines for applying Roll force
lsel,r,loc,x,-cylinder2,-cylinder2+200
lplot
/rep
sfl,all,pres,roll                       ! apply roll force distributed over small length
lsel,s,loc,y,height-201,height-199      ! select lines for applying PITCH force
lsel,r,loc,z,cylinder2-200,cylinder2
lplot
/rep
sfl,all,pres,pitch                      ! PITCH
```

```
CSYS,5
lsel,s,loc,x,2480,2520          ! select lines on which TP stands
CSYS,0
lsel,r,loc,y,980,1020           ! select all lines on which TP stands
lsel,r,loc,x,2200,2501          ! only if one beam is selected
! sfl,all,pres,downall          ! apply vertical load of TP on all beams of grillage
sfl,all,pres,downone            ! apply vertical load on three beams of grillage
allsel
aplot
FINISH
/SOL
/STATUS,SOLU
SOLVE
FINISH
/POST1
/DSCALE,ALL,10                  ! show deformed shape plus scale factor
/EFACET,1
PLNSOL, S,EQV, 0,1.0            ! show von mises stress
/rep
```

Appendix J7: ANSYS script cylinder plus attachements

```
finish                  ! stops all running processors
/clear                  ! clears database
/prep7                  ! enter preprocessor
k,1                     ! create keypoints
k,2,10000               ! create keypoints
k,3,,2500               ! create keypoints
k,4,10000,2500          ! create keypoints
l,3,4                   ! create line
arota,1,,,,,,1,2        ! rotate line around keypoints
et,1,shell181           ! TP
sectype,1,shell
secdata,85,1
MP,EX,1,2e5             ! Young's modulus
MP,PRXY,1,0.3           ! Poisson's ratio
et,2,shell181           ! Fenders
sectype,2,shell
secdata,20,2
MP,EX,2,2e5             ! Young's modulus
MP,PRXY,2,0.3           ! Poisson's ratio
et,3,shell181           ! Fender connection
sectype,3,shell
secdata,25,3
MP,EX,3,2e5             ! Young's modulus
MP,PRXY,3,0.3           ! Poisson's ratio
et,4,shell181           ! ladder + ladder connection
sectype,4,shell
secdata,14.2,4
MP,EX,4,2e5             ! Young's modulus
MP,PRXY,4,0.3           ! Poisson's ratio
et,5,shell181           ! steps (ladder)
sectype,5,shell
secdata,5,5
MP,EX,5,2e5             ! Young's modulus
MP,PRXY,5,0.3           ! Poisson's ratio
dl,5,,ux,0              ! constrain model
dl,7,,ux,0              ! constrain model
dl,9,,ux,0              ! constrain model
dl,11,,ux,0             ! constrain model
dk,5,uy,0               ! constrain model
dk,9,uy,0               ! constrain model
dk,9,uz,0               ! constrain model
wpoffs,5950             ! offset workplane
wprota,,,90             ! rotate workplane
asbw,all                ! divide areas by workplane
wpoffs,,,600            ! offset workplane
asbw,all                ! divide areas by workplane
asel,,area,,13,16
wprota,,,-90            ! rotate workplane
```

```
wprota,,-6.875              ! rotate workplane
asbw,all                    ! divide areas by workplane
wprota,,13.751              ! rotate workplane
asbw,all                    ! divide areas by workplane
wprota,,31.250              ! rotate workplane
asbw,all                    ! divide areas by workplane
wprota,,13.751              ! rotate workplane
asbw,all                    ! divide areas by workplane
wprota,,31.250              ! rotate workplane
asbw,all                    ! divide areas by workplane
wprota,,13.751              ! rotate workplane
asbw,all                    ! divide areas by workplane
wprota,,31.250              ! rotate workplane
asbw,all                    ! divide areas by workplane
wprota,,13.751              ! rotate workplane
asbw,all                    ! divide areas by workplane
asel,all
aplot
WPCSYS,-1,0                 ! align workplane with global cartesian
k,51,1000,900,3526          ! fenders
k,52,10000,900,3526
k,53,1000,727.2,3526
k,54,10000,727.2,3526
l,53,54                     ! create line
arota,23,,,,,,51,52,
k,61,1372,900,3526          ! connection fenders to TP
k,62,1372,536,2100
k,63,1544.8,900,3526
k,64,1544.8,536,2100
l,63,64
arota,89,,,,,,61,62,        ! rotate line around keypoints
aovlap,all
asel,s,loc,z,2100,2400
asel,r,loc,y,400,750
adele,all
allsel
/rep
asel,s,loc,x,1200,1550
asel,r,loc,z,3353,3700
adele,all
/rep
asel,s,loc,x,1200,1551
agen,2,all,,,5000           ! generate second connection fender
/rep
allsel
aplot
k,93,1000,325,2930          ! ladder
k,94,8000,325,2930
k,95,1000,410,2930
k,96,8000,410,2930
l,95,96
arota,139,,,,,,93,94,
```

```
k,103,2000,325,2930          ! connection ladder
k,104,2000,325,2200
k,105,2085,325,2930
k,106,2085,325,2200
l,105,106
arota,151,,,,,,103,104,      ! rotate line around keypoints
allsel
aplot
asel,s,loc,x,1920,2090
agen,2,all,,,4000            ! generate second connection ladder
asel,s,loc,z,2501,3900
asel,u,loc,y,0,410
LOCAL,11,CYLIN,0,0,0,,,90    ! create local coordinate system
agen,2,all,,,,28.636         ! generate and rotate fenders
allsel
aplot
CSYS,0                       ! cartesian coordinate system
asel,s,loc,z,2201,3900
asel,r,loc,y,150,410
agen,2,all,,,,-650           ! generate second half of ladder plus connection
k,177,1300,325,2930
k,178,1300,-325,2930
k,179,1312.50,325,2930
k,180,1312.50,-325,2930
l,179,180
arota,257,,,,,,177,178       ! rotate line around keypoints
asel,s,loc,x,1286,1313
agen,24,all,,,281            ! generate multiple ladder steps
allsel
aovlap,all
asel,s,loc,y,-390,390
asel,r,loc,z,2200,2350
adele,all                    ! delete excessive areas
allsel
aplot
asel,s,loc,x,5950,6550
asel,u,loc,z,2500,4000
! *SET,PRESS,3.28            ! use this q if modular height is 8 m
*SET,PRESS,3.98                      ! use this q if modular height is 6 m
sfa,16,,pres,PRESS
sfa,30,,pres,PRESS
sfa,10,,pres,PRESS
sfa,17,,pres,PRESS
sfa,22,,pres,PRESS
sfa,19,,pres,PRESS
sfa,25,,pres,PRESS
sfa,29,,pres,PRESS
sfa,6,,pres,PRESS
sfa,14,,pres,PRESS
sfa,646,,pres,PRESS
sfa,507,,pres,PRESS
sfa,645,,pres,PRESS
```

```
sfa,506,,pres,PRESS
allsel
aplot
! TP cylinder
LOCAL,11,CYLIN,0,0,0,,,90      ! create local coordinate system
asel,s,loc,x,2501
type,1                         ! turn on element type 1
real,1                         ! turn on real constant set 1
mat,1                          ! turn on material properties 1
secnum,1                       ! turn on section data 1
aesize,all,50                  ! set mesh size
amesh,all                      ! mesh all selected areas
allsel
aplot
! Fenders
asel,s,loc,x,3300,4000
type,2                         ! turn on element type 2
real,2                         ! turn on real constant set 2
mat,2                          ! turn on material properties 2
secnum,2                       ! turn on section data 2
aesize,all,50                  ! set mesh size
amesh,all                      ! mesh all selected areas
allsel
aplot
! Fender connection
asel,s,loc,x,2550,3400
CSYS,0
asel,u,loc,y,-420,420
/rep
type,3                         ! turn on element type 3
real,3                         ! turn on real constant set 3
mat,3                          ! turn on material properties 3
secnum,3                       ! turn on section data 3
aesize,all,50                  ! set mesh size
amesh,all                      ! mesh all selected areas
allsel
aplot
! ladder + ladder connection
asel,s,loc,y,-420,420
asel,r,loc,z,2500,4000
asel,u,loc,y,-220,220
/rep
type,4                         ! turn on element type 4
real,4                         ! turn on real constant set 4
mat,4                          ! turn on material properties 4
secnum,4                       ! turn on section data 4
aesize,all,25                  ! set mesh size
amesh,all                      ! mesh all selected areas
allsel
aplot

! ladder steps
```

```
asel,s,loc,z,2500,4000
asel,r,loc,y,-220,220
/rep
type,5                          ! turn on element type 5
real,5                          ! turn on real constant set 5
mat,5                           ! turn on material properties 5
secnum,5                        ! turn on section data 5
aesize,all,25                   ! set mesh size
amesh,all                       ! mesh all selected areas
allsel
aplot
WPCSYS,-1,0                     ! align workplane with global cartesian
! solve
FINISH
/SOL
/STATUS,SOLU
SOLVE
FINISH
! plot results
/POST1
PLNSOL, S,EQV, 0,1.0            ! show von Mises stress
/RGB,INDEX,100,100,100, 0       ! reverse colours
/RGB,INDEX, 80, 80, 80,13
/RGB,INDEX, 60, 60, 60,14
/RGB,INDEX, 0, 0, 0,15
/REPLOT
/VIEW,1,-1
/ANG,1
/ANG,1,30,XS,1
/ANG,1,30,XS,1
/ANG,1,30,XS,1
/ANG,1,-30,YS,1
/ANG,1,-30,YS,1
/ANG,1,-30,YS,1
/replot
```